STUDY ON SOME ADVANCED CONTROL TECHNIQUES OF PERMANENT MAGNET SYNCHRONOUS MOTOR FOR MINIMIZING THE TORQUE RIPPLE

A thesis is submitted to fulfill the requirement of the degree

Master in Control System Engineering

Submitted by

Aritra Pal

Examination Roll no. – **M4CTL22010**

Registration no. – **154060** of **2020-2021**

Year – **2nd**, Semester – **4th**

Under the guidance of

Prof. Susanta Ray

and

Dr. Sayantan Chakraborty

Department of Electrical Engineering

Jadavpur University

Kolkata – 700032

June, 2022

Faculty of Engineering and Technology
Jadavpur University, Kolkata - 700032

Certificate

This is to certify that the thesis entitled "**Study on some Advanced Control Techniques of Permanent Magnet Synchronous Motor for Minimizing the Torque Ripple**", submitted by **Mr. Aritra Pal** (Examination Roll No. M1CTL22010), under our supervision and guidance during the session of 2020-22 in the department of Electrical Engineering, Jadavpur University. We are satisfied with his work, which is being presented for the partial fulfillment of the degree of **Master in Control System Engineering** from Jadavpur University, Kolkata-700032.

……..

Prof. Susanta Roy
Associate Professor
Department of Electrical Engineering
Jadavpur University
Kolkata, 700032

……

Dr. Sayantan Chakraborty
Assistant Professor
Department of Electrical Engineering
Jadavpur University
Kolkata, 700032

……

Prof. Chandan Mazumdar
Dean of Faculty Council of
Engineering and Technology
Jadavpur University
Kolkata, 700032

……

Prof. Saswati Mazumdar
Head of the Department of
Electrical Engineering
Jadavpur University
Kolkata, 700032

Faculty of Engineering and Technology
Jadavpur University, Kolkata - 700032

Certificate of Approval

The forgoing thesis entitled "**Study on some Advanced Control Techniques of Permanent Magnet Synchronous Motor for Minimizing the Torque Ripple**" is hereby approved as a creditable study of an Engineering subject carried out and presented in a manner that fulfills its acceptance as a prerequisite to the degree for which it is submitted. It is understood that by this approval, the undersigned does not necessarily endorse or approve any statement made, opinion expressed, or conclusion drawn therein but approves the thesis only for the purpose for which it is submitted.

The final examination for evaluation of the thesis

Signature of the examiners

……

……

……

Declaration of Originality

I hereby declare that this thesis contains a literature survey and original research work done by me. All the information in this document has been obtained and presented according to academic rules and ethical conduct. I also declare that, as required by these rules and conduct, I have fully cited and referenced all material and results that are not original to this work.

Name: ARITRA PAL

Examination Roll No: M4CTL22010

Thesis Title: Study on some Advanced Control Techniques of Permanent Magnet Synchronous Motor for Minimizing the Torque Ripple

Signature with Date:

ACKNOWLEDGMENTS

I express my sincere gratitude to my supervisor, Prof. Susanta Ray for his encouragement, suggestion, and advice, which made the thesis possible to be completed successfully. I am very much grateful to Dr. Sayantan Chakraborty for being a constant source of encouragement, and inspiration and for his valuable suggestions coupled with his technical expertise throughout my research work. It was a great honor for me to pursue my research under their supervision.

I would also like to thank my co-worker SK Nasim Ali, all the staff of the Drives and Simulation laboratory, and the research scholars of our department for providing constant encouragement throughout my thesis work.

Last but not least I extend my words of gratitude to my parents for personally motivating me to carry out the work smoothly.

ABSTRACT

This thesis consists of the mathematical equations of Permanent Magnet Synchronous Motor (PMSM), a general idea of the Direct Torque Control (DTC) method, and a DTC based on Sliding Mode Control for PMSM as well as PI control. Space Vector Modulation (SVM) is used to select the voltage vectors of the inverter for different time instances. Look-Up Table (LUT) is used to select the voltage vectors for different values of torque and flux with different phases. Here, twelve sectors modified DTC have been introduced to get a better response. And then PMSM control system simulations are accomplished with the two methods mentioned above in the MATLAB® SIMULINK environment. Then the ripples produced in speed, torque, and flux responses of DTC with PI control and SMC are compared. This is evident that DTC has a specific disadvantage is that it has a significant torque and current ripple. This problem can be well tackled by Sliding Mode Control (SMC). In this thesis work, this is justified that the twelve-sector modified SVM method is preferable to suppress the ripple percentage to a great extent. It can suppress the ripples produced while the load variations are there. This method has only one disadvantage it creates a chattering effect but this will not affect the system significantly.

Chapter No.	CONTENTS	Page No.
	Acknowledgment	**5**
	Abstract	**6**
	List of Acronyms	**10**
	List of Figures	**11-13**
	List of Tables	**14**
1	**Introduction and Literature Review**	**15-18**
1.1	The motivation for the work	15
1.2	Literature Review	15-18
1.3	Organization of the Thesis	18
2	**Permanent Magnet Synchronous Motor**	**19-36**
2.1	Introduction	19
2.2	Construction	19-26
2.2.1	Merrill's Rotor	21-22
2.2.2	Interior-type PM Rotors	22-23
2.2.3	Surface PM Rotors	23
2.2.4	Inset-type PM Rotor	24
2.2.5	Buried PM Rotors	24-25
2.2.6	Comparison of PMSM with Surface and Buried Magnets	26
2.3	Operating Principle	26
2.4	Starting	26-27
2.5	System Parameters	27-28
2.6	Nonlinearities in PMSM	28
2.7	Basic Equations of PMSM	28-33
2.7.1	Park and Clarke Transformation	28-32
2.7.2	Electrical Equations	32-33
2.7.3	Mechanical Equations	33

List of Acronyms

Short Form	Full-Form
AC	Alternating Current
BJT	Bipolar Junction Transistor
BLDCM	Brush Less Direct Current Motor
DC	Direct Current
DTC	Direct Torque Control
FPGA	Field Programmable Gate Array
GA	Genetic Algorithm
HEV	Hybrid Electric Vehicle
LQR	Linear Quadratic Regulator
LUT	Look-Up Table
MOSFET	Metal Oxide Semiconductor Field Effect Transistor
MPC	Model Predictive Control
MPCC	Model Predictive Current Control
MPTC	Model Predictive Torque Control
PI	Proportional Integral
PMACM	Permanent Magnet Alternating Current Motor
PMSM	Permanent Magnet Synchronous Motor
PRC	Proportional Resonance Control
PSO	Particle Swarm Optimization
PWM	Pulse Width Modulation
SFC	State Feedback Control
SMC	Sliding Mode Control
SPMSM	Surface-mounted Permanent Magnet Synchronous Motor
SVM	Space Vector Modulation
VC	Vector Control
VFD	Variable Frequency Drive
VSD	Variable Speed Drive
VSI	Voltage Source Inverter
VVVF	Variable Voltage Variable Frequency

List of Figures

List of Tables

CHAPTER 1

INTRODUCTION AND LITERATURE REVIEW

1.1 The motivation for the work

Power semiconductor devices help AC Drives grow rapidly. Permanent Magnet Synchronous Motor (PMSM) is a very efficient and powerful motor for high-speed AC drive applications like Traction, Aerospace, Robotics, Electric Vehicles, Machine Tools, Washing machines, refrigerators, etc. This not only has a wide range of applications but also has easier control operations.

There are different types of control methods of PMSM. Here, I used Direct Torque Control (DTC) to get the desired speed as this method is most advantageous compared to the others. This method has a wide range of control. The only disadvantage is the torque and flux ripple which can be suppressed by another control method named Sliding Mode Control (SMC). SMC can help to suppress the ripple and it can work with lower torque limits. These controllers were used for both six sectors and twelve sector operations. It can be used in other plants also.

The main motivation of my work is to get an almost ripple-free speed response as the desired output of the drive system by controlling the electromagnetic torque and flux of the PMSM. Also, here I am introducing SMC with twelve sectors modified DTC to control not only speed but also to suppress other important parameters of the system like torque, current, etc.

1.2 Literature Review

Permanent magnet synchronous motors (PMSM) are mostly used as Electric drive applications to control the motion of any system. It has very good dynamic behavior and it has a compact structure. For this, the major use of this machine is in servo-drive applications like robotics and machine tools [1]. As PMSM has superior power density and high efficiency, nowadays it is used in power electronic converter-controlled drive systems such as Variable

Speed Drive (VSD) in Electric Vehicle (EV), Hybrid Vehicle (HV), Hybrid Electric Vehicle (HEV), Electric Power Steering (EPS), etc. It is also used as auxiliary drive-in heating, ventilating, and air conditioning (HVAC) systems [2]-[5].

Speed control of PMSM using VSD is the most rarely implemented in cascade control structures with PI controllers [6]. SMC [7] or non-linear control can also be used based on fuzzy logic [8] and neural networks [9] there to ensure the drive is very robust to use.

State Feedback Control (SFC) is an alternative way of controlling PMSM. Here, a state-space model is designed, and by tuning the system gain matrix, the system is controlled. Here, only one controller can be used [10]. Conventionally, SFC is tuned in the trial-and-error method. But, later Linear Quadratic Regulator (LQR) takes the responsibility to calculate the gain matrix by using Bryson's rule [11]. Besides that, the SFC gain matrix can be obtained by applying Particle Swarm Optimization (PSO) [12] or Genetic Algorithm (GA) [13] in computer-aided optimization.

Model Predictive Control (MPC) is one of the best algorithms to control Voltage Source Inverter (VSI) fed PMSM drive if anyone has very good knowledge to design mathematical model of the drive [14]. Here, we can deal with the constraint which has two ways to approach [15]. We can consider the constraint while controlling the system. Otherwise, we can apply the constraint later, which is known as the posterior constraint. The first approach is more complex as compared to the other and it can be implemented by using MPC [16]-[19]. In this method, it is required to solve the optimal control problem over a finite horizon. As we have to give more effort to computing using this technique, we need to implement it with the help of fast processing units.

In [18], an FPGA control board is used to control PMSM using an MPC algorithm. Here, we have to consider the two constraints, current limitation and voltage saturation for defining the befitting reference, current, and voltage PWM.

Advanced methods such as MPC, SMC, or Proportional Resonance Control (PRC) help the designers to operate smoothly. These methods are applied to improve the control performance of PMSM and these can solve the major problems like the dependence and disturbance of the system in the motor and also, the problems occurred due to parameter insensitivity [19]-[20].

MPC is preferred for its easy scheme and faster control operation. It follows the mathematical representation of the system to determine the forecasted value in the discrete domain and obtain the optimized cost function to use the predicted value to find a more accurate value on the next step to reach the desired output. Two types of MPC are based on control

parameters such as Model Predictive Current Control (MPCC) and Model Predictive Torque Control (MPTC). MPCC cannot perform well as it is dependent on the accuracy of the parameters. However, temperature, magnetic field saturation, and operating state affect the control performance of the parameter that causes parameter drift and model mismatch, and especially the control accuracy and the control performance are decreased [21], [22].

The basic and conventional methods were applied to control PMSM before using the MPC algorithm. Conventional control methods were Vector Control (VC) and Direct Torque Control (DTC). Vector Control is used to control DC motors for implementing the current decoupling by using coordinate transformation as well as the decoupling of the magnetic field and torque. But VC cannot fulfill practical requirements when the motor experiences disturbances externally or changes in parameters internally [23]-[24].

When Vector Control fails to fulfill the requirement, we have to follow another way, i.e., DTC. Here in DTC, neither decoupling nor coordinate transformation is required. So, the system does not need to depend so much on the parameter. As the inverter switch is not constant, it caused flux linkage and torque ripple very large [25]-[28].

As per we know, PMSM is highly efficient and it has high torque density and good reliability. These machines are widely used in many applications in practical fields that growing interest in researchers [29]-[31]. Electromagnetic torque and speed have to perform excellently to control the motion of PMSM [32]-[34].

Vector Control can implement the decoupling control of the torque and the flux obtained from the stator currents [35]-[36], and the Proportional-Integral (PI) controller can be applied to converge the reference torque value.

DTC can enhance the dynamic characteristics of the electromagnetic torque [37]-[38]. In a DTC system, the electromagnetic torque can be controlled precisely dependent on the stator voltage vector selection, the loop is closed by the speed with the PI controller, and a comparator for pulse width modulation (PWM) is not needed in the system [39]. DTC can reach a faster torque response by using hysteresis control in comparison with PWM current control [40]-[42].

As the electromagnetic torque has superior dynamic performance, DTC has been studied and developed frequently such as Space Vector Modulation DTC (SVM-DTC) which can decrease the ripples in electromagnetic torque and stator flux, like cascaded with PI regulator [43], parallel with two PI regulators [44] and Model Predictive DTC (MP-DTC) [45]-[48].

Though the traditional DTC is so much advantageous, it has also some disadvantages such as large torque and flux ripples. This leads to noise, vibrations, and power loss. SMC is an efficient method to deal with nonlinear uncertainties that operate very fast to switch any control quantity to obtain a faster and more robust dynamic response. The SMC is best suited in the case of the uncertain system model, parameter variance, and the presence of large disturbances [49].

1.3 Organization of the Thesis

The thesis is organized as follows:

- Chapter 1 introduces the preliminary idea of the thesis work. It includes my motivation for the work and the previous works related to my working area on this project.
- Chapter 2 consists of the detailed information regarding Permanent Magnet Synchronous Motor where construction, starting, parameters, etc. everything was discussed. Also, the advantages, disadvantages, applications, and comparisons with other machines were mentioned.
- Chapter 3 has the concept of a three-phase voltage source inverter with sufficient theory, necessary tables, and relevant diagrams which describe the switching operation properly.
- Direct Torque Control is discussed in chapter 4. It tells about the theory, advantages, disadvantages, and necessary formulas. Here, both classical and modified DTC were shown for both six sectors and twelve sector operations with sector selection diagram and relevant Look-up tables.
- Chapter 5 discussed the Sliding Mode Control Technique with formulas and diagrams where needed. This shows the ripple minimization techniques for both first-order and higher-order SMC. Also, the applications of SMC in practical fields were mentioned.
- Chapter 6 is the most important chapter where I showed the responses obtained from MATLAB for all the important parameters for all cases. I compared the responses with each other, mentioned the ripple percentages and observations from the results, and discussed the values for different cases.
- Chapter 7 is the conclusion of my thesis where I mentioned my contributions to project work and the future scopes that may come from my work.

CHAPTER 2

PERMANENT MAGNET SYNCHRONOUS MOTOR

2.1 Introduction

PMSM has a permanent magnet in the inductor in the rotor. It has a difference from the induction motor in only efficiency and speed. The rest is almost the same. PMSM has efficiency more than Induction Motor and it runs at synchronous speed. But it has the same stator design and same variable frequency drive. PMSM is selected in the practical field for its high-power operation and high torque output to serve high load torque [50].

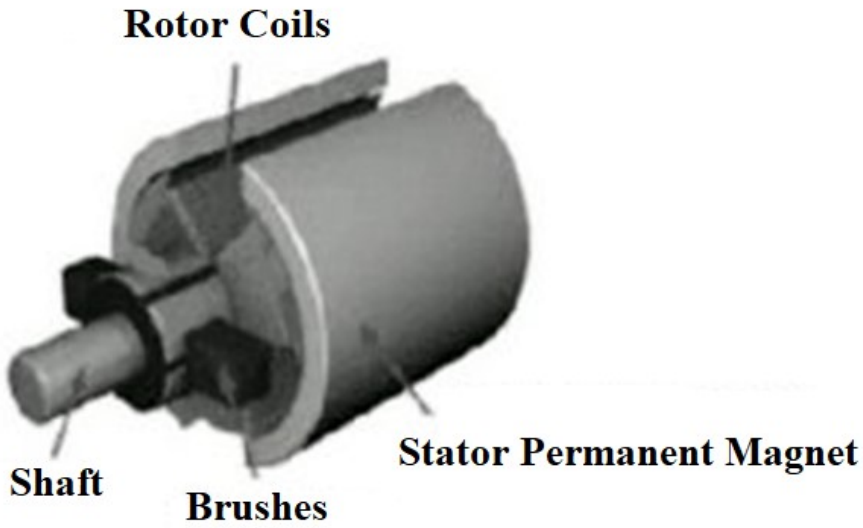

Fig. 2.1: Outside view of PMSM [50]

2.2 Construction

The stationary part in PMSM is the stator. The stator has distributed winding. The rotating part is the rotor. Here, the rotor has in-rotor construction, i.e., the rotor is located inside the stator. The rotor consists of a permanent magnet made of high permeable and high coercive material [50].

Here, in Fig. 2.2 and 2.3, the rotor is of non-salient pole type, i.e., the direct and quadrature axis inductances are the same. The permanent magnet is mounted on the outer surface of the rotor. Rotor poles are interlocked with the rotating magnetic field of the stator.

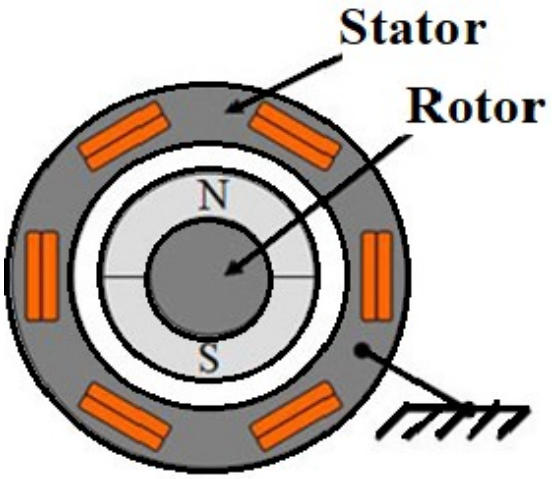

Fig 2.2: In-rotor construction [50]

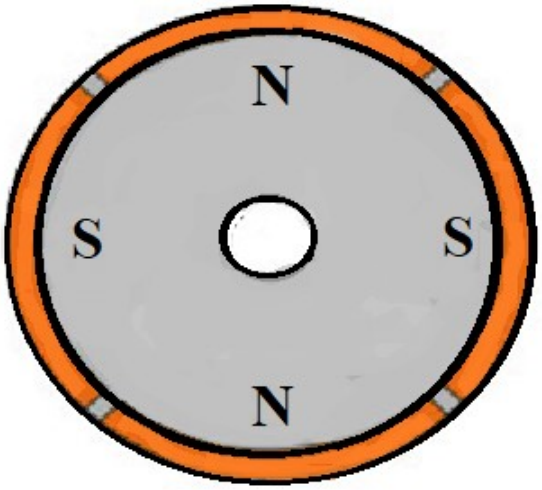

Fig. 2.3: Rotor of SPMSM [50]

Synchronous motors run at a constant speed in exact synchronism with the line frequency. According to the design of the rotor, construction, materials, and operation, synchronous motors are classified into the four categories which are given below -

1. Electromagnetically-excited Motors

2. PM Motors
3. Reluctance Motors
4. Hysteresis Motors

A cage winding is mostly mounted on salient-pole rotors in electromagnetically excited and PM motors for providing a start asynchronously and for damping the oscillations under transient conditions, which is called a damper [51].

A new prospect has been opened based on the development of rare-earth PM materials and power electronics which leads to the design, construction, and application of PMSM. The applications of static inverter-fed servo drives have been increasing day by day. Commonly, PM servo motors have nearly 15 kW of output power which rotates at 1500 RPM. Commercially, the drives with PMAC motors have ratings up to at least 746 kW. Recently, in large power synchronous motors rated, rare-earth PMs have also been used at more than 1 MW. Large PM motors have the uses in both high-speed drives (pumps and compressors) and low-speed drives (Ship propulsion) [51].

PMSMs are usually made with one of the following rotor configurations [51] mentioned below -

1. Classical rotor or Merrill's rotor (Salient poles, laminated pole shoed, and cage winding).
2. Interior-type PM rotor.
3. Surface-type PM rotor.
4. Inset-type PM rotor.
5. Rotor with buried magnets distributed symmetrically.
6. Rotor with buried magnets distributed asymmetrically.

2.2.1 Merrill's Rotor

F.W. Merrill patented the first fruitful manufacture of a PM rotor rated at high frequencies for small synchronous motors. This four-pole motor was similar to the two-pole motor. Between each of the magnet poles, there are deep narrow slots in the laminated external ring. We have to change the width of those narrow slots to change the leakage flux of the magnet. At starting and speed reversal, the armature flux passes through the laminated rings. Here, the narrow slots omit the magnet, so the alnico magnet is to be guarded against demagnetization. With the aid of an aluminum or zinc alloy sleeve, the magnet is mounted on the shaft. The thickness of the laminated rotor ring should be such that when the rotor and stator

are assembled, its magnetic flux density is approximately 1.5 T. In rotor teeth, magnetic flux density can be up to 2 T [51].

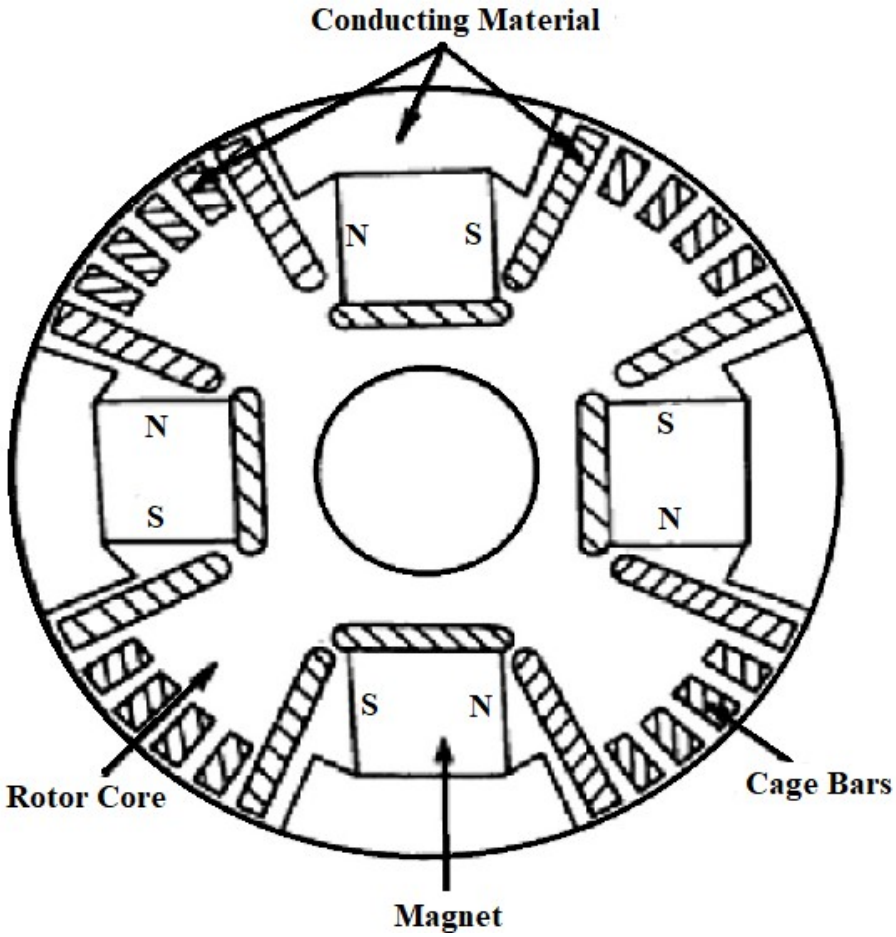

Fig. 2.4: Merrill's Rotor [51]

2.2.2 Interior-type PM Rotors

The rotor of the interior magnet has magnetized radially and poles are placed alternatively. On the open circuit, the air gap flux density is lesser compared to the magnetic flux density, because the pole area of the magnet is smaller than the pole area of the rotor surface. Since without crossing the magnets, the Q-axis magnetic flux can pass through the steel pole pieces, so the synchronous D-axis reactance is smaller than the Q-axis reactance. Against the centrifugal forces, the magnet is protected well. We can recommend such a design for high-speed motors at high frequencies [51].

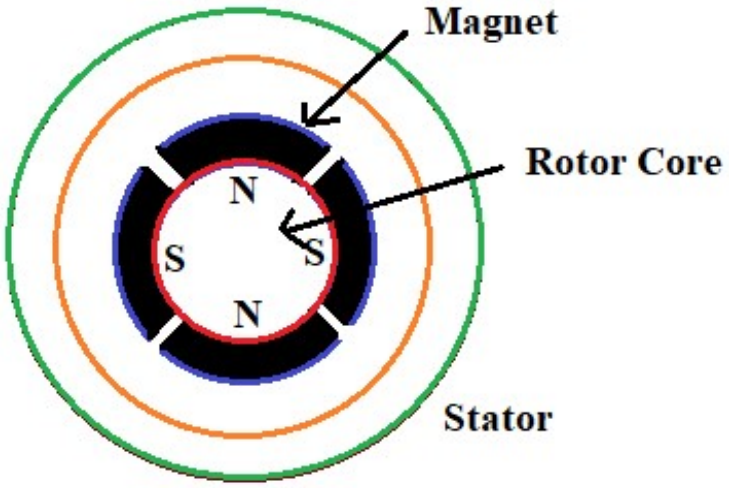

Fig. 2.5 Interior-type PM Rotor [51]

2.2.3 Surface PM Rotors

Sometimes, the magnetizations are done circumferentially or radially in the surface magnet motor. Sometimes, we use a nonferromagnetic cylinder externally with high conductivity. This can guard the magnets against the demagnetization effect of armature reaction and centrifugal forces. It provides an asynchronous starting torque that acts as a damper. If we use rare-earth magnets, the D- and Q-axis synchronous reactances are practically the same [51].

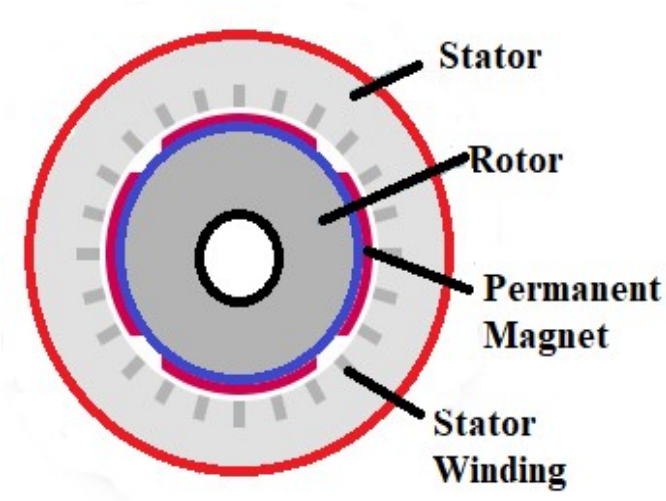

Fig. 2.6 Surface PM Rotor [51]

2.2.4 Inset-type PM Rotor

Magnetizations are done radially and embedded in shallow slots in the case of inset-type rotor magnets. The magnetic circuit of the rotor is laminated or made of solid steel. We require either a starting cage winding or an external nonferromagnetic cylinder in the first case. The Q-axis synchronous reactance is larger than the D-axis reactance. Generally, the EMF induced here is lower compared to the surface PM rotors [51].

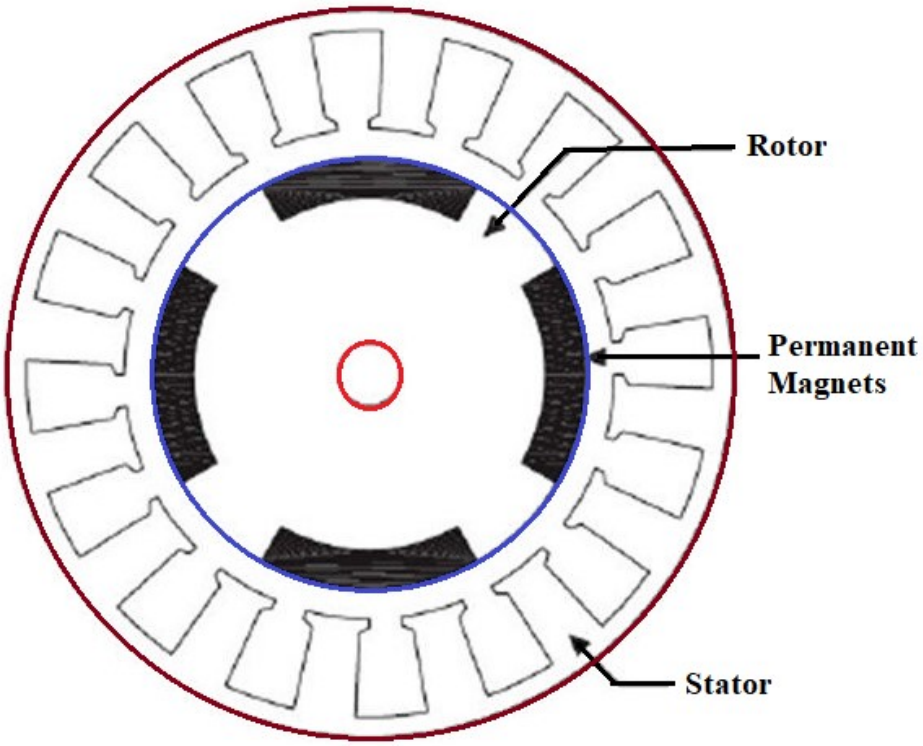

Fig. 2.7: Inset-type PM Rotor [51]

2.2.5 Buried PM Rotors

Magnetization is done circumferentially embedded in deep slots in the case of a buried-magnet rotor. For this, the height of the magnet is directed tangentially, i.e., along with the pole pitch. The coefficient of the effective pole arc is dependent on the width of the slot. The Q-axis synchronous reactance is greater compared to the D-axis reactance. In the rotor pole shoes with the aid of both a cage winding incorporated in slots or mild steel-made solid salient pole shoes, an asynchronous torque is produced at the start. Between the inner ends of the neighboring

magnet, we have to carefully select the width of the iron bridge. It is important to apply a nonferromagnetic shaft. A large portion of useless magnetic flux goes through the shaft with a ferromagnetic shaft. Between the rotor core and ferromagnetic shaft, a nonferromagnetic sleeve should be used. Or, with a nonferromagnetic shaft, a buried-magnet rotor should be equipped [51].

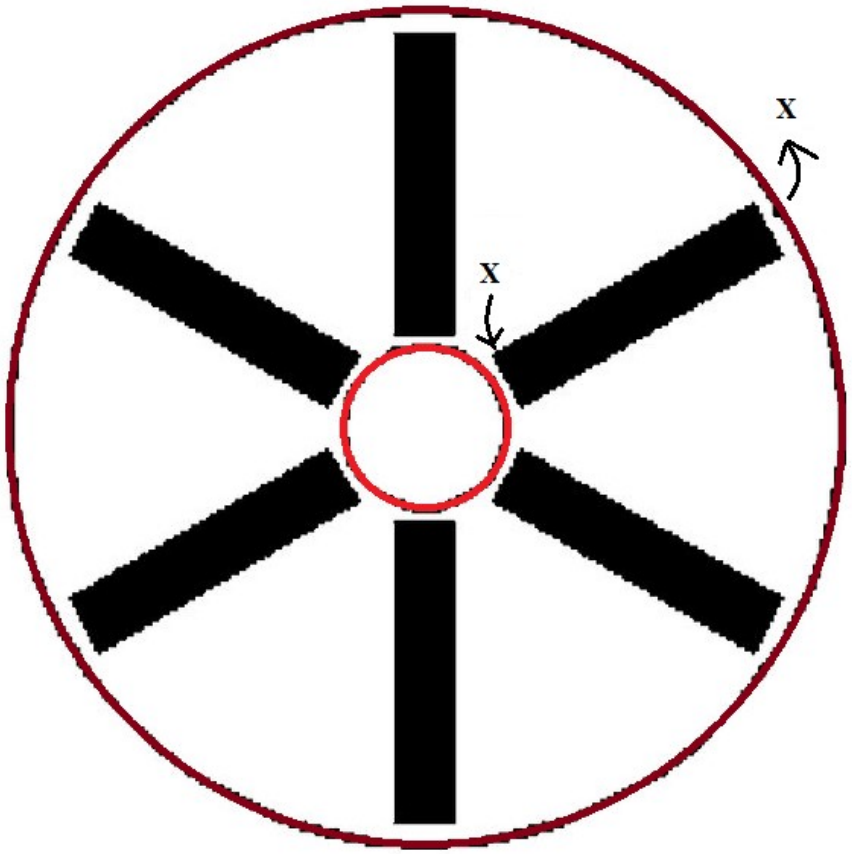

Fig. 2.8: Buried PM Rotor [51]

2.2.6 Comparison [51] of PMSM with Surface and Buried Magnets

Table 2.1: Comparison of PMSM with Surface and Buried Magnets [51]

Factors	Surface Magnets	Buried Magnets
Magnetic flux density at the air gap	Smaller	Greater
Motor construction	Simple	Relatively complicated
Armature reaction flux	Small	Higher
Protection of permanent magnet against armature fields	No	Yes
Eddy-current losses	Yes	No
Damper	Expensive	Less expensive
Winding	Cylinder or slotless	Cage

2.3 Operating Principle

The principle of operation of a synchronous motor is that the rotating magnetic field of the stator interacts with the constant magnetic field of the rotor. According to Ampere's law, the magnetic field of the rotor interacts with the synchronous alternating current of the stator windings that creates torque and forces the rotor to rotate [50].

2.4 Starting

The PMSM is similar to any synchronous motor. It is dependent on the rotating magnetic field generating electromotive force at the synchronous speed [52].

Synchronous motors are not self-starting motors above a certain size. It cannot instantly follow the rotation of the magnetic field of the stator due to the inertia of the rotor. However, at standstill, the synchronous motors do not produce any inherent average torque. So, without some supplemental mechanism, it cannot accelerate to synchronous speed [53].

For the starting of large synchronous motors with electromagnetic excitation, auxiliary induction motors are mostly used. This auxiliary starting motor is placed on the shaft of the synchronous motor so that it can be capable of reaching the synchronous speed at which time synchronizes with the power circuit. Using a smaller induction motor, the unexcited synchronous motor is accelerated to nearly synchronous speed. When the speed is close to the synchronous speed, the armature voltage is switched on first and secondly, the excitation voltage is switched on. Then, the synchronous motor is pulled into synchronism. But, under load, it is not possible to start the motor. This is one of the disadvantages of this method. So, it is not feasible to use the same rating of the auxiliary motor with the synchronous motor. This installation is very much expensive [51].

Between the air gaps, a magnetic field is created when a 3-phase supply energizes the stator winding. When the rotor field poles hold the rotating magnetic field, at synchronous speed, a torque is produced and the rotor starts rotating continuously [52].

The frequency of the voltage is applied to the motor efficiently which changes from the value tend to zero to the rated value. During the entire starting period, the motor runs synchronously. We commonly use Variable Voltage Variable Frequency (VVVF) solid-state inverters [51].

2.5 System Parameters [54]

1. Instantaneous voltage of A-B-C phase stator windings
2. Resistance of three-phase stator windings
3. Mutual inductance of three-phase stator windings
4. Mutual inductance between three-phase stator windings
5. Instantaneous current of three-phase stator windings
6. Induced rotating electromotive force of three-phase stator windings
7. Differential operator
8. Instantaneous current of two-phase static $\alpha\beta$-coordinates
9. Instantaneous current of DQ-axis
10. Instantaneous angle of DQ-phase
11. Magnetic-chain amplitude of DQ-axis current after an amplitude-invariant principal transformation
12. Equivalent winding inductance of stator DQ-axis

13. Magnetic chain of the rotor
14. Phase resistance of the stator
15. Voltage amplitude of DQ-axis
16. Electrical angular frequency of the rotor
17. Electromagnetic torque
18. Pole pairs
19. Rotational inertia moment
20. Load torques
21. Resistance coefficient
22. Motor powers
23. Viscous friction coefficient
24. Time

2.6 Nonlinearities [55] in PMSM

(a) Direct Axis Inductance
(b) Quadrature Axis Inductance
(c) Direct Axis Flux
(d) Quadrature Axis Flux
(e) Mutual Flux between two axes
(f) Torque (Coupling between current and flux)
(g) States (Coupling between current and angular frequency)

2.7 Basic Equations of PMSM

2.7.1 Park and Clarke Transformation [56]-[57]

PMSM is modeled best in the DQ reference frame for easy operation and calculation. But the supply voltage and currents are in a three-phase AC source. So, we need to transform the reference frame from ABC on the stator side to DQ on the rotor side and vice versa. Fig.2.4 demonstrates a conceptual cross-sectional view of a three-phase two-pole interior PMSM along with two reference frames.

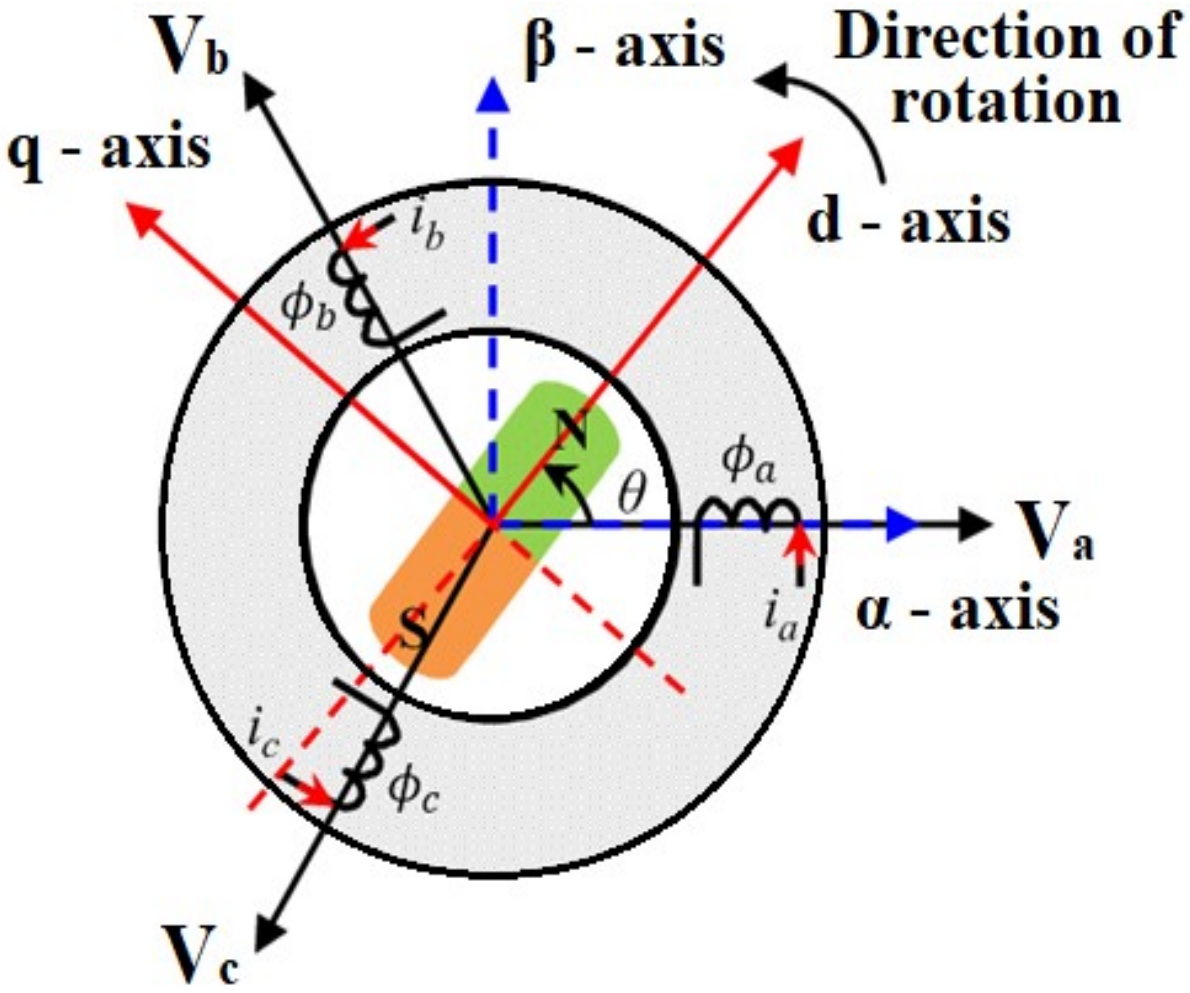

Fig. 2.9: Three-Phase and Two-Phase Winding Axis [56]

The Clarke transformation is used to transfer [**abc**] to [**αβ0**] frame as,

$$\mathbf{F_{\alpha\beta 0} = T_1\, F_{abc}}$$

The Park transformation is used to transfer [**αβ**] to [**dq**] frame as,

$$\mathbf{F_{dq0} = T_2\, F_{\alpha\beta 0} = T_2\, T_1\, F_{abc} = T\, F_{abc}}$$

So, we have, $\mathbf{T_1} = \frac{2}{3}\begin{bmatrix} 1 & -\frac{1}{2} & -\frac{1}{2} \\ 0 & \frac{\sqrt{3}}{2} & -\frac{\sqrt{3}}{2} \\ \frac{1}{2} & \frac{1}{2} & \frac{1}{2} \end{bmatrix}$ and $\mathbf{T_2} = \begin{bmatrix} \cos\theta & \sin\theta & 0 \\ -\sin\theta & \cos\theta & 0 \\ 0 & 0 & 1 \end{bmatrix}$

So, the transformation matrix [56]-[58] is

$$\mathbf{T} = \begin{bmatrix} \cos(\theta) & \cos(\theta - \frac{2\pi}{3}) & \cos(\theta + \frac{2\pi}{3}) \\ -\sin(\theta) & -\sin(\theta - \frac{2\pi}{3}) & -\sin(\theta + \frac{2\pi}{3}) \\ \frac{1}{3} & \frac{1}{3} & \frac{1}{3} \end{bmatrix}$$

So, the inverse transformation matrix [56]-[58] is

$$\mathbf{T^{-1}} = \begin{bmatrix} \cos(\theta) & -\sin(\theta) \\ \cos(\theta - \frac{2\pi}{3}) & -\sin(\theta - \frac{2\pi}{3}) \\ \cos(\theta + \frac{2\pi}{3}) & -\sin(\theta + \frac{2\pi}{3}) \end{bmatrix}$$

We consider the permanent magnet rotor produces magnetic flux towards the d-axis as ψ_r. The components of this rotor flux along stator a-phase, b-phase, and c-phase axes are $\psi_r \cos(\theta)$, $\psi_r \cos(\theta - \frac{2\pi}{3})$ and $\psi_r \cos(\theta + \frac{2\pi}{3})$ respectively.

Thus, phase flux linkages can be expressed as follows:

$$\psi_a = L_{aa} i_a + L_{ab} i_b + L_{ac} i_c + \psi_r \cos(\theta) \ldots\ldots (1)$$

$$\psi_b = L_{ba} i_a + L_{bb} i_b + L_{bc} i_c + \psi_r \cos(\theta - \tfrac{2\pi}{3}) \ldots\ldots (2)$$

$$\psi_c = L_{ca} i_a + L_{cb} i_b + L_{cc} i_c + \psi_r \cos(\theta + \tfrac{2\pi}{3}) \ldots\ldots (3)$$

Where, L_{kk} is the self-inductance of the k-th phase and L_{ij} is the mutual inductance of the i-th phase due to the j-th phase.

Considering the balanced mode of PMSM with symmetrical alignments of the inductances, we consider, $L_{kk} = L$ for $k = a, b$ or c and $L_{ij} = M$ for all i and j.

Moreover, in a balanced condition, the sum of the stator currents of each phase is equal to zero.

So, $\mathbf{i_a + i_b + i_c = 0}$**……. (4)**

This reveals the simplified the phase flux linkage equations lead as follows:

$$\boldsymbol{\psi_a = (L - M)i_a + \psi_r \cos(\theta)} \text{……. (5)}$$

$$\boldsymbol{\psi_b = (L - M)i_b + \psi_r \cos(\theta - \frac{2\pi}{3})} \text{……. (6)}$$

$$\boldsymbol{\psi_c = (L - M)i_c + \psi_r \cos(\theta + \frac{2\pi}{3})} \text{……. (7)}$$

Now, in the balanced mode of the stator, the stator phase voltages can be represented as

$$\boldsymbol{V_a = Rsi_a + \frac{d\psi_a}{dt}} \text{……. (8)}$$

$$\boldsymbol{V_b = Rsi_b + \frac{d\psi_b}{dt}} \text{……. (9)}$$

$$\boldsymbol{V_c = Rsi_c + \frac{d\psi_c}{dt}} \text{……. (10)}$$

Where, **Rs** represents the resistance of stator coil per phase.

If we consider, $[\mathbf{F_{abc}}] = [\mathbf{F_a\ F_b F_c}]^{\mathbf{T}}$, then the above set of equations can be written as,

$$\boldsymbol{[v_{abc}] = R[I]_{3\times3}\ [i_{abc}] + \frac{d}{dt}\ [\psi_{abc}]} \text{……. (11)}$$

Here, the expression of $[\boldsymbol{\psi_{abc}}]$ will be,

$$\boldsymbol{[\psi_{abc}] = (L - M)\ [I]_{3\times3}\ [i_{abc}] + \psi_r\ [A_{cos}]} \text{……. (12)}$$

Here, we have, $[\mathbf{A_{cos}}] = \begin{bmatrix} \cos(\theta) \\ \cos\left(\theta - \frac{2\pi}{3}\right) \\ \cos\left(\theta + \frac{2\pi}{3}\right) \end{bmatrix}$

The transformation of $[\boldsymbol{\psi_{abc}}]$ to $[\boldsymbol{\psi_{dq}}]$ reference frame will be,

$$\boldsymbol{[\psi_{dq}] = (L - M)\ [I]_{2\times2}\ [i_{dq}] + \psi_r \begin{bmatrix} 0 \\ 1 \end{bmatrix}} \text{……. (13)}$$

So, the frame $\boldsymbol{[V_{dq}]}$ can be as follows:

$$\boldsymbol{[V_{dq}] = R[I]_{2\times2}\ [i_{dq}] + T\frac{d}{dt}T^{-1}[\psi_{dq}]} \text{……. (14)}$$

Now, following simple calculus on matrix expressions in previous equations, we can get DQ-axis voltages as given below -

$$\boldsymbol{[V_{dq}] = R[I]_{2\times2}\ [i_{dq}] + (L - M)[I]_{2\times2}\frac{d}{dt}[i_{dq}] + \begin{bmatrix} 0 & -1 \\ 1 & 0 \end{bmatrix} \omega e\ [\psi_{dq}]} \text{……. (15)}$$

So, the equation of flux will be,

$$\boldsymbol{[\psi_{dq}] = (L - M)\ [I]_{2\times2}\ [i_{dq}] + \psi_r \begin{bmatrix} 0 \\ 1 \end{bmatrix}} \text{……. (16)}$$

So, equation **(16)** implies that,

$$\begin{bmatrix} 0 & -1 \\ 1 & 0 \end{bmatrix} \omega_e \ [\psi_{dq}] = \begin{bmatrix} -(L-M)\ \omega_e\ i_q \\ (L-M)\ \omega_e\ i_d + \omega_e\ \psi_r \end{bmatrix} \ldots\ldots. (17)$$

And, finally, from the previous equations, we obtain the equations of DQ-axis voltages shown below -

$$V_d = R\ i_d - (L-M)\omega_e\ i_q + (L-M)\frac{di_d}{dt} \ldots\ldots. (18)$$

$$V_q = R\ i_q + (L-M)\omega_e\ i_d + (L-M)\frac{di_q}{dt} + \omega_e\ \phi_r \ldots\ldots. (19)$$

Where, V_d = D-axis voltage, V_q = Q-axis voltage, i_d = D-axis current, i_q = Q-axis current, ω_e = electrical angular velocity of motor.

2.7.2 Electrical Equations

Considering, $L - M = L_d = L_q$ in balanced mode, we get the basic electrical equations [56] of PMSM are as below,

$$V_d = R_s\ i_d + L_d\ \frac{di_d}{dt} - \omega_e\ L_q\ i_q \ldots\ldots. (20)$$

$$V_q = R_s\ i_q + L_q\ \frac{di_q}{dt} + \omega_e\ L_d\ i_d + \omega_e\ \psi_r \ldots\ldots. (21)$$

Where, L_d = d-axis inductance, L_q = q-axis inductance. The two-axis inductances are kept equal for salient pole machines.

The electromagnetic torque [48], [56]-[57], [59]-[65],

$$T_e = \frac{3}{2}\ p\ [\psi_r\ i_q + (L_d - L_q) i_d\ i_q] = \frac{3}{2}\ p\ [\psi_d\ i_q - \psi_q\ i_d] \ldots\ldots. (22)$$

Where, p = no. of pair of poles, ψ_d = d-axis flux, ψ_q = q-axis flux.

So, the expression of DQ-axis fluxes [49] is,

$$[\psi_{dq}] = \begin{bmatrix} \psi_d \\ \psi_q \end{bmatrix} = \begin{bmatrix} L_d.\ i_d + \psi_r \\ L_q.\ I_q \end{bmatrix} \ldots\ldots. (23)$$

Stator flux [48], [57], [59],

$$\psi_s = \sqrt{\{(\psi_d)^2 + (\psi_q)^2\}} = \int (V_s - I_s\ R_s) dt \ldots\ldots. (24)$$

where, V_s = stator voltage, I_s = stator current.

And, flux angle,

$$\theta = \tan^{-1}\left(\frac{\psi_d}{\psi_q}\right) \ldots\ldots. (25)$$

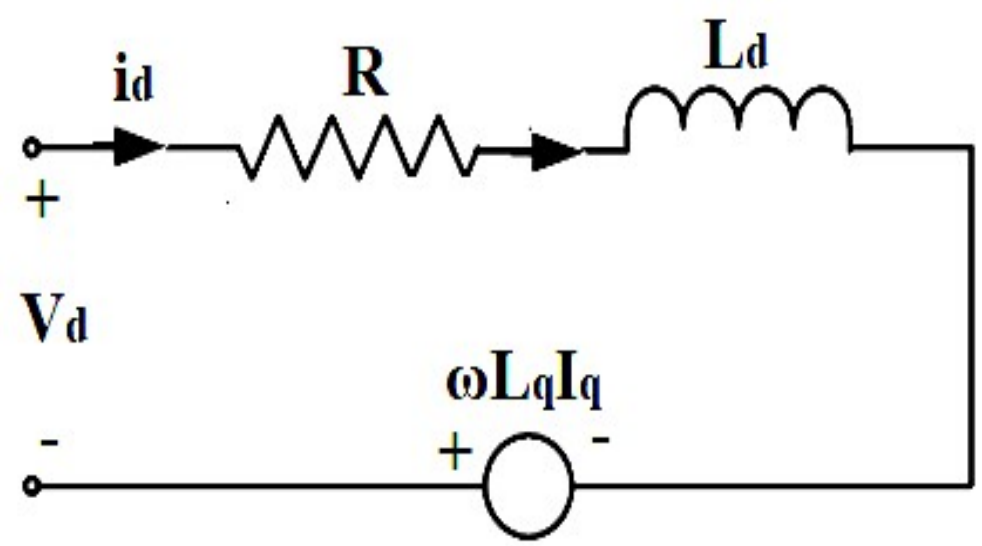

Fig. 2.10: D-axis Circuit of PMSM

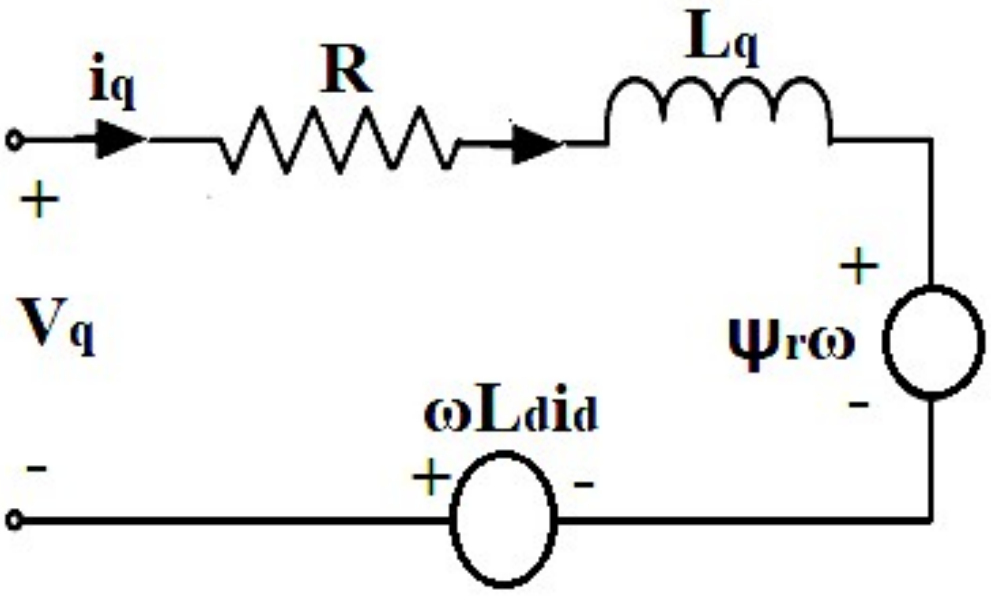

Fig. 2.11: Q-axis Circuit of PMSM

2.7.3 Mechanical Equations

The basic mechanical speed and angle equations [60] are –

$$\omega_e = -\frac{B}{J}\omega_e + \frac{p}{J}(T_e - T + T_{load}) \text{ and } \frac{d}{dt}(\theta) = \omega_e \ldots\ldots (26)$$

where, **B** = Viscous damping coefficient, **J** = Inertia Constant.

2.8 Advantages [52] of PMSM

PMSM provides higher efficiency at high speeds. It is also available in small sizes in different packages. It is highly efficient and reliable. Core loss is lesser than other motors.

PMSM is capable of maintaining full torque at low speeds. It gives smooth torque and dynamic performance. Harmonics are also fewer than BLDC. It creates lesser noise.

The maintenance and installation of PMSM are very easy than the induction motor. It has a better starting performance than the induction motor.

2.9 Disadvantages [52] of PMSM

PMSM is not self-starting, so, it is difficult to start the motor. Control of PMSM is more complex than the other machines.

The Nonferromagnetic air gap is higher, so the loss is also higher. It has a higher switching loss. These types of motors are very expensive compared to induction motors.

2.10 Comparison [51] of Synchronous Motor and Induction Motor

Table 2.2: Comparison of Synchronous Motor and Induction Motor [51]

Factors	Synchronous Motor	Induction Motor
Speed and load dependence	No	Load increases, speed decreases
Power factor	Adjustable	Constant
Nonferromagnetic air gap	Large (from a fraction of mm to a few centimeters)	small (from a fraction of mm to a maximum of 3 mm)
Torque	Directly proportional to the input voltage	Directly proportional to the square of the input voltage
Starting performance	Better	No much good
Cost	Expensive	Reasonable

2.11 Comparison [66] of BLDCM and PMSM

Table 2.3: Comparison of BLDCM and PMSM [66]

Factors	BLDCM	PMSM
Synchronous machine	Yes	Yes
Fed currents	DC	AC
Back emf	Trapezoidal	Sinusoidal
Position of the stator flux	60° Commutation each	Continuous alteration
ON phases at the same time	Only two	Able to be three
Commutation torque ripple	Yes	No
Harmonics	Low order inaudible range	Fewer because of sinusoidal excitation
Core losses	High because of harmonic content	Less
Switching losses	Less	High at the same switching frequency
Control algorithms	Relatively simple	Mathematically intensive
Control	Easier (six trapezoidal states)	More complex (continuous 3Ø sine wave)
Speed	Better at lower	Maximum achievable higher
Noisy	Higher	Low
Work with distributed winding	No	Yes, at low-cost
Efficiency	Lesser	Higher
Torque	Lower	Higher
Cost	Low	Higher
Current waveforms	Rectangular	Sinusoidal or quasi-sinusoidal

2.12 Applications [52] of PMSM

PMSMs are used in home appliances such as air conditioners, refrigerators, washing machines, AC compressors, etc. These are also used in industries like machine tools, data storage units, robotics, etc.

Transport systems also have PMSM applications such as control of traction, servo drives, aerospace, automotive electrical power steering, etc. Last but not the least, it is also used in large power systems to improve power.

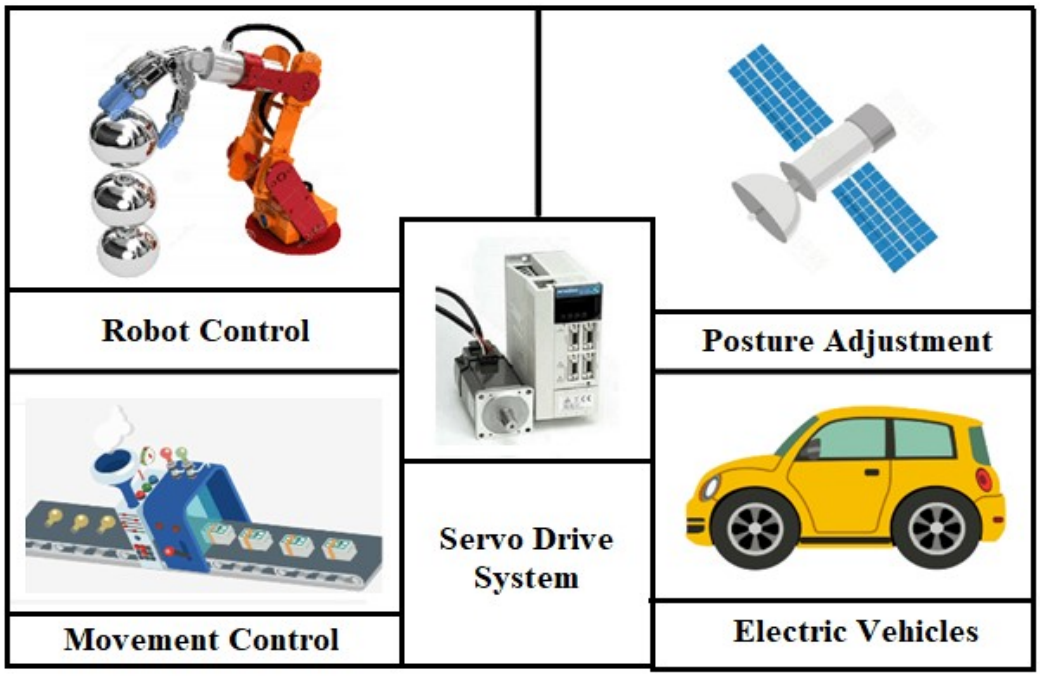

Fig. 2.12: Applications of PMSM [52]

2.13 Chapter Summary

In this chapter, the construction, operating principle, starting, and the internal and external structure of PMSM were shown. System parameters, nonlinearities, Clarke and Park transformation equations and matrices, and electrical and mechanical equations were provided in detail with the necessary diagram. Apart from that, the basic differences between BLDCM and PMSM were enlightened. Finally, the advantages, disadvantages, and different applications of PMSM are discussed.

CHAPTER 3

THREE-PHASE VOLTAGE SOURCE INVERTER

3.1 Introduction

The inverter is a DC to Variable AC converter. PMSM is a not self-starting machine. So, it has to be driven externally. Therefore, a three-phase voltage source inverter is best suited in this aspect. Here, we can also vary both the magnitude of the output voltage and the frequency of the input signal. MOSFET or IGBT are used in most of these as a power electronic switch for good switching response in high power applications. The three-phase inverter consists of six switches and one anti-parallel diode is used with each switch for a free-wheeling path for inductive load. Here, PMSM is an inductive load, so an anti-parallel diode is a must for good output response. Space Vector Modulation (SVM) or Space Vector Pulse Width Modulation (SVPWM) technique can be used for better output response and good control operation of PMSM. This technique is used to select the proper voltage vector applied in each switch for each time instant for different time durations and magnitudes. This technique is mandatory for Direct Torque Control (DTC) of PMSM. Presently, Look Up Table (LUT) is used in DTC for being an easier, advanced, and more efficient method of SVM. Detailed LUT technique will be discussed in upcoming chapters while discussing DTC. The inverter has both 180° and 120° of conduction mode. For 180° conduction, three switches are activated at a time and for 120° conduction, two switches are activated at a time. Here, for SVM or LUT, we need three switches to be activated at a time in the 180° conduction and this is a better operation compared to the 120° conduction [56]-[57].

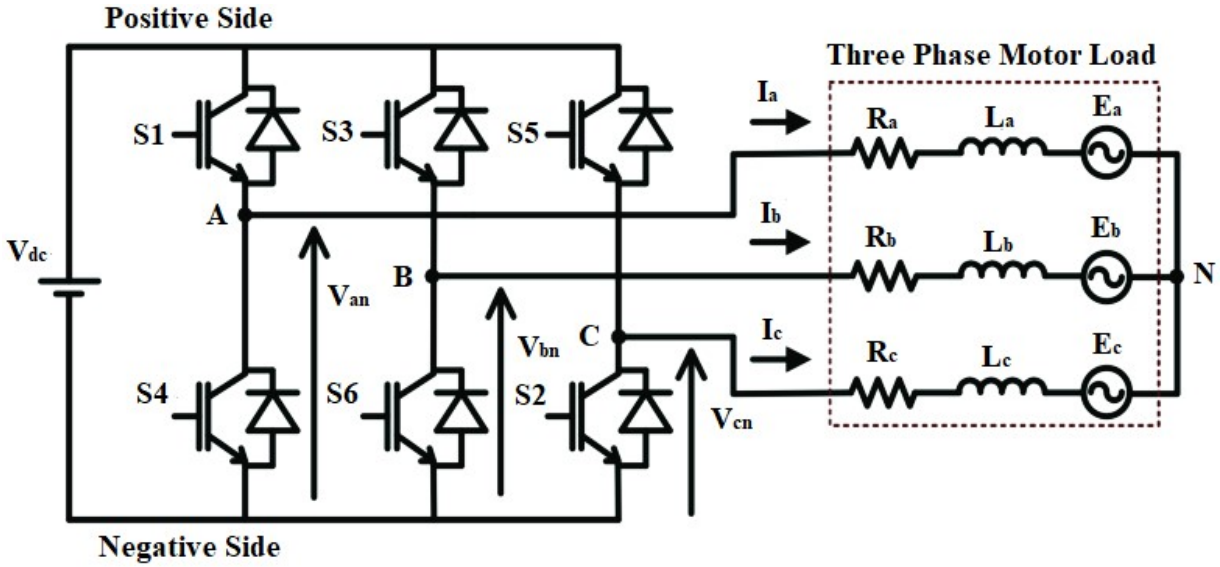

Fig. 3.1: Three-Phase Voltage Source Inverter with Balanced Three-Phase Motor Load [67]

3.2 Voltage Vector Selection

The voltage vector table is given below where we can know which switch should be "**ON**" or "**OFF**" every time instant for different voltage vectors. Here, "**1**" denotes the upper switch is conducting and "**0**" indicates the lower switch is conducting. This table is based on the anti-clockwise rotations of three phases [67].

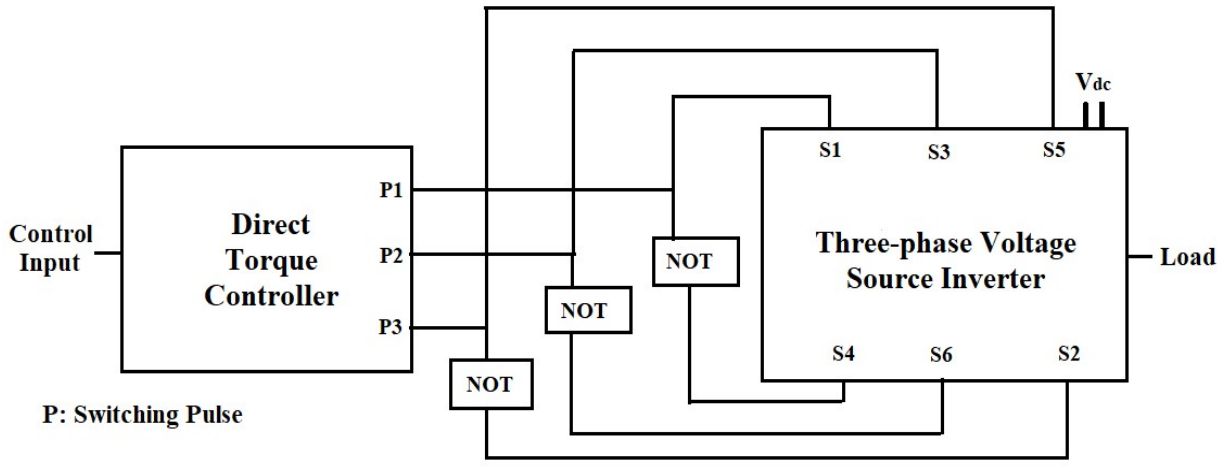

Fig. 3.2: Voltage Vector Selection of Three-phase Voltage Source Inverter by Direct Torque Controller

Table 3.1: Voltage Vector Selection Table of Voltage Source Inverter [67]

Voltage Vectors	S_1	S_2	S_3	S_4	S_5	S_6	V_a	V_b	V_c
V_0	0	1	0	1	0	1	0	0	0
V_1	1	1	0	0	0	1	$2V_{dc}/3$	$-V_{dc}/3$	$-V_{dc}/3$
V_2	1	1	1	0	0	0	$V_{dc}/3$	$V_{dc}/3$	$-2V_{dc}/3$
V_3	0	1	1	1	0	0	$-V_{dc}/3$	$2V_{dc}/3$	$-V_{dc}/3$
V_4	0	0	1	1	1	0	$-2V_{dc}/3$	$V_{dc}/3$	$V_{dc}/3$
V_5	0	0	0	1	1	1	$-V_{dc}/3$	$-V_{dc}/3$	$2V_{dc}/3$
V_6	1	0	0	0	1	1	$V_{dc}/3$	$-2V_{dc}/3$	$V_{dc}/3$
V_7	1	0	1	0	1	0	0	0	0

3.3 Circuit Diagrams for Different Voltage Vectors

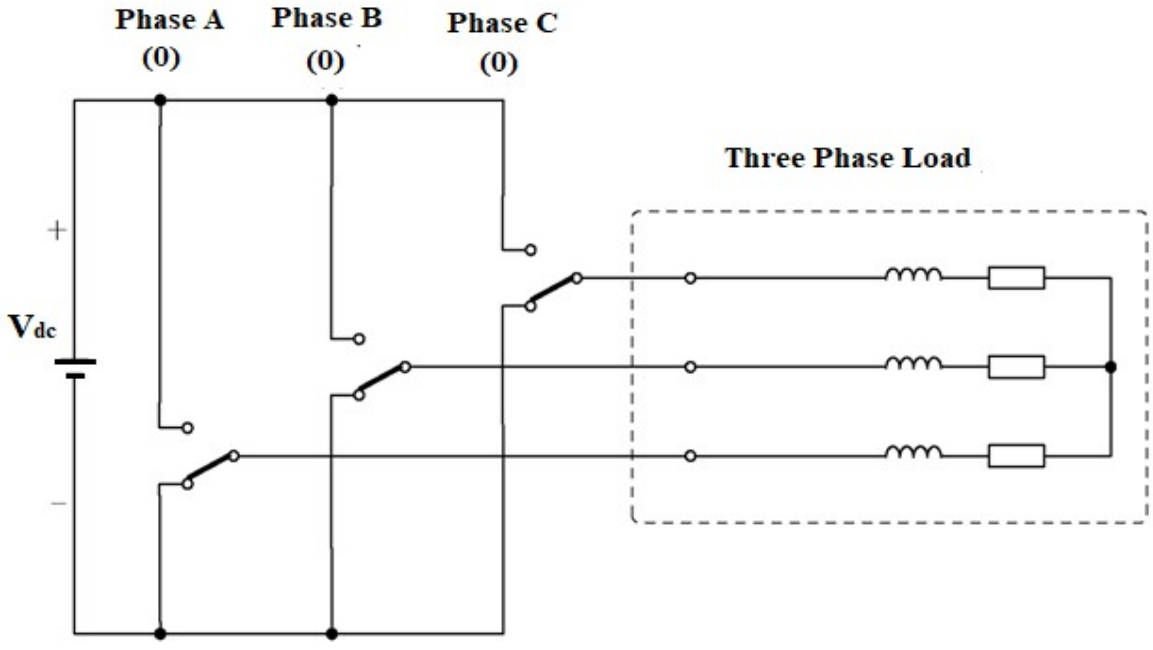

Fig. 3.3: Circuit Diagram for V0 (000) [67]

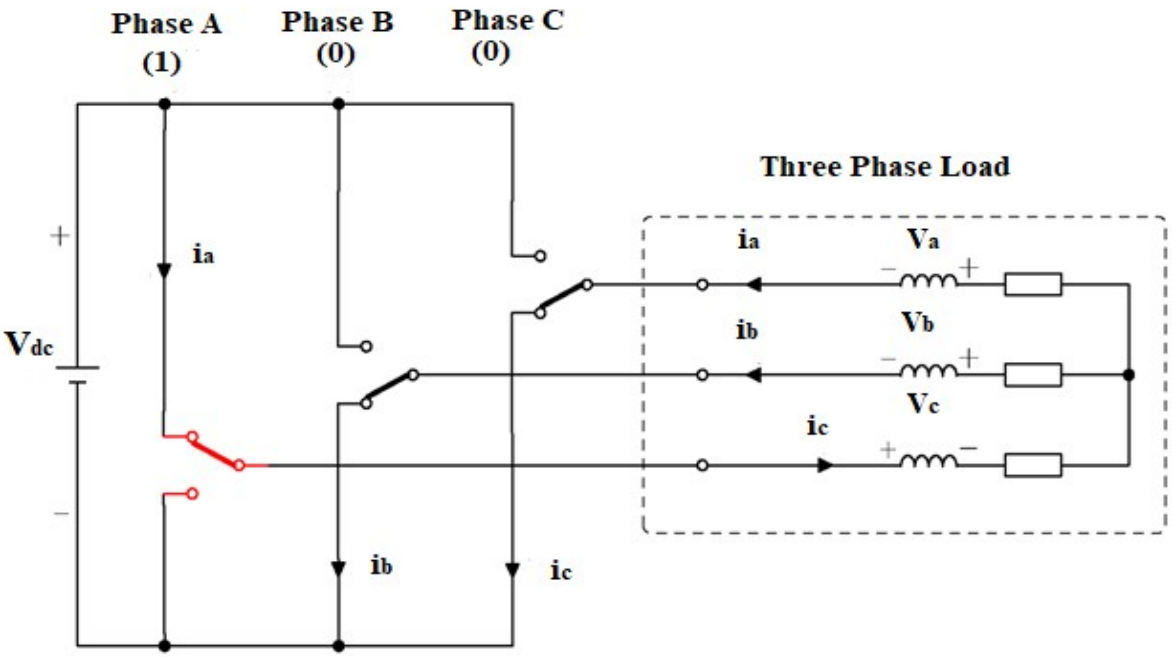

Fig. 3.4: Circuit Diagram for V1 (100) [67]

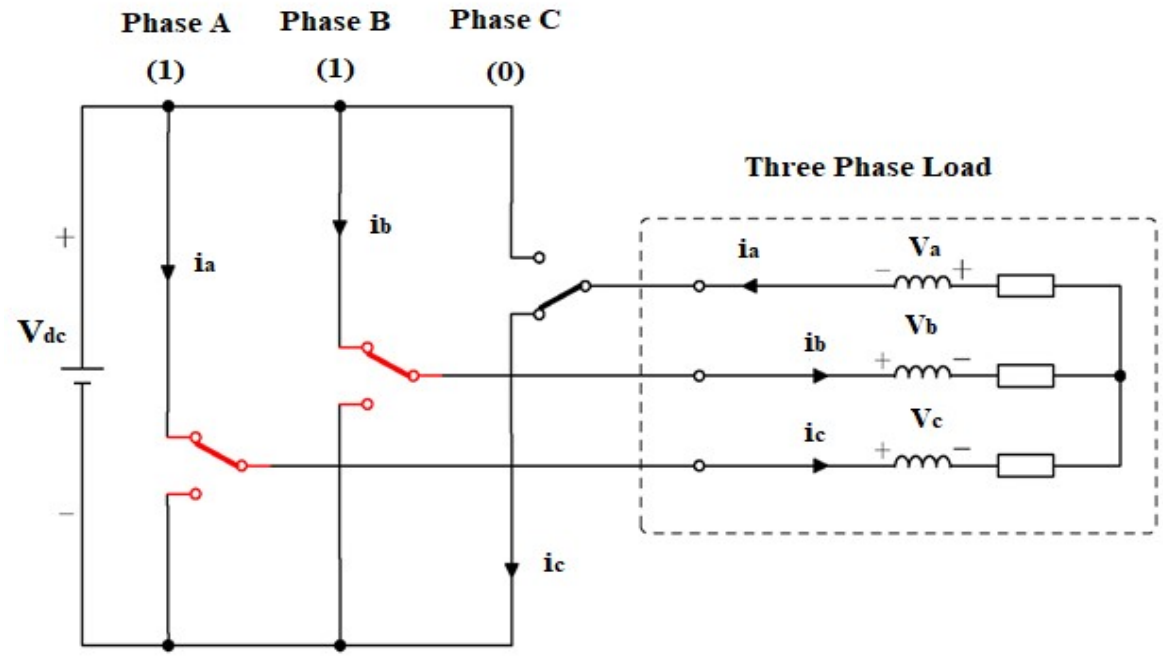

Fig. 3.5: Circuit Diagram for V2 (110) [67]

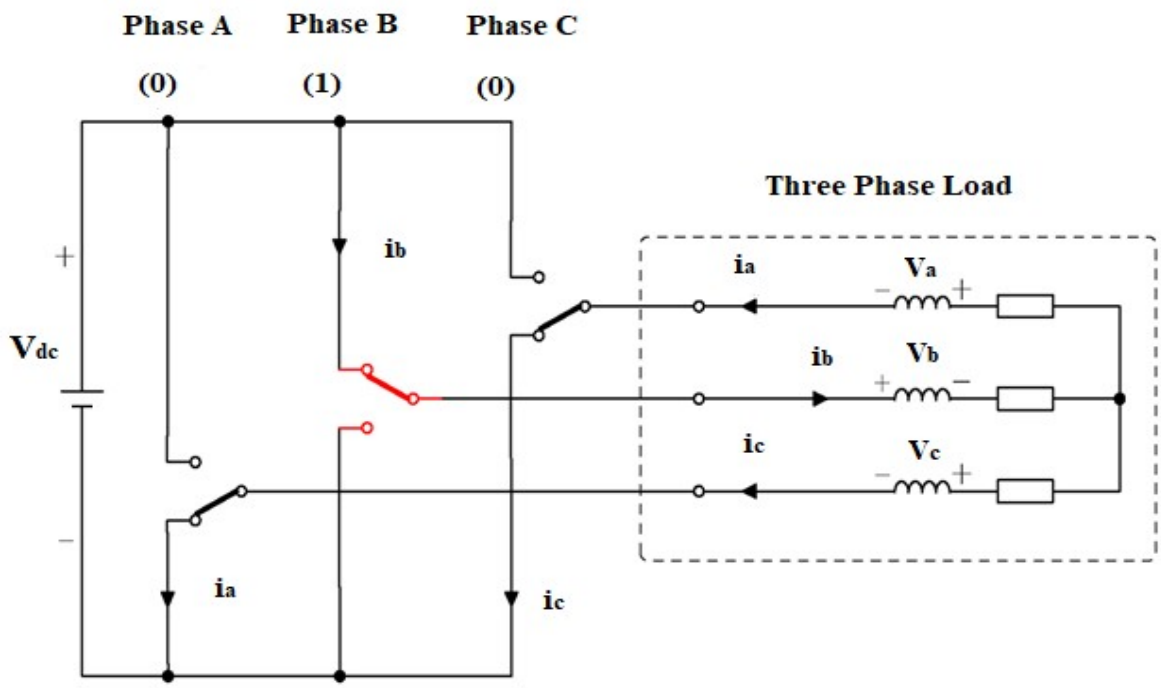

Fig. 3.6: Circuit Diagram for V3 (010) [67]

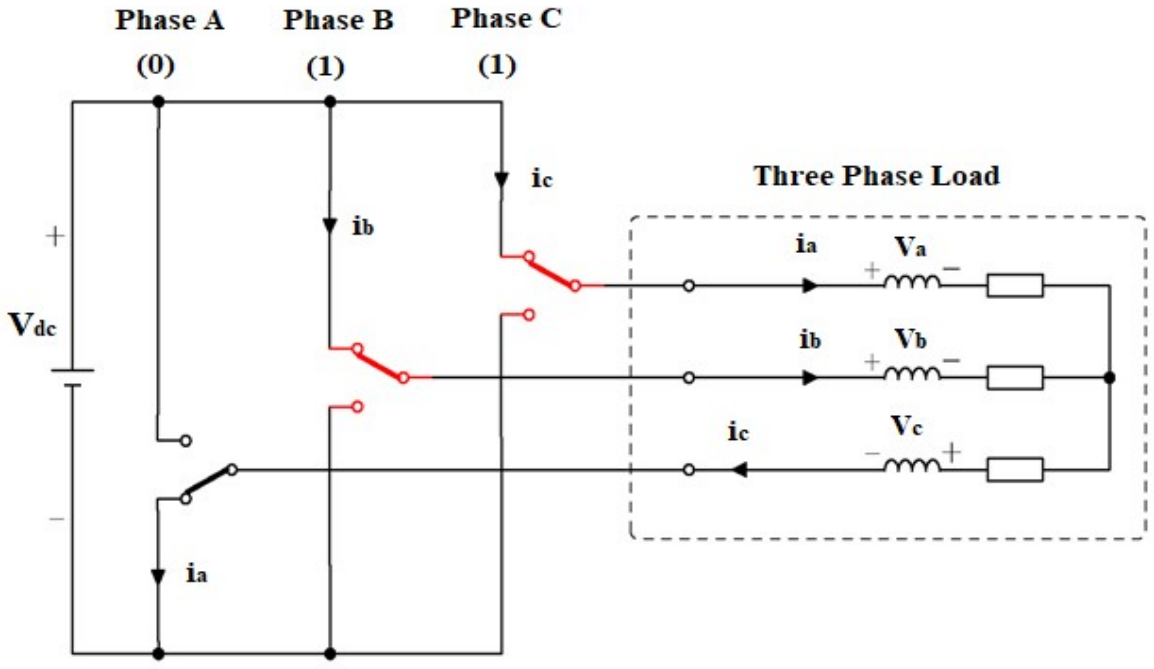

Fig. 3.7: Circuit Diagram for V4 (011) [67]

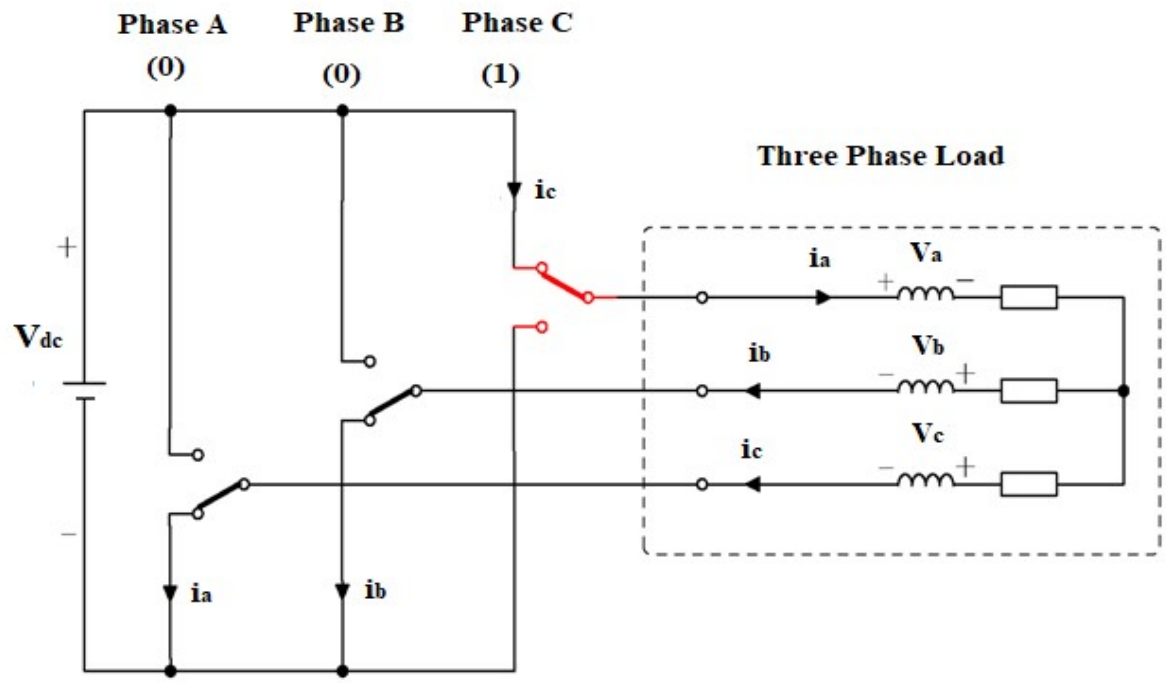

Fig. 3.8: Circuit Diagram for V5 (001) [67]

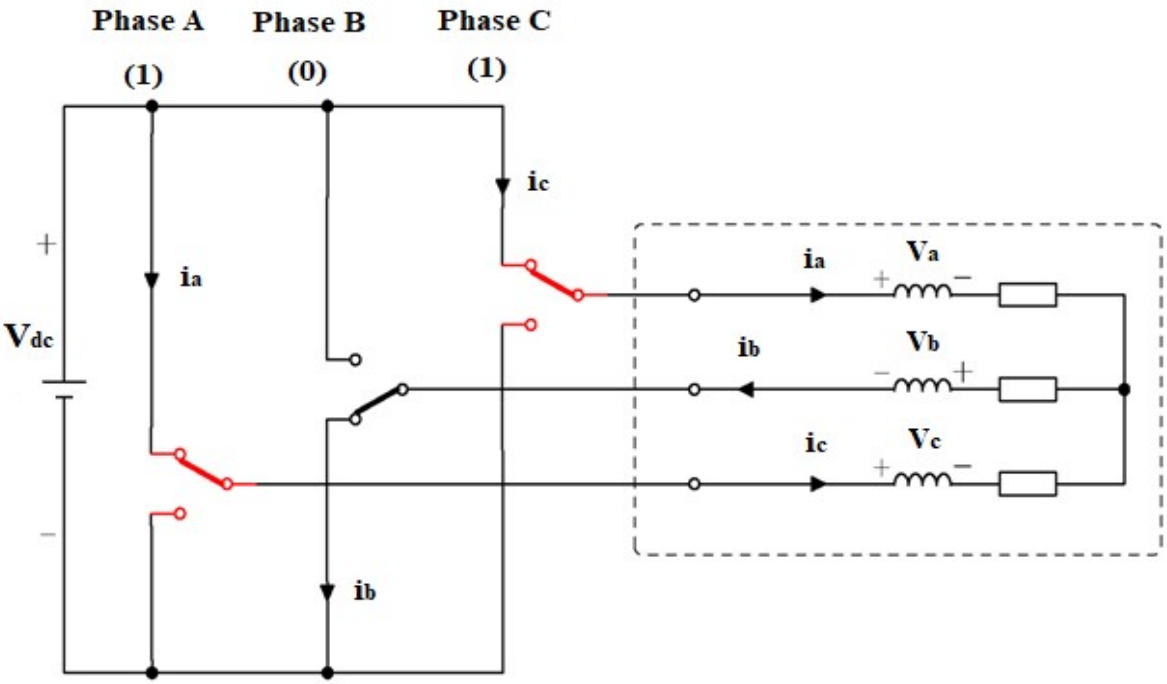

Fig. 3.9: Circuit Diagram for V6 (101) [67]

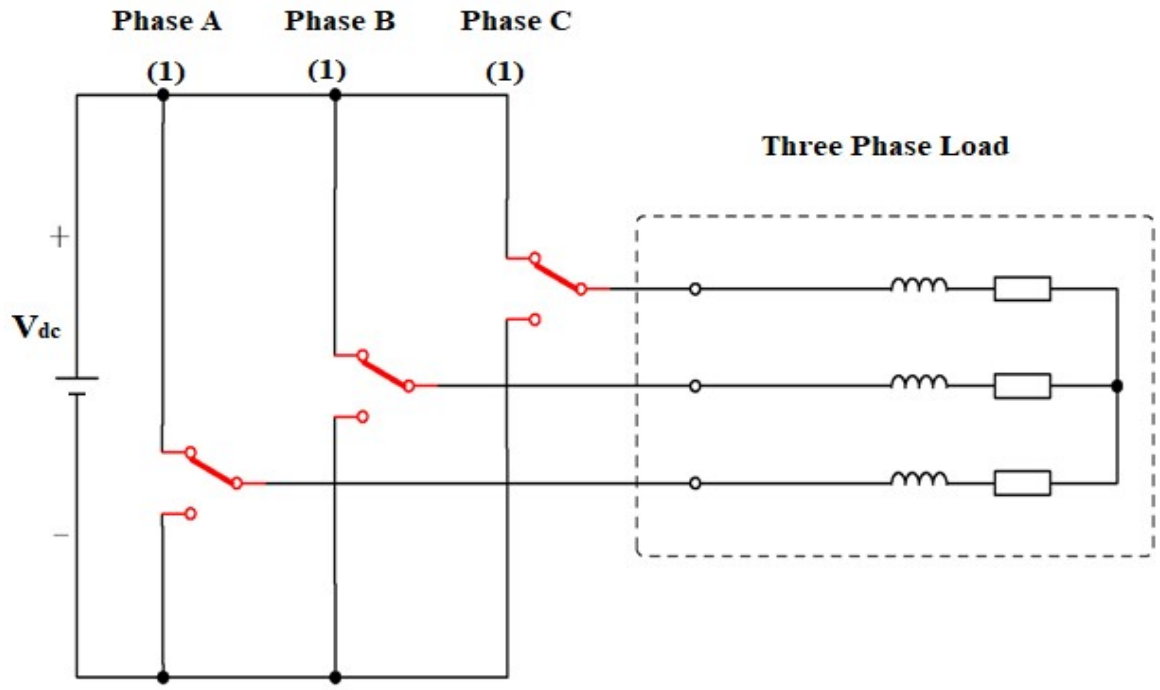

Fig. 3.10: Circuit Diagram for V7 (111) [67]

3.4 Chapter Summary

In this chapter, the basic concept of a three-phase voltage source inverter was discussed with a relevant circuit diagram. Then, the switching sequence of different voltage vectors and voltage values for each phase were provided in a table. Then, the equivalent circuit diagrams for different switching sequences of different voltages vectors were shown.

CHAPTER 4

DIRECT TORQUE CONTROL

4.1 History

The basic history behind Direct Torque Control is a little bit longer. There are several speed control techniques of PMSM including this. These techniques are of two types. One is scalar control and another is vector control. The scalar control scheme is easier but its performance is not up to the mark as the researchers expect. So, vector control techniques were applied for better performance. This is also of two types. One is using a position sensor and the other is without a position sensor. Using a sensor, the rotor detection is easier, but it increases the complexity and cost of the system. So, the estimation method was introduced, i.e., the speed is estimated through other parameters. Later, Field Oriented Control (FOC) was introduced where the flux is used to control the frequency which ultimately controls the speed. There is neither any need to use any sensor nor any need to estimate the speed. The speed is easily controlled using the flux. Next, the Direct Torque Control (DTC) was introduced where using either torque or flux or both torque and flux, the frequency can be controlled which controls the speed ultimately. Here also, position sensor and speed estimation are not required. We only estimate the torque and flux by using voltage and current. We can either calculate the switching time or we can take the e help of the Look-Up Table (LUT) to select the voltage vector applied to the inverter. This control technique is so much advantageous as it has a wide range of control operations. The only disadvantage is the production of torque, flux, and current ripple which can be easily eliminated by other controllers. This does not affect the system much [68]-[70].

4.2 Introduction

Presently, so many researchers are working with Direct Torque Control (DTC) as it has simple control operation, faster torque response, and outstanding dynamic performance to change in load. DTC-based PMSM drive system becomes very much famous in the field of AC

Electric Drives because it has a smooth control operation using faster torque response and stator flux which can be realized very easily. DTC takes the voltage and current information from the system and calculates torque and flux value. Then, it compares the estimated value with the reference value, Next, depending on the requirement of increasing or decreasing the torque or flux, it selects the voltage vector for the inverter switches to minimize the error for every instant using the hysteresis controller. DTC has a simple control structure so that it can obtain a faster dynamic response [68]-[70].

But DTC has to witness several noticeable issues such as current and torque ripples, variable switching frequency, and high sampling requirements during implementation in the discrete domain. Additionally, the voltage vector is used in restricted ways which usually affects the accuracy of torque control. The torque ripple magnitude is dependent on the DC-link voltage magnitude and the operating status of PMSM, and the control sample time. A very small control sample time must be needed to decrease the ripples which causes the increment of the switching loss. Additionally, it is hard to originally implement a very high-performance processor to achieve a faster sampling time of control [61].

4.3 Main Features [57]

The main feature of DTC is that it controls the torque and stator flux directly by controlling the switching frequency of the inverter. But it controls the stator currents and voltages indirectly.

Stator fluxes and stator currents are approximately sinusoidal. Also, the rotor may be locked due to the high dynamic performance.

4.4 Advantages [57]

The main advantage of DTC is that coordinate transformation is not required here. Also, the torque response time is minimum which is even better than the vector controllers.

Apart from that, the voltage modulator block is absent, as well as other controllers like PID for flux and torque are also absent.

4.5 Disadvantages [57]

Torque and flux estimators are required which implies the parameters identification consequently. Torque and flux ripples are present inherently.

DTC may create problems at the start. So, we need another controller to avoid this issue.

4.6 Control Action [57]

The required stator flux is imposed to select the best suited Voltage Source Inverter (VSI) state. For simplicity, we can ignore the voltage drops across the resistances. So, the voltage of the stator must be directly proportional to the stator flux as shown in the equation below -

$$\frac{d\psi s}{dt} = V_s$$

$$\text{Or, } \Delta\psi_s = V_s \, \Delta t \ldots\ldots \text{ (27)}$$

We can achieve the decoupled control of the modulus of the stator flux and the torque by working on the tangential and radial components respectively of the space vector of the stator flux linkage in its path. The equation [49] for electromagnetic torque is

$$T_e = \frac{3}{2}\frac{p}{L_s} |\psi_s| |\psi_r| \sin(\delta)$$

$$\text{Or, } \Delta T_e = \frac{3}{2}\frac{p}{L_s} |\psi_s| |\psi_r| (\Delta\delta) \sin(\Delta\delta) \ldots\ldots \text{ (28)}$$

These two parameters are directly proportional to the same voltage space vector components in the same direction.

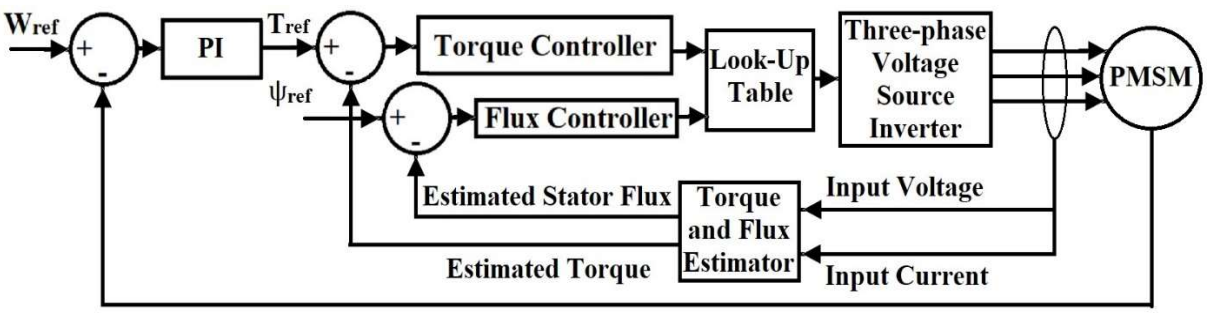

Fig. 4.1: Block Diagram of PI Controller based Direct Torque Control of Permanent Magnet Synchronous Motor Drive System

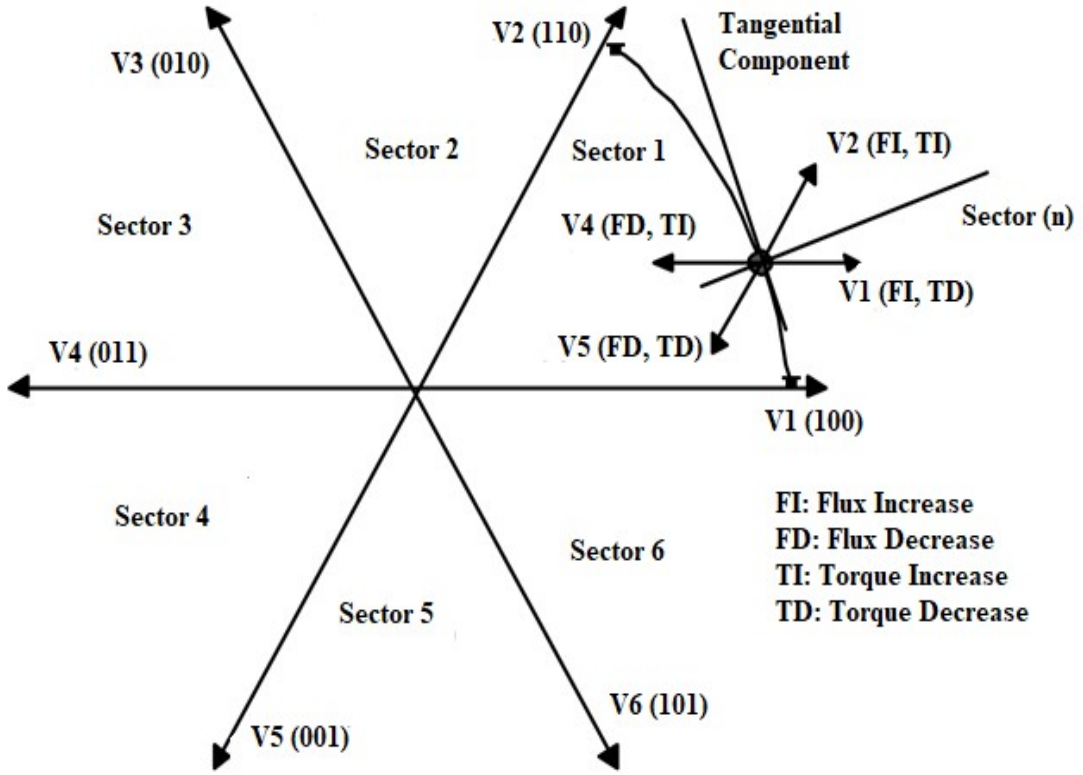

Fig. 4.2: Stator flux vector locus and different possible switching voltage vectors for Classical DTC [57]

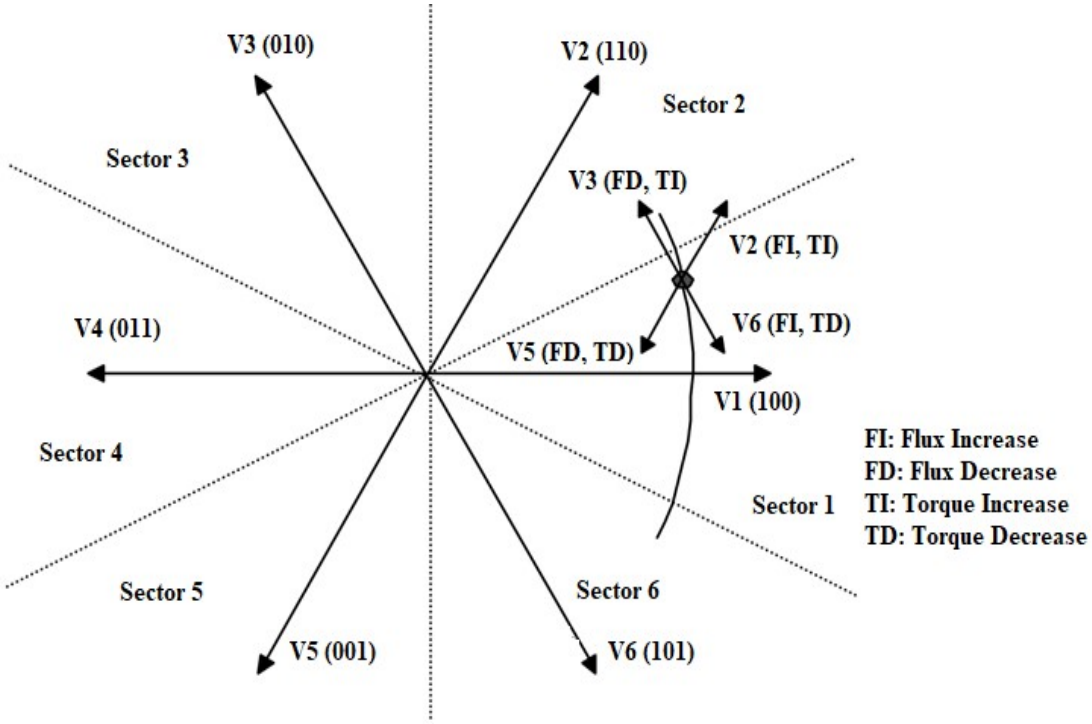

Fig. 4.3: Stator flux vector locus and different possible switching voltage vectors for six sectors Modified DTC [49], [71]

Figure 4.2 and 4.3 show the probable dynamic stator flux locus and its different variations depending on the selected VSI states. The possible global locus is split into six different sectors separated by a discontinuous line. In classical DTC, the sectors were on either side of the voltage vector. But, in modified DTC, the sectors are present on both sides of the voltage vector.

Hysteresis Control is applied here. Torque and Flux limits are set as a Hysteresis loop and then depending on the value of torque and flux, the corresponding voltage vector is selected based on the Look-Up Table for Direct Torque Control [57].

The sectors of the space vector of the stator flux are denoted from S_1 to S_6. After the hysteresis control block, stator flux modulus error can take just two values. Torque error after the hysteresis control block can take three different values. The zero voltage vectors V_0 and V_7 are chosen when the torque error is within the specified hysteresis limits and must be kept constant [57].

The calculated values of Flux and Electromagnetic Torque are sent to hysteresis control blocks to calculate the error signal for torque and flux. Based on the values, voltage vectors are selected to give pulse to the electronic switches of the inverter. No sensor is used here.

The Look-Up Tables for different Direct Torque Control methods are given below which consist of the voltage vectors for different sectors for different toque and flux conditions.

Table 4.1: Look Up Table for Classical Direct Torque Control (Increase = 1, Constant = 0, Decrease = -1) [57]

H_ψ	H_{Te}	S_1	S_2	S_3	S_4	S_5	S_6
1	**1**	V_2	V_3	V_4	V_5	V_6	V_1
	0	V_0	V_7	V_0	V_7	V_0	V_7
	-1	V_1	V_2	V_3	V_4	V_5	V_6
-1	**1**	V_4	V_5	V_6	V_1	V_2	V_3
	0	V_7	V_0	V_7	V_0	V_7	V_0
	-1	V_5	V_6	V_1	V_2	V_3	V_4

Table 4.2: Look Up Table for six sectors Modified Direct Torque Control (Increase = 1, Constant = 0, Decrease = -1) [49], [71]

H_ψ	H_{Te}	S_1	S_2	S_3	S_4	S_5	S_6
1	**1**	V_2	V_3	V_4	V_5	V_6	V_1
	0	V_7	V_0	V_7	V_0	V_7	V_0
	-1	V_6	V_1	V_2	V_3	V_4	V_5
-1	**1**	V_3	V_4	V_5	V_6	V_1	V_2
	0	V_0	V_7	V_0	V_7	V_0	V_7
	-1	V_5	V_6	V_1	V_2	V_3	V_4

There is another DTC method available, i.e., twelve sector DTC where the sectors are divided into two parts for better control operation which is shown in figure 4.3. However, it must be presented the concept of a small torque increase as a substitute for a torque increase, mainly because the tangential voltage vector component is very small and subsequently its torque variation will be small as well.

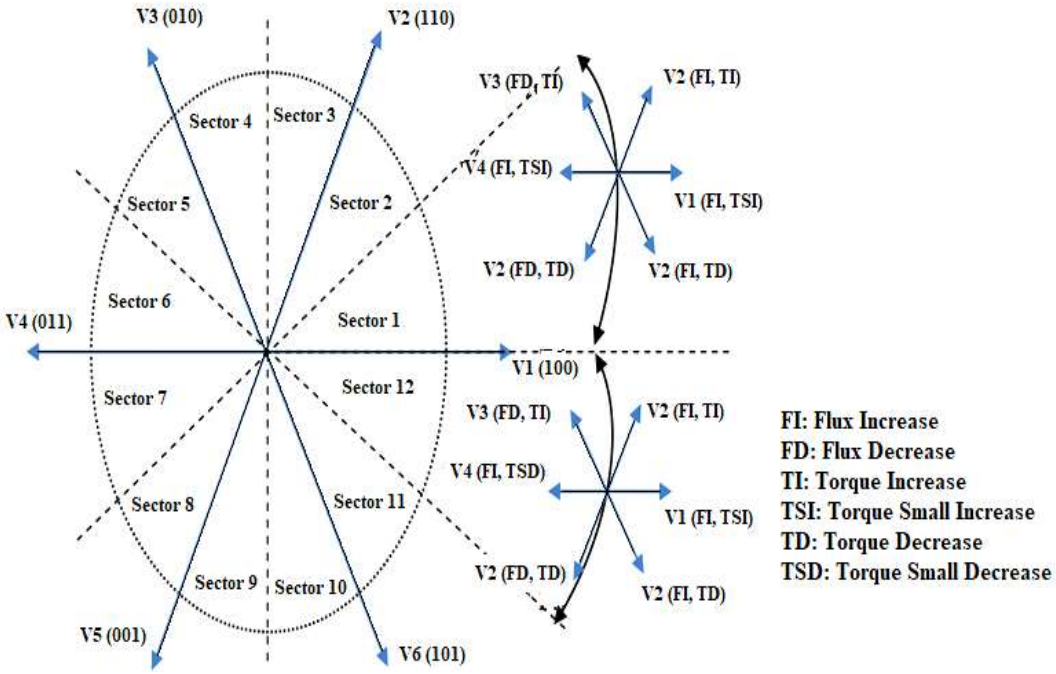

Fig. 4.4: Stator flux vector locus and different possible switching voltage vectors for twelve sectors Modified DTC [72]

Table 4.3: Switching Table of twelve sectors DTC [72]

		Augmentation	Diminution
S_{12}	Flux	V_1, V_2, V_6	V_3, V_4, V_5
	Torque	V_1, V_2, V_3	V_4, V_5, V_6
S_1	Flux	V_1, V_2, V_6	V_3, V_4, V_5
	Torque	V_2, V_2, V_4	V_5, V_6, V_1

Table 4.4: Look Up Table for twelve sectors Modified Direct Torque Control (FI: H = 1, FD: H = 0, TI: H = 2, TSI: H = 1, TSD: H = -1, TD: H = -2) [72]

H_ψ	H_{Te}	S_1	S_2	S_3	S_4	S_5	S_6	S_7	S_8	S_9	S_{10}	S_{11}	S_{12}
1	2	V_2	V_3	V_3	V_4	V_4	V_5	V_5	V_6	V_6	V_1	V_1	V_2
	1	V_2	V_2	V_3	V_3	V_4	V_4	V_5	V_5	V_6	V_6	V_1	V_1
	-1	V_1	V_1	V_2	V_2	V_3	V_3	V_4	V_4	V_5	V_5	V_6	V_6
	-2	V_6	V_1	V_1	V_2	V_2	V_3	V_3	V_4	V_4	V_5	V_5	V_6
0	2	V_3	V_4	V_4	V_5	V_5	V_6	V_6	V_1	V_1	V_2	V_2	V_3
	1	V_4	V_4	V_5	V_5	V_6	V_6	V_1	V_1	V_2	V_2	V_3	V_3
	-1	V_7	V_5	V_0	V_6	V_7	V_1	V_0	V_2	V_7	V_3	V_0	V_4
	-2	V_5	V_6	V_6	V_1	V_1	V_2	V_2	V_3	V_3	V_4	V_4	V_5

4.7 Chapter Summary

In this chapter, different DTC methods are discussed with necessary control action and relevant formulas, and a system diagram. The concepts of a selection of sectors and their Look-Up tables for classical, modified, and twelve sector DTCs were provided in detail.

CHAPTER 5

SLIDING MODE CONTROL

5.1 Basic Principle

Sliding mode control (SMC) is a nonlinear control method that has the noticeable properties of robustness, accuracy, easy tuning, and easy realization. SMC is designed to drive the total system states on sliding surfaces in the state space. Once we can reach the sliding surface, SMC keeps the states in the close neighborhood of that surface. Meanwhile, SMC is a bipartite controller scheme. The first part consists of the design of that surface so that the sliding motion fulfills design specifications. The second part consists of the selection of a control law as it can make the switching surface convincing to the state of the system [73].

The SMC method has two important advantages. The first one is the dynamic conduct of the system which may be fitted by the particular selection of the sliding function. The second one is the closed-loop response which becomes oblivious to some uncertainties particularly. The principle of SMC encompasses model parameter uncertainties, disturbances, and nonlinearities that are circumscribed. Practically, SMC can allow for controlling nonlinear processes with the presence of external disturbances and heavy model uncertainties up to a certain limit [74]-[75].

5.2 Simple Description [76]-[77]

Consider the nonlinear SISO system

$$\mathbf{X} = \mathbf{f}(\mathbf{x}, \mathbf{t}) + \mathbf{g}(\mathbf{x}, \mathbf{t})\mathbf{u} \ldots\ldots. \textbf{(29)}$$

$$\mathbf{Y} = \mathbf{h}(\mathbf{x}, \mathbf{t}) \ldots\ldots. \textbf{(30)}$$

Here, u and y indicate the scalar input and output variable, and the $\mathbf{x} \in \mathbf{R^n}$ vector represents the state vector.

The objective of the control technique is to lead the output variable y to follow a desired profile of $\mathbf{y_{DES}}$ so that it is needed that after a transient of acceptable duration, the output error variable $\mathbf{e = y\text{-}y_{DES}}$ tends to some small vicinity of zero.

As we know, SMC consists of two phases:

Phase 1: Design of the Sliding Surface

Phase 2: Design of the Control Input

The first phase defines a precise scalar function of the system state given below -

$$\boldsymbol{\sigma}\,(\mathbf{x}): \mathbf{R^n} \rightarrow \mathbf{R} \ldots\ldots. \mathbf{(31)}$$

Sometimes, the sliding surface is dependent on the tracking error, e_y together with a certain number of its differentials,

$$\boldsymbol{\sigma} = \boldsymbol{\sigma}\,(\mathbf{e}, \dot{\mathbf{e}}, \ldots.., \mathbf{e^{(k)}}) \ldots\ldots. \mathbf{(32)}$$

The function $\boldsymbol{\sigma}$ should be elected in such a way that its disappearing factor, $\boldsymbol{\sigma} = \mathbf{0}$, can reach such a "stable" differential equation as if any of the solutions $\mathbf{e_y(t)}$ can tend to zero easily. A usual form for the sliding surface is provided below, which is dependent on just a single scalar parameter, **p**.

$$\boldsymbol{\sigma} = \left(\frac{\mathbf{d}}{\mathbf{dt}} + \mathbf{p}\right)^{\mathbf{k}} \mathbf{e} \ldots\ldots. \mathbf{(33)}$$

$$\mathbf{k = 1,}\ \boldsymbol{\sigma} = \dot{\mathbf{e}} + \mathbf{pe} \ldots\ldots. \mathbf{(34)}$$

$$\mathbf{k = 2,}\ \boldsymbol{\sigma} = \ddot{\mathbf{e}} + \mathbf{2p\dot{e} + p^2 e} \ldots\ldots. \mathbf{(35)}$$

The most typical selection of the sliding manifold is a linear sequence of the types below-

$$\boldsymbol{\sigma} = \dot{\mathbf{e}} + \mathbf{c_0 e} \ldots\ldots. \mathbf{(36)}$$

$$\boldsymbol{\sigma} = \ddot{\mathbf{e}} + \mathbf{c_1 \dot{e} + c_0 e} \ldots\ldots. \mathbf{(37)}$$

$$\boldsymbol{\sigma} = \mathbf{e^{(k)}} + \sum_{\mathbf{i=0}}^{\mathbf{k}} \mathbf{c_i\, e^{(i)}} \ldots\ldots. \mathbf{(38)}$$

The number of differentials to be included (the "**k**" coefficient in **(38)**) should be $\mathbf{k = r\text{-}1}$, where **r** is the input-output comparative degree of **(29)-(30)**. With correctly picked $\mathbf{c_i}$ coefficients, if one leads to zero the $\boldsymbol{\sigma}$ variable, the exponential disappearing of the error and its differentials are achieved. If this happens, then the finite time zeroing of $\boldsymbol{\sigma}$ will be the control task, "forgetting" any other aspects. From a geometrical point of view, the equation, $\boldsymbol{\sigma} = \mathbf{0}$ is the definition of a surface in the error space named "sliding surface". Along which the system behavior matches the design specifications, the control trajectories are forced onto the sliding surface. We have almost an arbitrary selection of the positive parameter **p** and when it is sliding, it states the unique pole of the occasioning "reduced dynamics" of the system. The integer parameter **k** is in the conflict rather crucial, it has to be equal to **r-1**, with **r** being the comparative degree between **y** and **u**. It means that the sigma variable has the relative degree

as one. The consecutive phase (Phase 2) is to find a control action that navigates the system trajectories onto the sliding manifold, i.e., the control can steer the $\boldsymbol{\sigma}$ variable to zero in finite time.

There are different methodologies based on the SMC given below -

1. Standard (or first-order) sliding mode control
2. High-order sliding mode control

Second-order SMC is emphasized mostly and there are also some references to the higher-order SMC methods. The usual aspect of all SMC procedures is that the exact knowledge about the fundamental system dynamics is not given properly. Here, the total controlled system is considered as a completely uncertain "Black Box" object.

5.3 First Order Sliding Mode Control [76]-[77]

The control is discontinuous across the manifold, $\boldsymbol{\sigma = 0}$.

$$\mathbf{u = -U\ sgn\ (\sigma)} \ldots\ldots\ \mathbf{(39)}$$

That means,

$$\mathbf{u} = \begin{cases} \mathbf{-U\ at\ \sigma > 0} \\ \mathbf{U\ at\ \sigma < 0} \end{cases} \ldots\ldots\ \mathbf{(40)}$$

So, U is a sufficiently large positive constant.

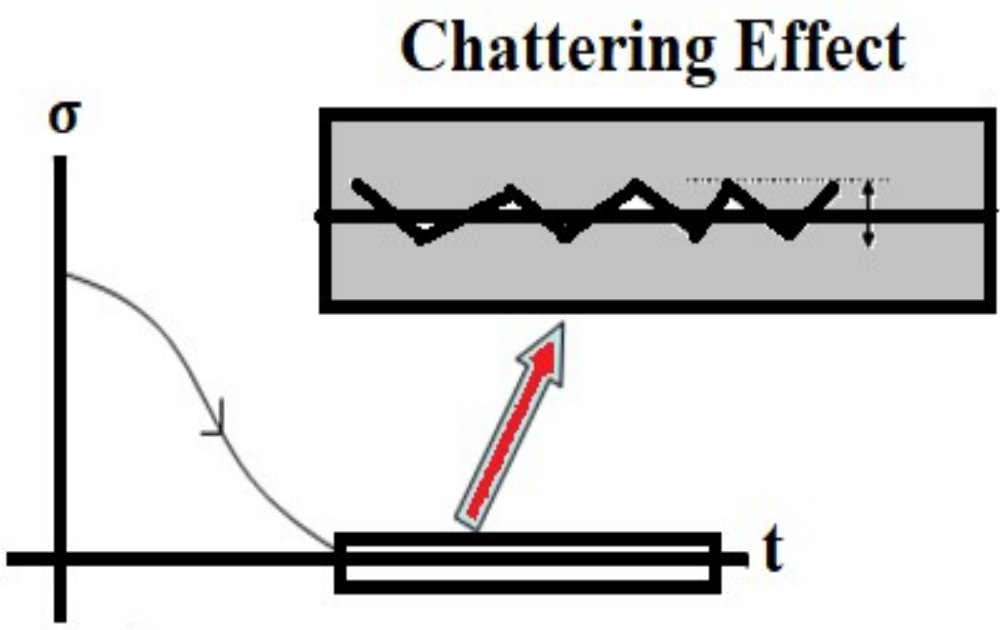

Fig. 5.1: Typical evolution of the $\boldsymbol{\sigma}$ variable starting from different initial conditions [76]

In a steady-state, the control variable u will transmute at a very high (hypothetically infinite) frequency between the values **u** = **U** and **u** = **-** **U** (See Fig. 5.2).

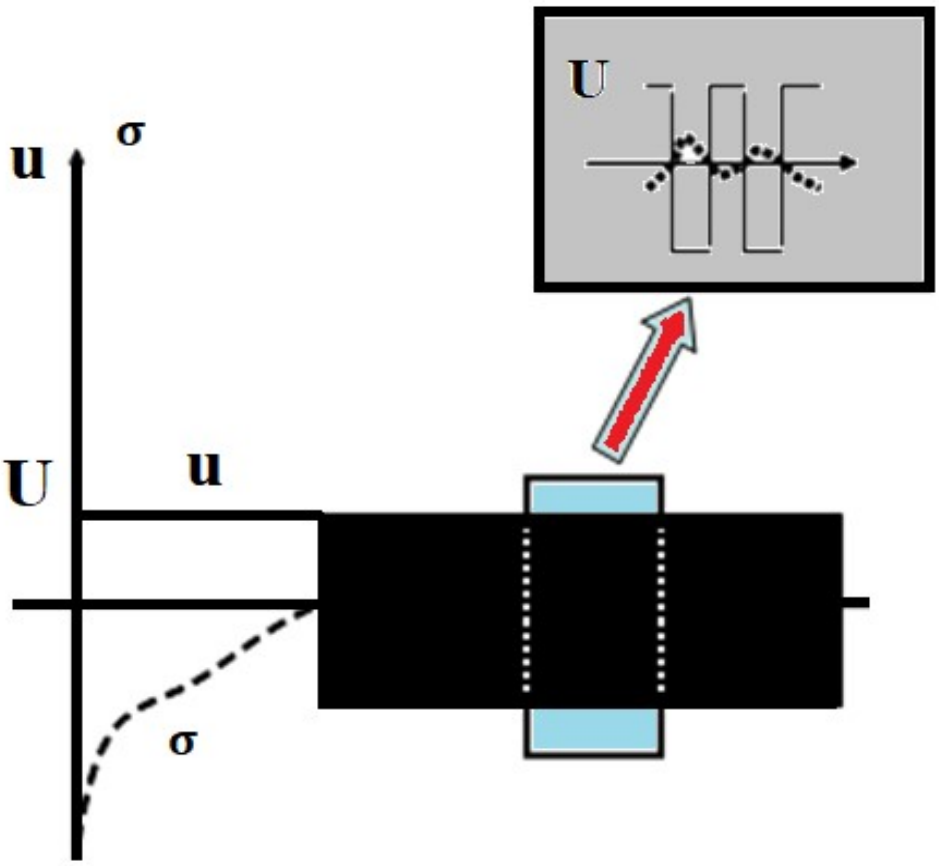

Fig. 5.2: Typical evolution of the control signal **u** (Dashed line represents **σ**) [77]

The irregular high-frequency switching control (Figure 5.2) is accurate in "electrical" applications (where PWM control signals are normally engaged) but creates oscillations and several issues in different fields like the control of mechanical systems etc.

For solving the problem shown above (referred to as the "chattering phenomenon") estimated (smoothed) realizations of SMC practices have been recommended where the discontinuous "sign" term is substituted by a continuous persuasive estimation.

Unfortunately, this way to move is applicable only in a precise case, it happens when hard uncertainties are absent and the counteracting control action can be fixed to zero in the sliding mode.

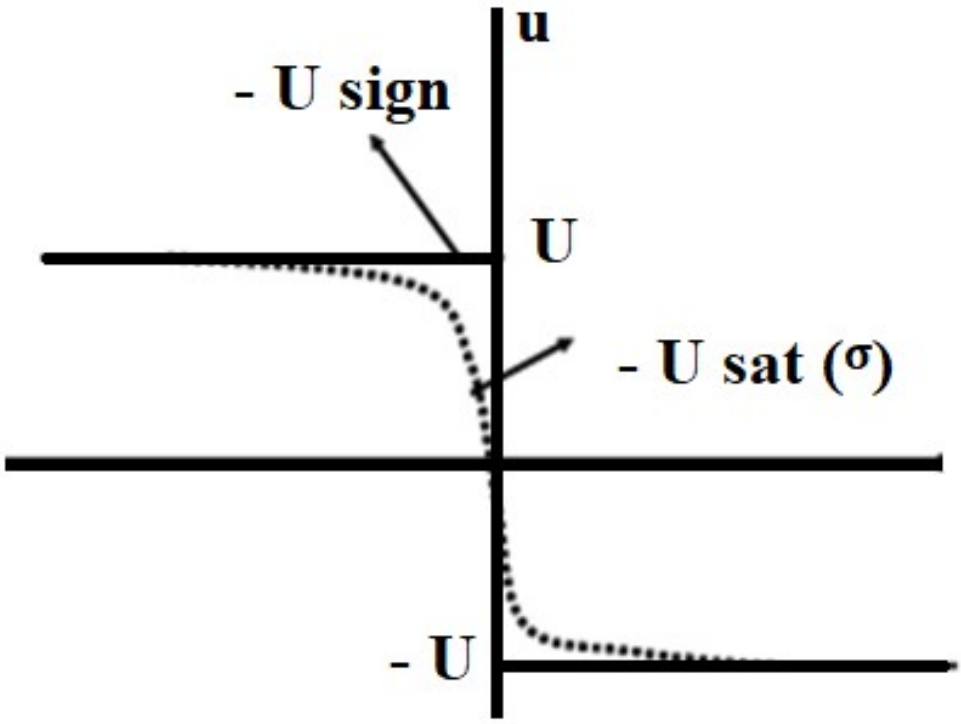

Fig. 5.3: Smooth approximations of Sliding Mode Control [77]

5.4 Second-Order Sliding Mode Control [78]-[79]

Using the previously expressed smooth estimations, some issues are reduced, at the price of a loss of robustness. Second-order SMC algorithms are an efficient alternative that solves the chattering effect without any adjustment to the robustness properties as well. One popular example of a second-order SMC algorithm, the "Super-Twisting Algorithm" is given below-

$$\mathbf{u} = -\boldsymbol{\lambda}\sqrt{|\boldsymbol{\sigma}|}\,\mathbf{sgn}\,(\boldsymbol{\sigma}) + \boldsymbol{\omega} \ldots\ldots \textbf{(41)}$$

$$\dot{\boldsymbol{\omega}} = -\mathbf{W}\,\mathbf{sgn}\,(\boldsymbol{\sigma}) \ldots\ldots \textbf{(42)}$$

A suitable way for tuning its parameters is the pair of the relationship as stated below -

$$\boldsymbol{\lambda} = \sqrt{\mathbf{U}} \ldots\ldots \textbf{(43)}$$

And, $\mathbf{W} = \mathbf{1.1\,U} \ldots\ldots$ **(44)**

Here, **U** is a positive constant to be taken sufficiently large. Practically, one has to progressively increase **U** until good performances are noticed in the closed-loop system. This kind of single-parameter "trial and error" tuning is particularly suitable in practical realization.

The super-twisting analogy can be seen as a nonlinear variant of the classical PI controller. This algorithm is clearer by referring to Fig. 5.4 and Fig. 5.5.

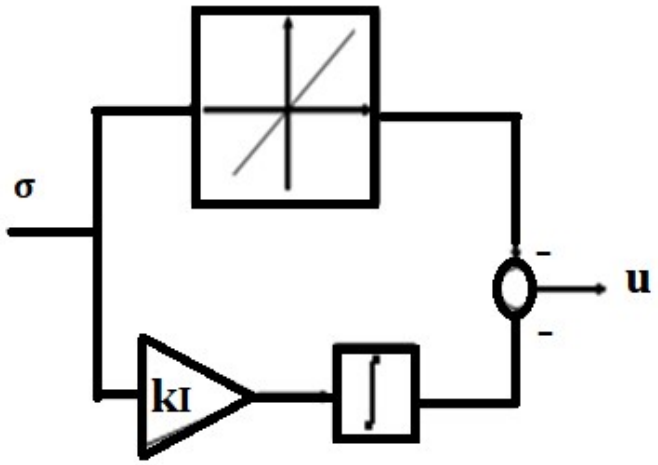

Fig. 5.4: Block Scheme of PI Controller [78]

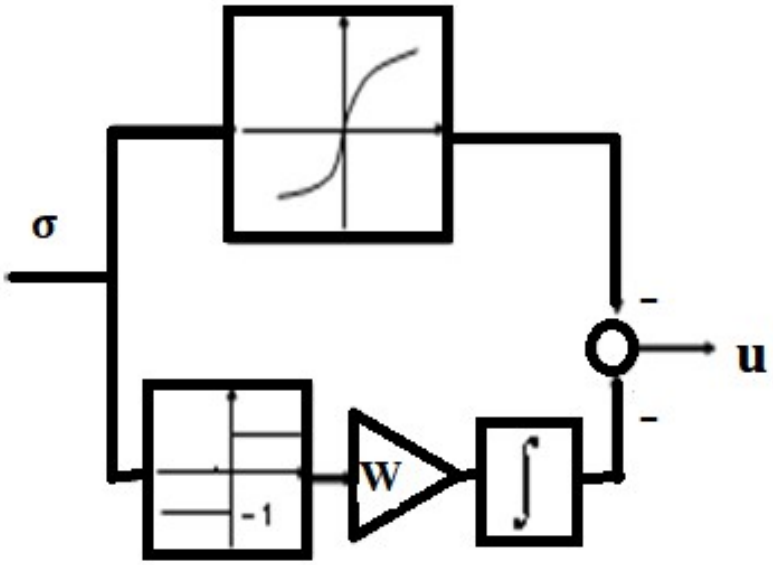

Fig. 5.5: Block Scheme of Super-Twisting Controller [78]

Second-order SMC solves the chattering issue since the control law is now a continuous function of time. Some residual chattering is present in the presence of unmodelled dynamics, but a few design approaches exist there to second-order SMCs that allow for limiting such an undesired phenomenon.

5.5 Control Action

It is designed that the sliding variable of the flux magnitude error is $S\omega = \omega_e^* - \omega_e$, according to the second-order SMC principle [78]-[79]. Based on a super-twisting algorithm, the flux controller can be designed as below -

$$T_e^* = K_p |S_\omega|^r \, sgn(S_\omega) + T_e \ldots\ldots (45)$$

$$\frac{d}{dt}(S_\omega) = K_i \, sgn(S_\omega) \ldots\ldots (46)$$

So, the final expression will be,

$$T_e^* = K_p |S_\omega|^r \, sgn(S_\omega) + \int K_i \, sgn(S_\omega) \, dt \ldots\ldots (47)$$

Here, $r = 0.5$ has been used in this system for good control operation [78]-[79].

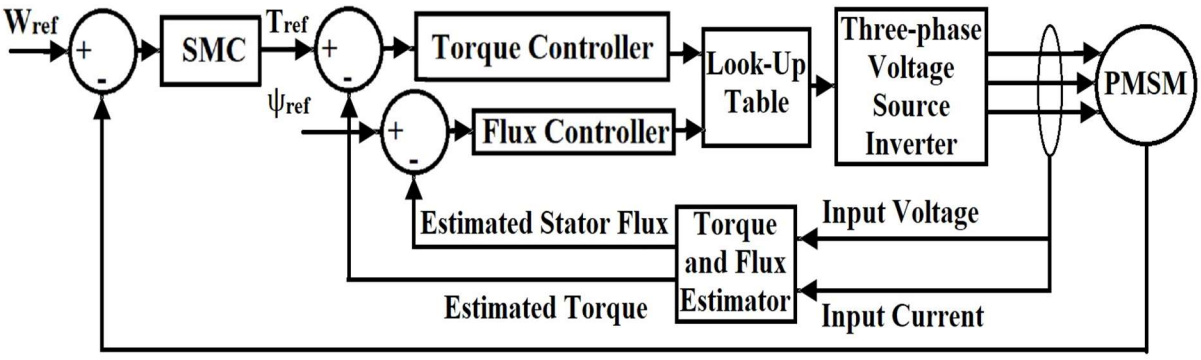

Fig. 5.6: Block Diagram of Sliding Mode Control based Direct Torque Control of Permanent Magnet Synchronous Motor Drive System

5.6 Applications of SMC

The main application of SMC is in the domain of Power Electronics and Electrical Drive with PWM converters [80]. Second-order SMC is used in DC Motor Control [81]. SMC is also used in the control of Power Systems [82] and Process Control [83]-[84].

Second-order SMC is applied to several types of mechanical systems (including cranes, robot manipulators, train pantographs, and more) [85], overhead cranes [86]-[87], marine vehicles [88]-[89], electrohydraulic valve actuator [90], combined-cycle plants, etc.

5.7 Chapter Summary

This chapter is discussed about basic principles and design of SMC. Both first-order and second-order SMC algorithms are discussed with necessary examples with characteristic diagrams. The applications of SMC are mentioned also in this chapter.

CHAPTER 6

SMC-BASED TWELVE SECTORS DTC

6.1 System Specifications

I simulated the system in MATLAB for both PI Controller and SMC for both six sectors and twelve sectors modified DTC. Here, I am providing the simulation results obtained from MATLAB/SIMULINK for the above-mentioned cases for each parameter in the system below. Before that, I would like to provide the values of the parameters used in the system for simulation in MATLAB/SIMULINK.

Table 6.1: System Specifications

Parameters	Values	Unit
No. of Pole Pairs	2	
Stator Resistance	0.767	Ω
Permanent Magnet Flux	0.1377	Wb
Q-axis Inductance	4.607	mH
D-axis Inductance	4.713	mH
Rated Power	0.4	kW
Rated Speed	1500	Rpm
Rated Current	4.66	A
Rated Torque	2.5	Nm
Rated Stator Flux	0.3	Wb
Inertia Constant	6.876×10^{-3}	Kgm^2
Viscous Damping	2.7504×10^{-3}	Nms.
Proportional Constant (K_p)	1	
Integral Constant (K_i)	5	
DC Supply Voltage of Inverter	100	V
Supply Frequency	50	Hz
Sample Time	10^{-4}	s
Torque Limit for PI Controller	20	Nm
Torque Limit for SMC	5	Nm

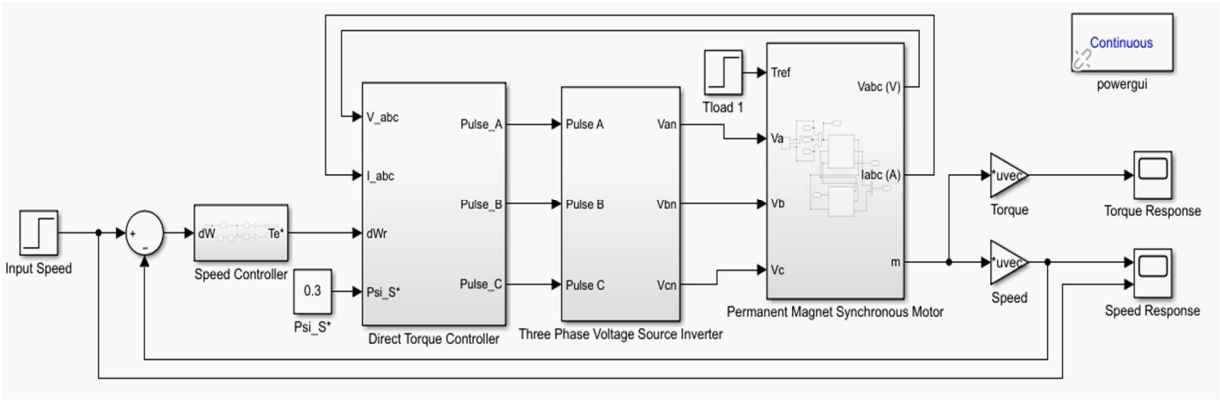

Fig. 6.1: Simulink Block Diagram for DTC of PMSM

6.2 Speed Response

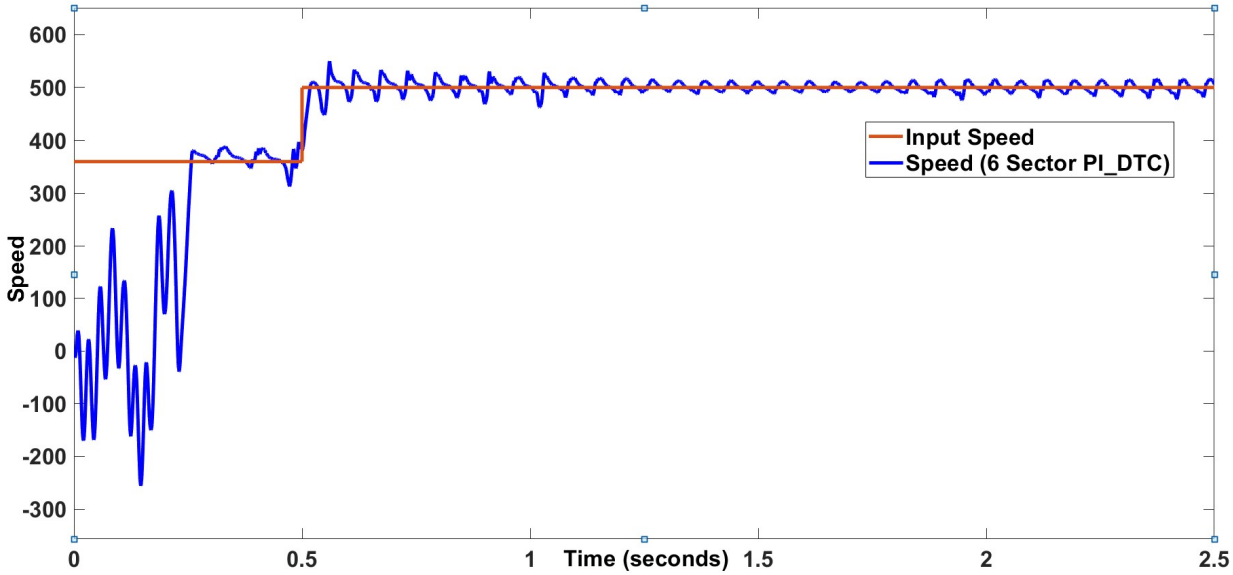

Fig. 6.2: Simulation Result of Speed Response of six sectors PI-DTC

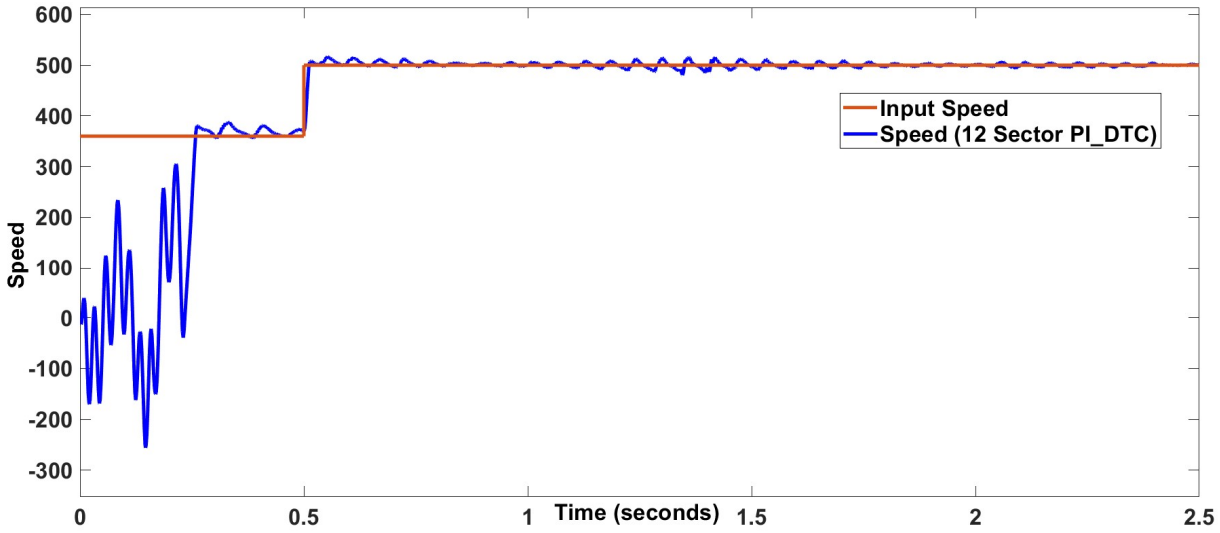

Fig. 6.3: Simulation Result of Speed Response of twelve sectors PI-DTC

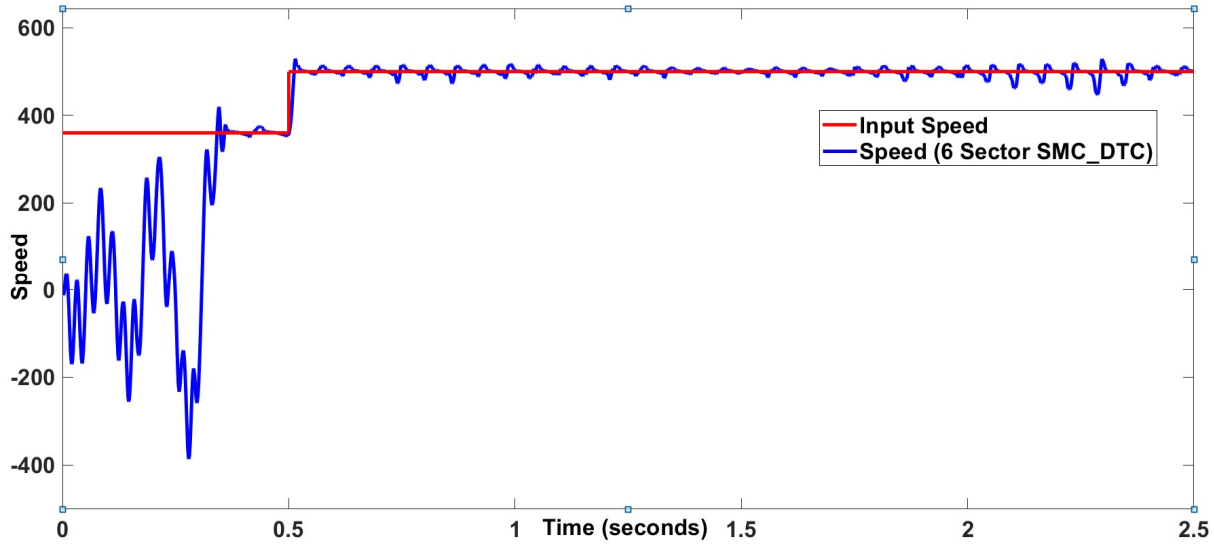

Fig. 6.4: Simulation Result of Speed Response of six sectors SMC-DTC

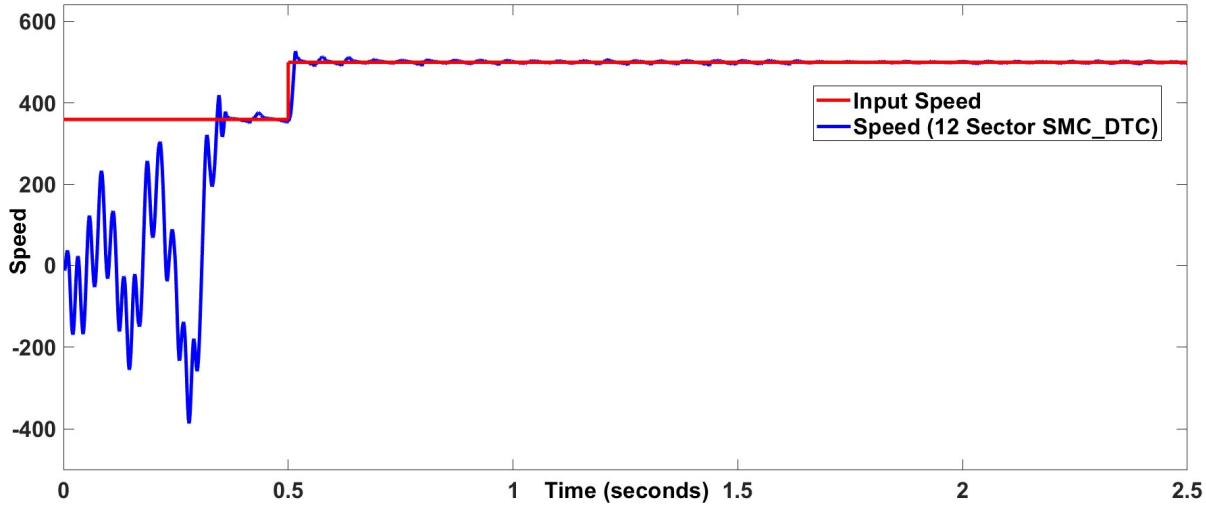

Fig. 6.5: Simulation Result of Speed Response of twelve sectors SMC-DTC

Observation: In the twelve sectors PI-DTC, the ripple is lesser than in six sectors PI-DTC. In twelve sectors SMC-DTC, the ripple is lesser than in six sectors SMC-DTC and it is also lesser than in PI-DTC.

6.3 Torque Response

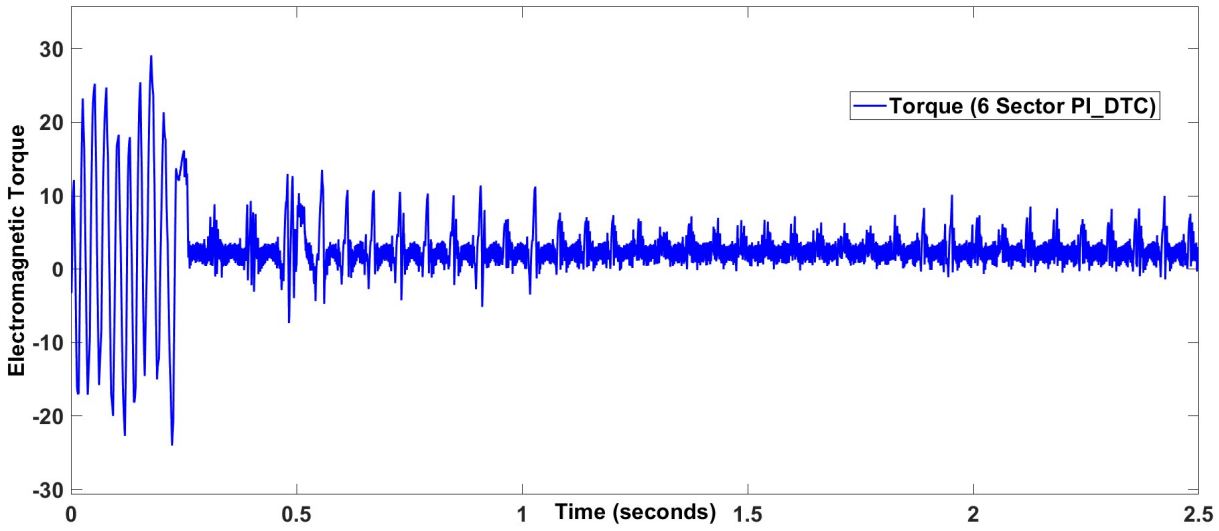

Fig. 6.6: Simulation Result of Torque Response of six sectors PI-DTC

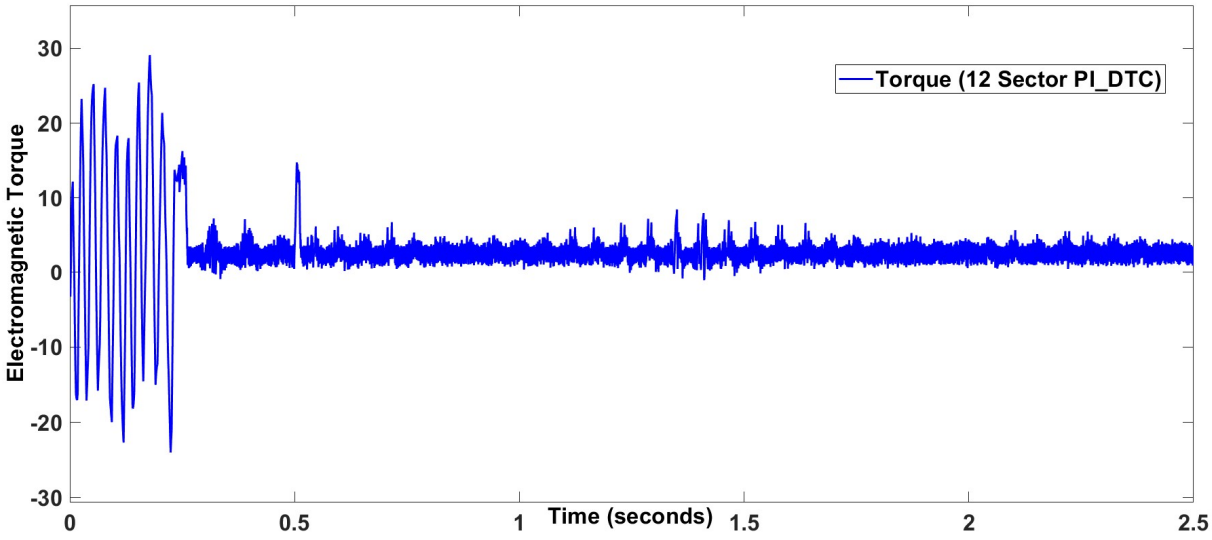

Fig. 6.7: Simulation Result of Torque Response of twelve sectors PI-DTC

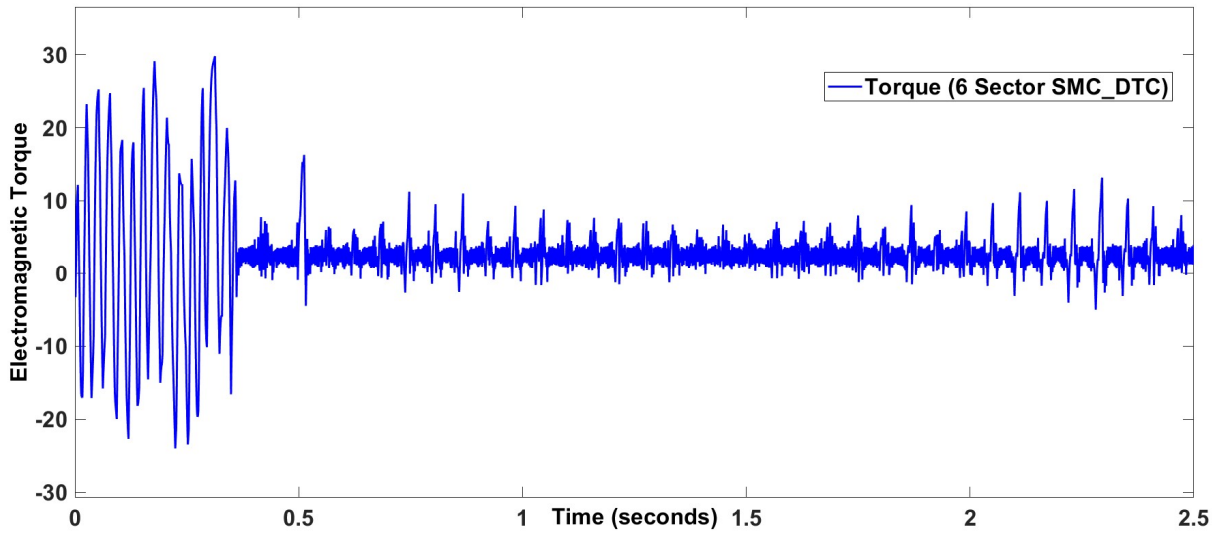

Fig. 6.8: Simulation Result of Torque Response of six sectors SMC-DTC

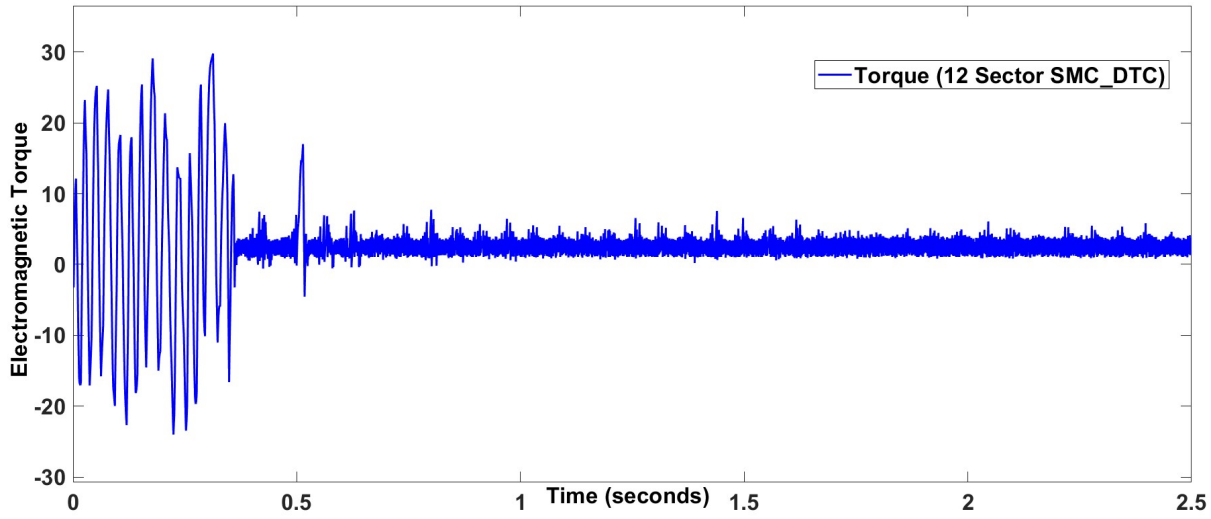

Fig. 6.9: Simulation Result of Torque Response of twelve sectors SMC-DTC

Observation: In the twelve sectors PI-DTC, the ripple is lesser than in six sectors PI-DTC. In twelve sectors SMC-DTC, the ripple is lesser than in six sectors SMC-DTC and it is also lesser than in PI-DTC.

6.4 Input Voltage Response

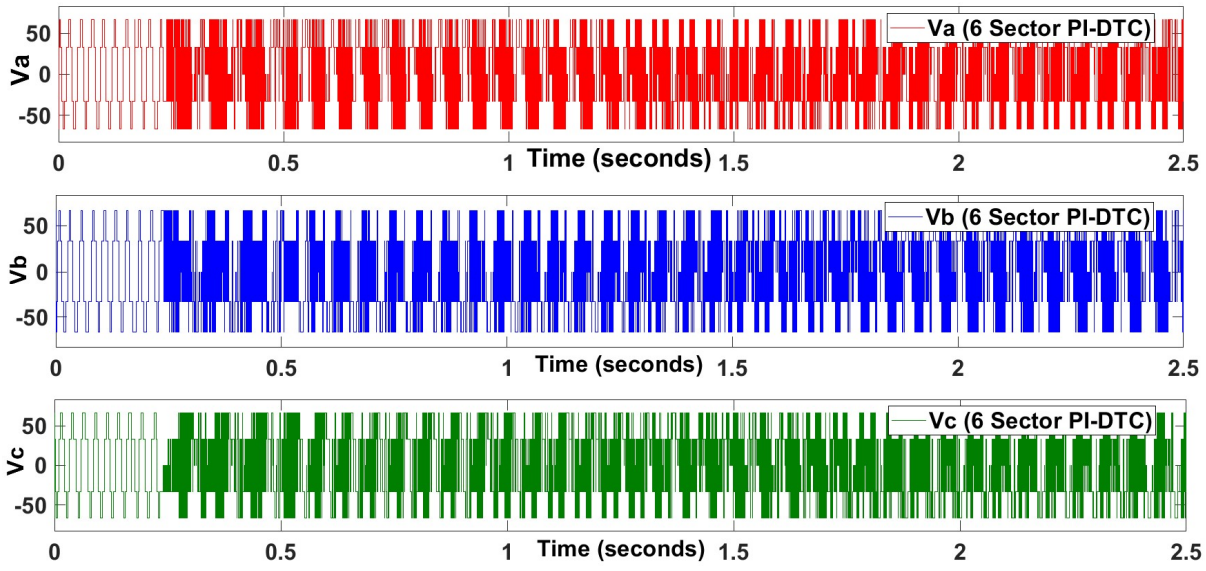

Fig. 6.10: Simulation Result of Input Voltage Response of six sectors PI-DTC

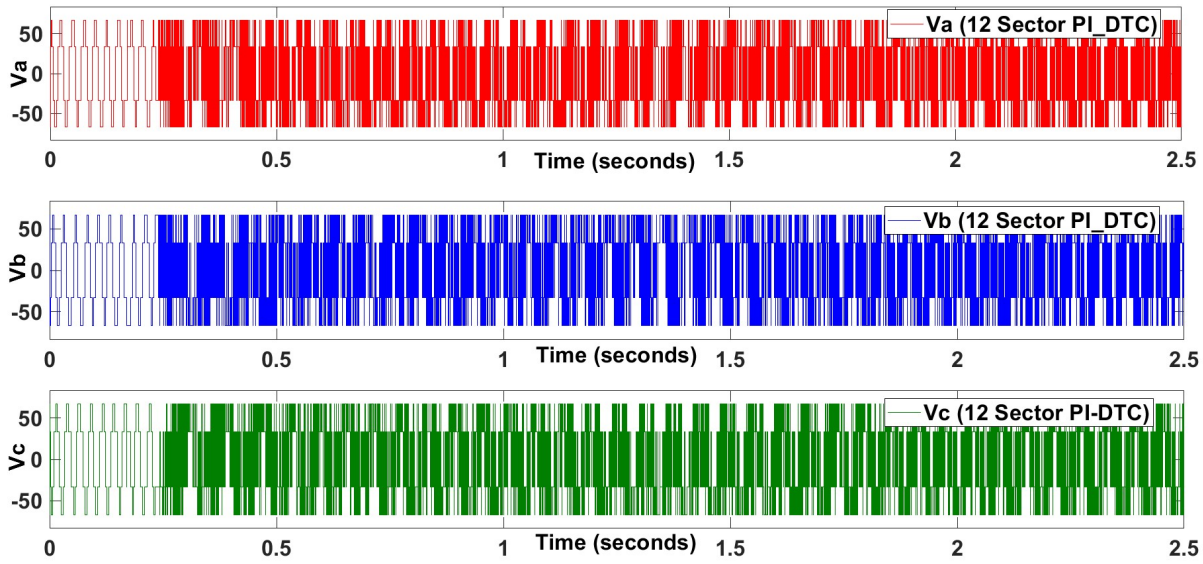

Fig. 6.11: Simulation Result of Input Voltage Response of twelve sectors PI-DTC

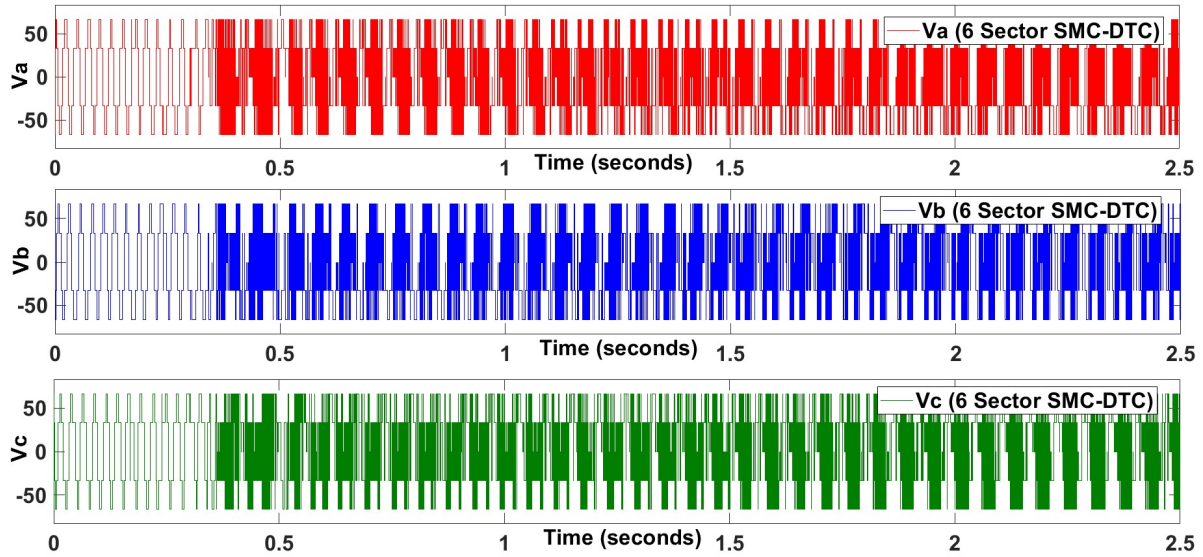

Fig. 6.12: Simulation Result of Input Voltage Response of six sectors SMC-DTC

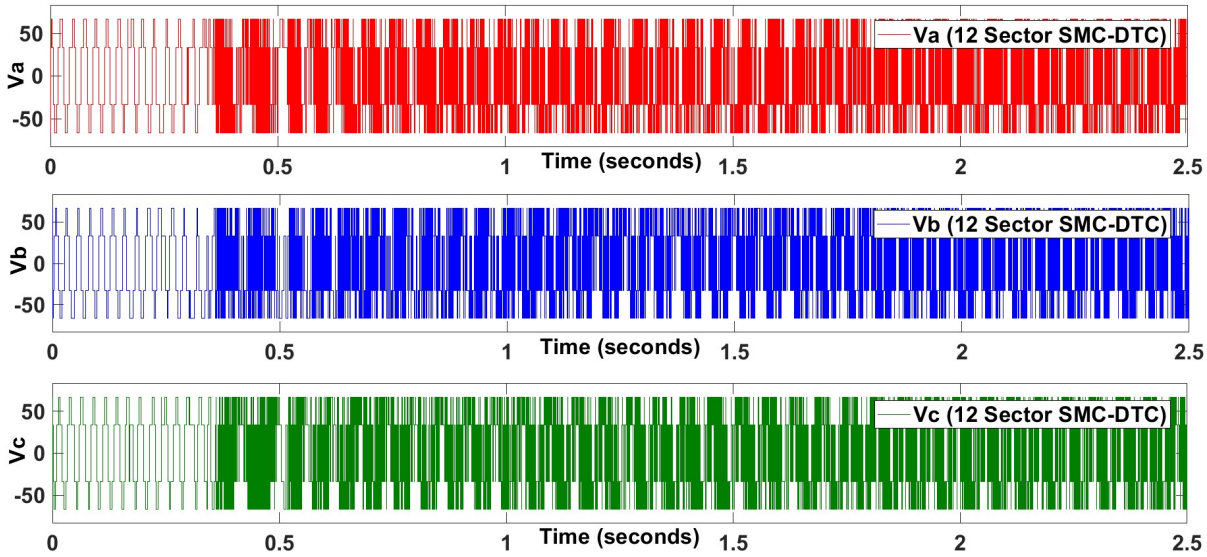

Fig. 6.13: Simulation Result of Input Voltage Response of twelve sectors SMC-DTC

Observation: The average value of voltage is more in twelve sector PI-DTC compared to six sectors PI-DTC. The average value of voltage is more in twelve sectors SMC-DTC compared to six sectors SMC-DTC and it is more than PI-DTC.

6.5 Input Current Response

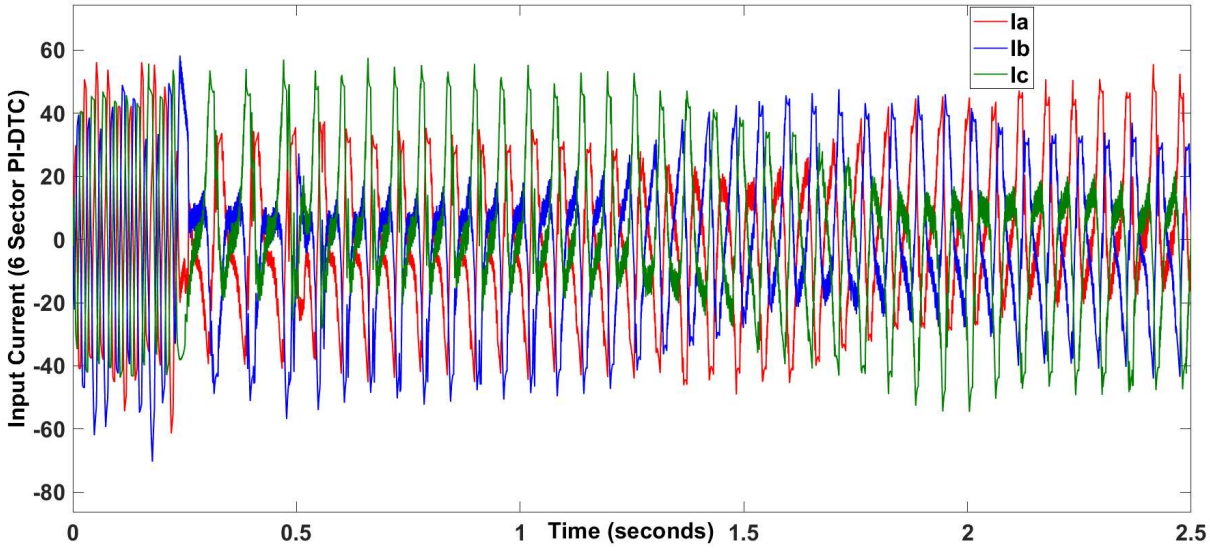

Fig. 6.14: Simulation Result of Input Current Response of six sectors PI-DTC

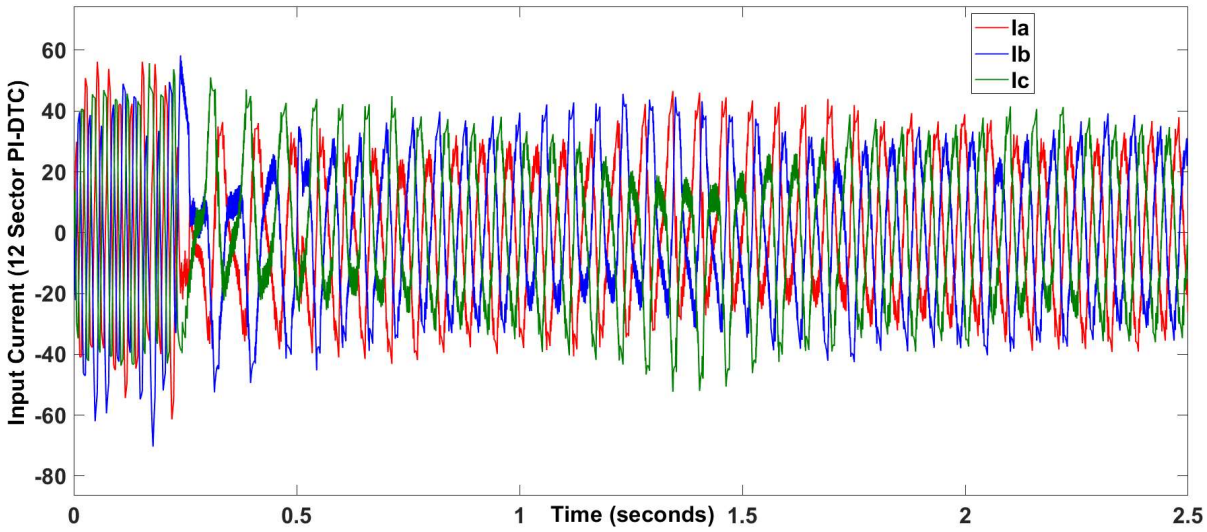

Fig. 6.15: Simulation Result of Input Current Response of twelve sectors PI-DTC

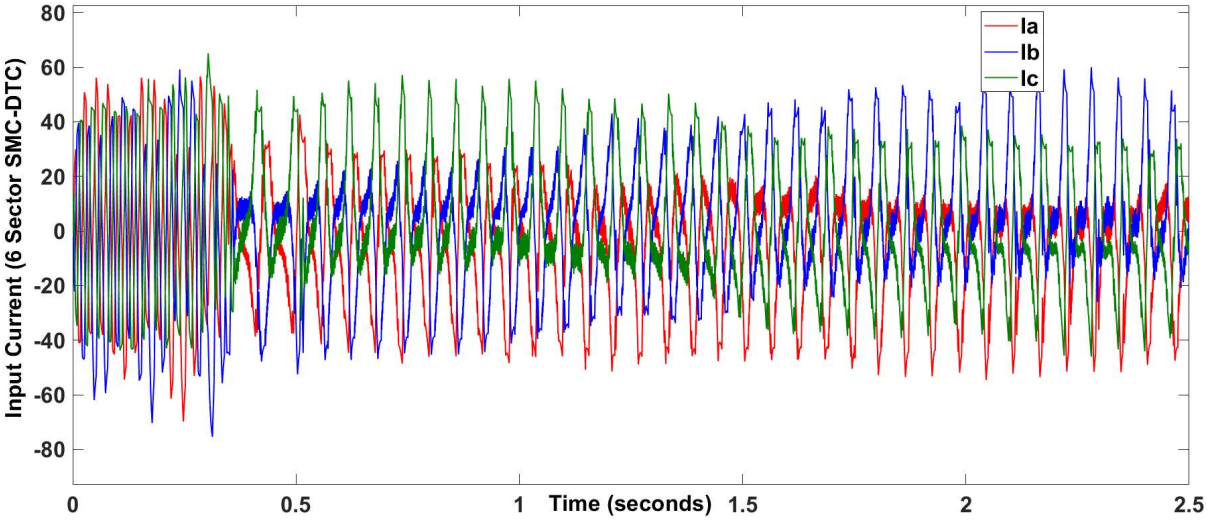

Fig. 6.16: Simulation Result of Input Current Response of six sectors SMC-DTC

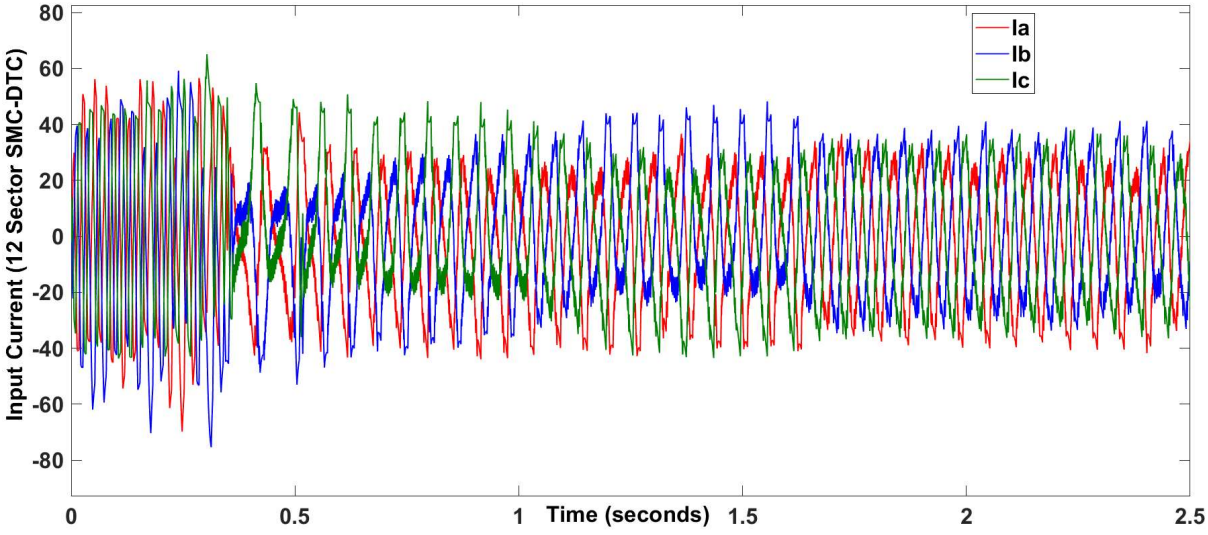

Fig. 6.17: Simulation Result of Input Current Response of twelve sectors SMC-DTC

Observation: In six sector PI-DTC, the average value of current of phase A is more, whereas, in twelve sectors PI-DTC, the average value of current of phase C is more. In six sector SMC-DTC, peak values of all phase currents are more compared to twelve sectors SMC-DTC, which means the current requirement is lesser in twelve sector SMC-DTC.

6.6 DQ-axis Current Response

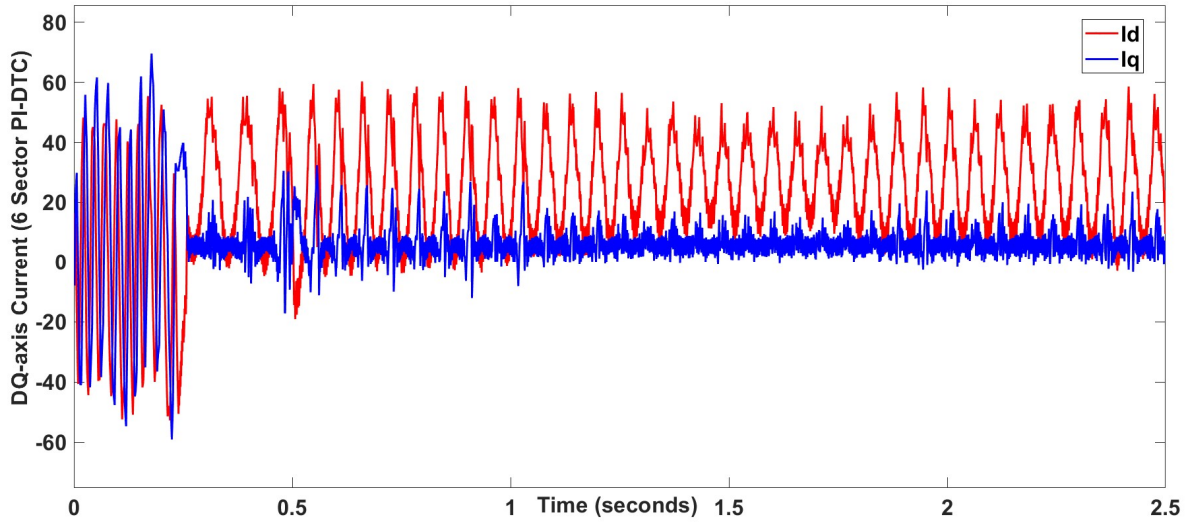

Fig. 6.18: Simulation Result of DQ-axis Current Response of six sectors PI-DTC

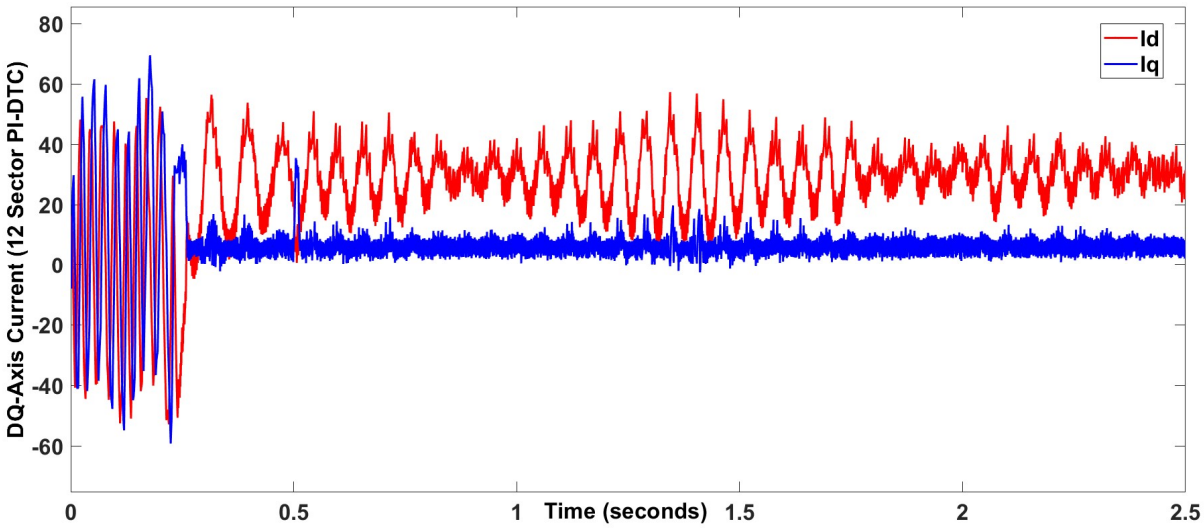

Fig. 6.19: Simulation Result of DQ-axis Current Response of twelve sectors PI-DTC

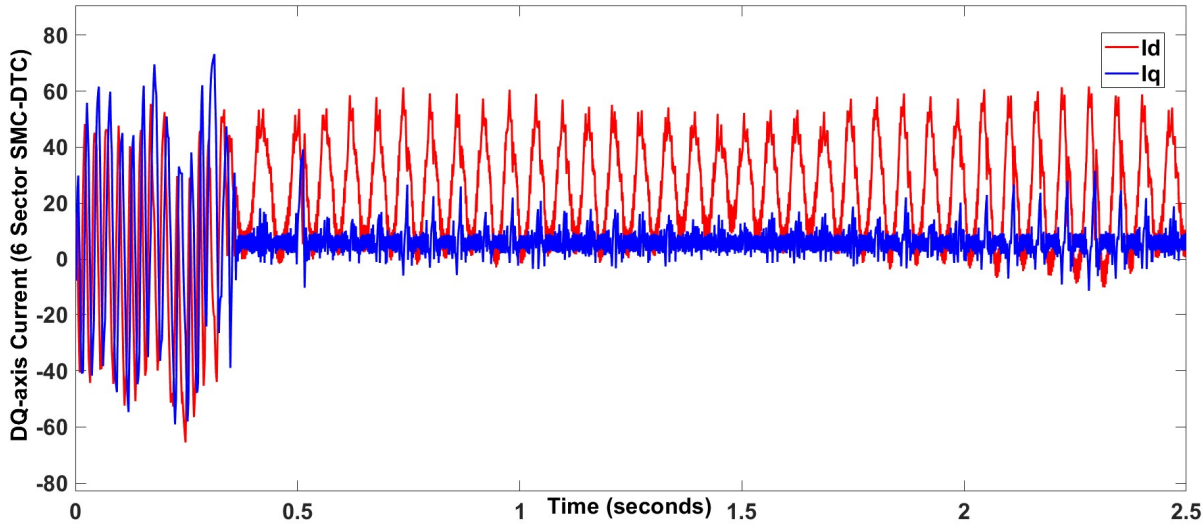

Fig. 6.20: Simulation Result of DQ-axis Current Response of six sectors SMC-DTC

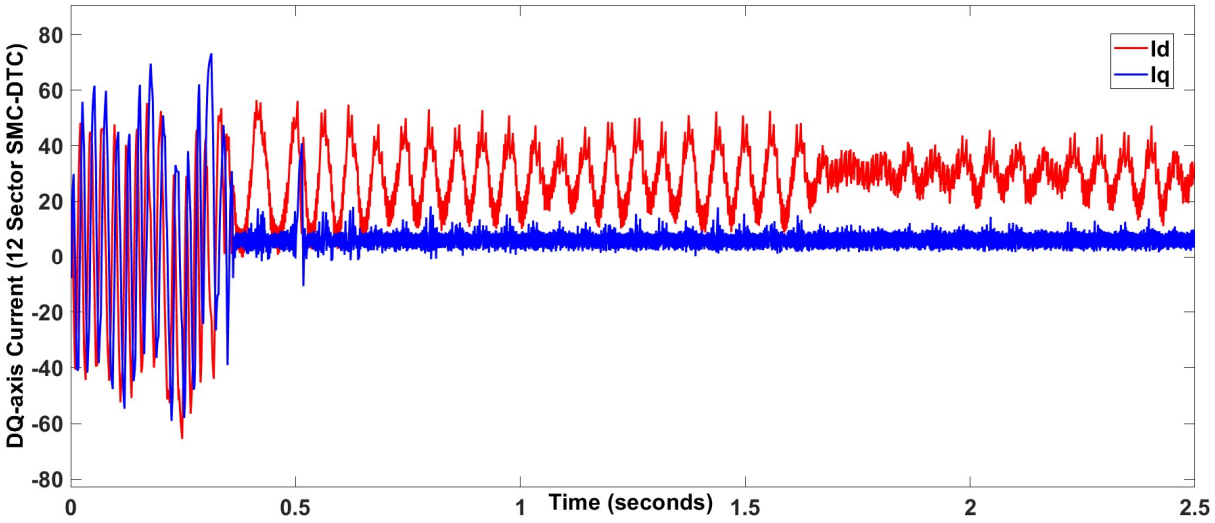

Fig. 6.21: Simulation Result of DQ-axis Current Response of twelve sectors SMC-DTC

Observation: In the twelve sectors of PI-DTC, the current requirement is more compared to the six sectors of PI-DTC. In twelve sector SMC-DTC, the current requirement is less compared to six sectors SMC-DTC and it is also lesser than PI-DTC.

6.7 DQ-axis Voltage Response

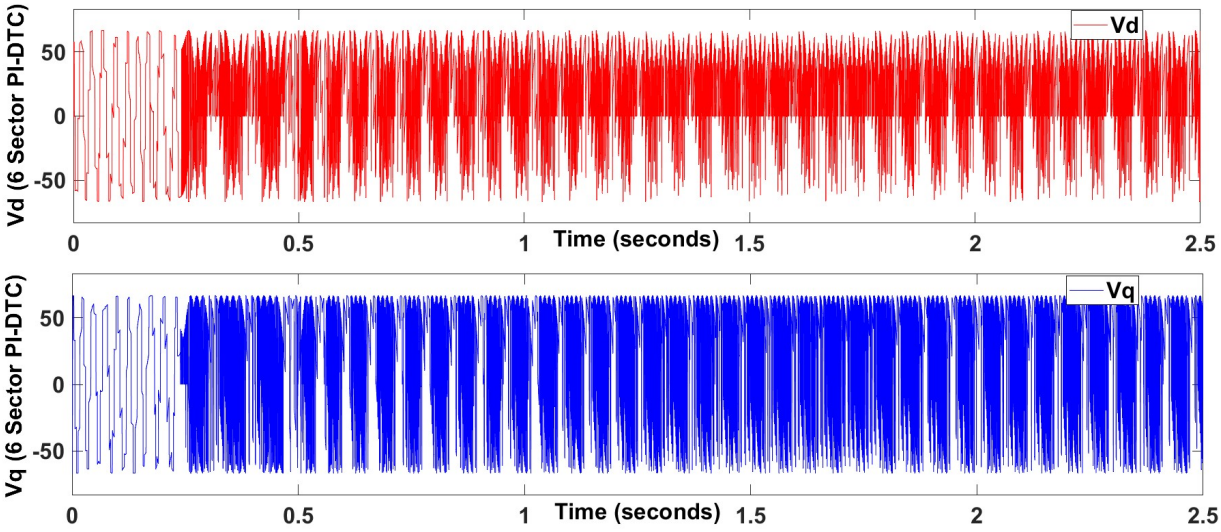

Fig. 6.22: Simulation Result of DQ-axis Voltage Response of six sectors PI-DTC

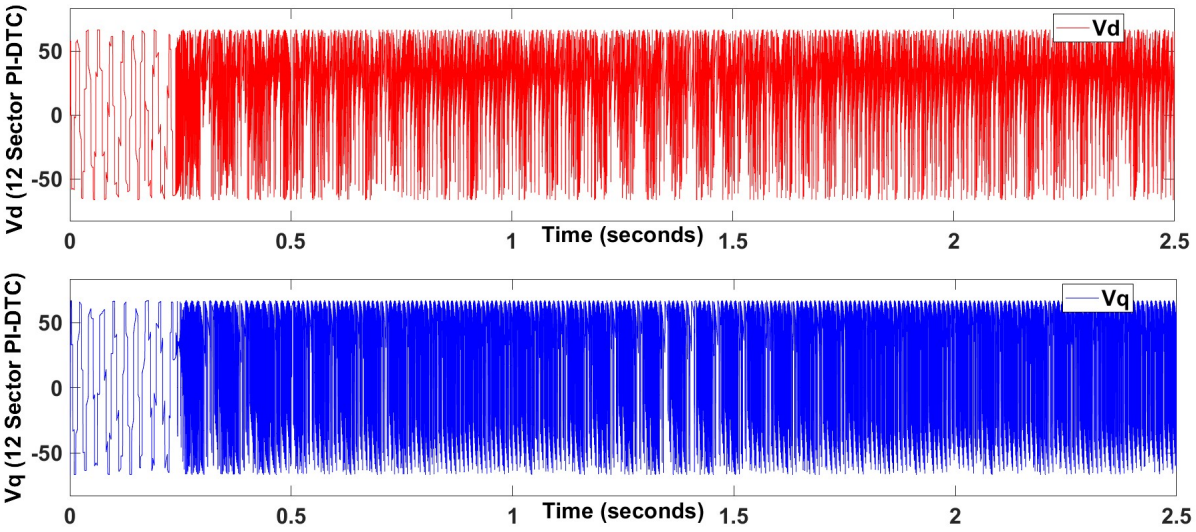

Fig. 6.23: Simulation Result of DQ-axis Voltage Response of twelve sectors PI-DTC

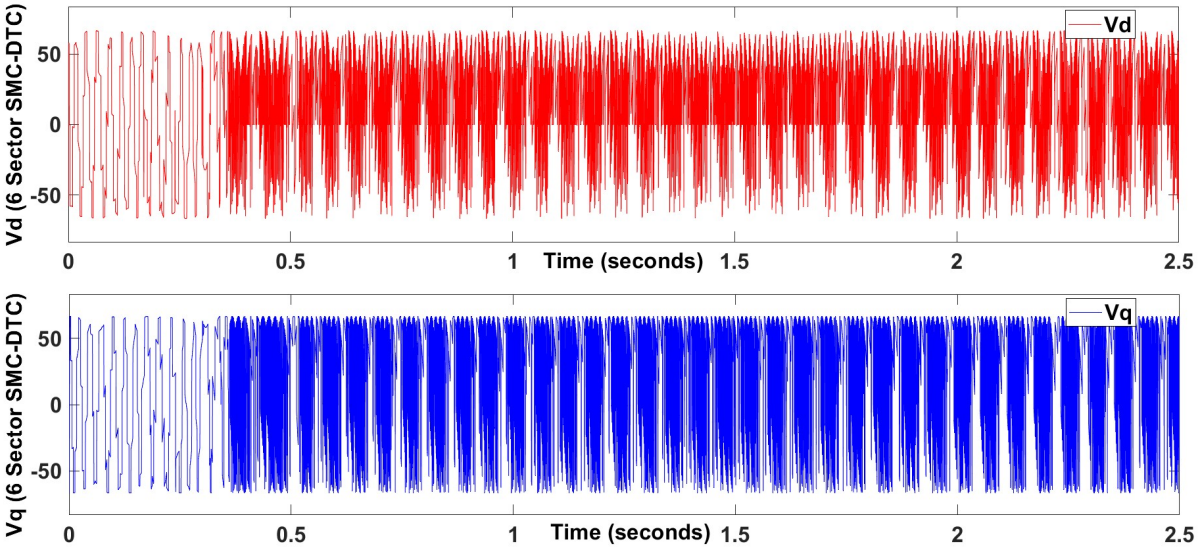

Fig. 6.24: Simulation Result of DQ-axis Voltage Response of six sectors SMC-DTC

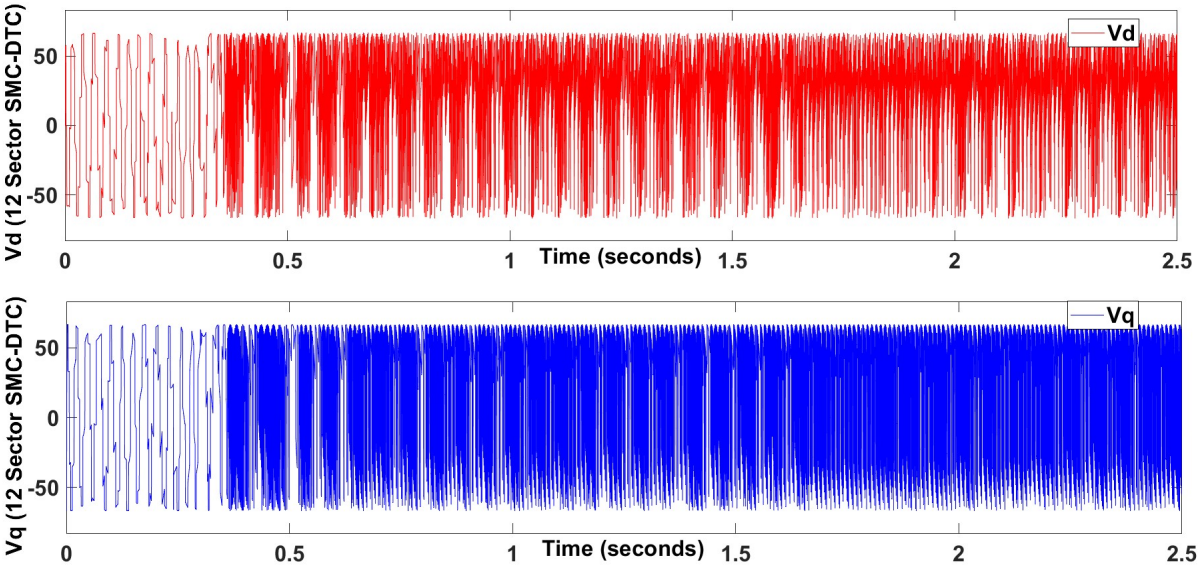

Fig. 6.25: Simulation Result of DQ-axis Voltage Response of twelve sectors SMC-DTC

Observation: Average value of d-axis voltage is more in the case of six sectors PI-DTC compared to twelve sectors PI-DTC. The average value of q-axis voltage is more in the case of twelve sectors SMC-DTC compared to six sectors SMC-DTC.

6.8 Stator Flux Response

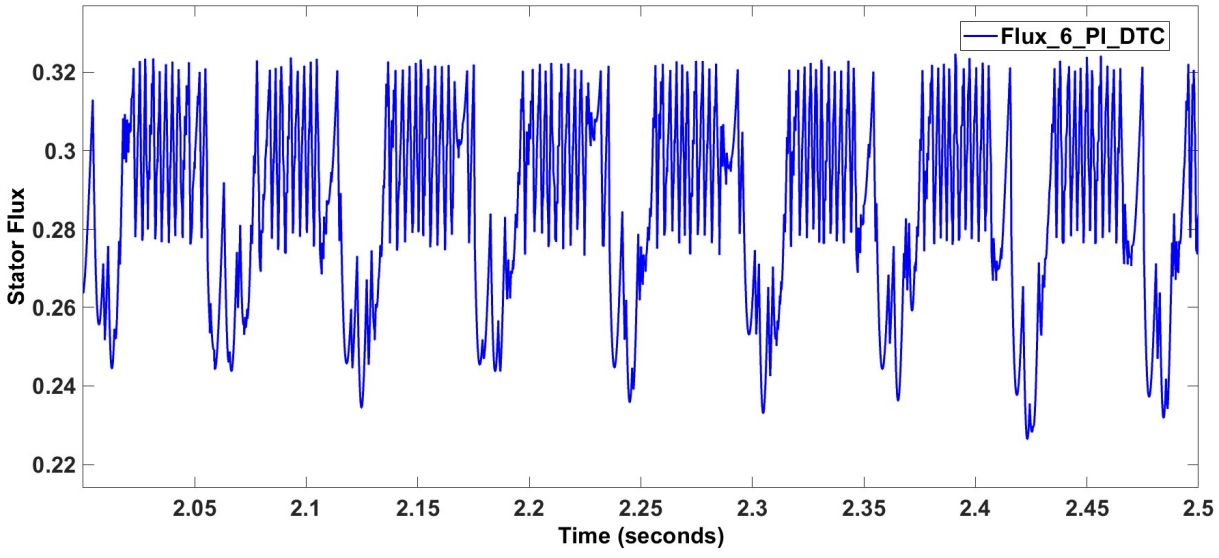

Fig. 6.26: Simulation Result of Stator Flux Response of six sectors PI-DTC

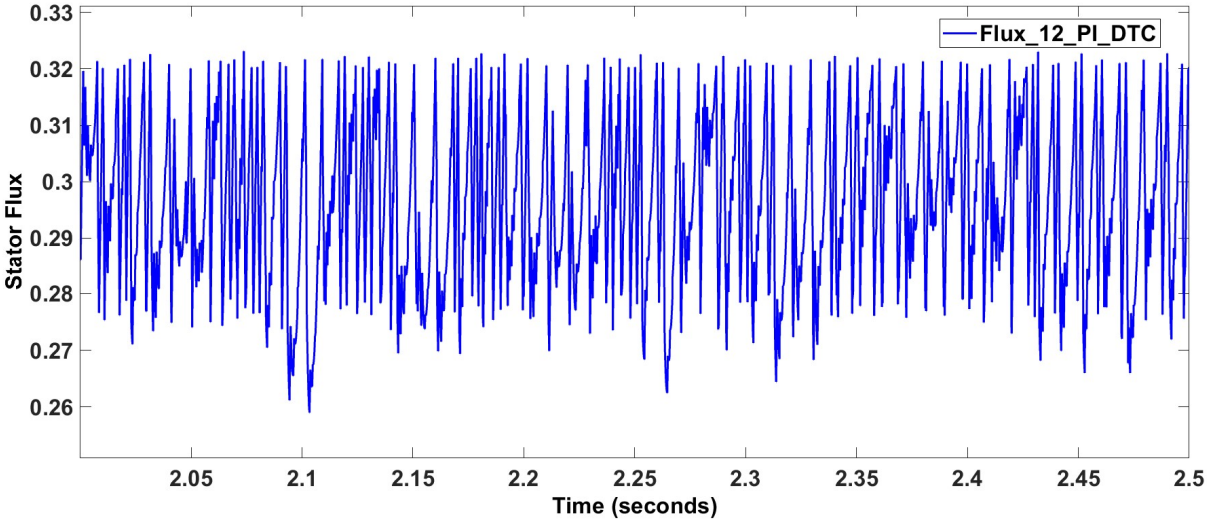

Fig. 6.27: Simulation Result of Stator Flux Response of twelve sectors PI-DTC

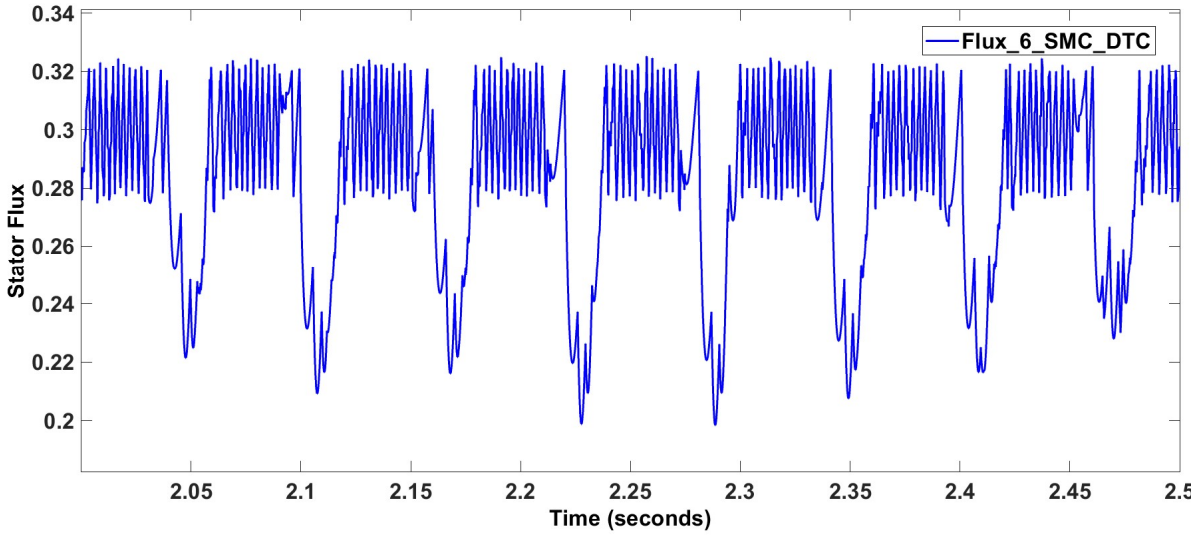

Fig. 6.28: Simulation Result of Stator Flux Response of six sectors SMC-DTC

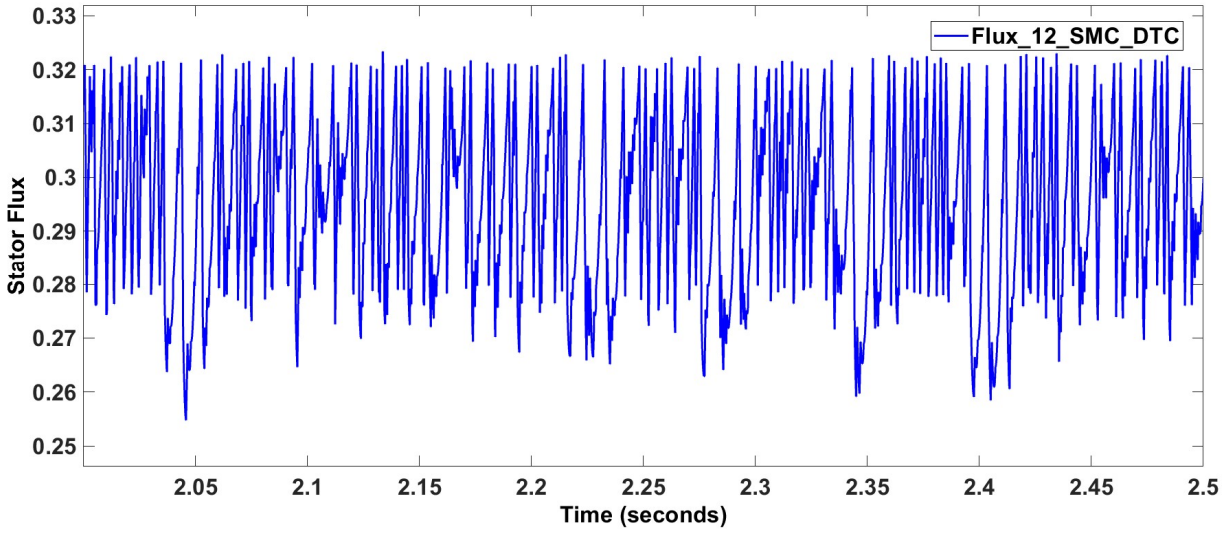

Fig. 6.29: Simulation Result of Stator Flux Response of twelve sectors SMC-DTC

Observation: Average value of stator flux is more in the case of twelve sectors PI-DTC compared to six sectors PI-DTC. Flux fluctuation is less in the case of twelve sectors SMC-DTC compared to six sectors SMC-DTC but not lesser than PI-DTC for twelve sectors operation. Twelve sectors of PI-DTC create the least flux ripples.

6.9 Comparison of the results

Table 6.2: Ripple Percentages of the Response of Different Parameters

Ripple Percentage (%)	Six Sectors PI-DTC	Twelve Sectors PI-DTC	Six Sectors SMC-DTC	Twelve Sectors SMC-DTC
Speed (RPM)	2.07	0.78	0.53	0.48
Torque (Nm)	71.75	40.59	64.41	38.81
Stator Flux (Wb)	9.1	5.25	9.01	5.6

6.10 Discussions

By observing the ripple percentages mentioned in the previous table, we can reach certain decisions given below -

The speed ripple for the case of six sectors PI-DTC is 2.07% and for the twelve sectors operation, the ripple (0.78%) is lesser. Also, for six sectors SMC-DTC, it is lesser, i.e., 0.53%. But, for the proposed scheme, twelve sectors SMC-DTC, the speed ripple is 0.48%, which is the least among all the cases. Though our purpose is to reduce torque ripple, this is also a good achievement from the proposed scheme as the speed response is best among all the cases mentioned here.

For the torque ripple, twelve sectors SMC-DTC, i.e., the proposed scheme, can produce the least ripple, 38.81%. For the other three cases, that means, for six sectors PI-DTC (71.75%), twelve sectors PI-DTC (40.59%), and six sectors SMC-DTC (64.41%), it is more. This means that if we use twelve sector operation in the case of SMC, the torque ripple will be the least so our purpose is solved.

If the flux ripple percentages are observed, we can see that when we proceed from six sectors operation to twelve sectors operation in the case of PI-DTC, flux ripples are going to be decreased, i.e., from 9.1% to 9.01%. But for SMC DTC, it is the opposite, i.e., 5.25% to 5.6%. But this will not affect the system much. For the proposed scheme, flux ripple is lesser than the six sectors operation for both PI and SMC except for the twelve sectors PI-DTC. Still, the ripple is lesser in the proposed scheme than in the first case, so it is permitted in the proposed scheme where the main purpose of reducing torque ripple has been served properly.

Here, the responses are given and compared for all four cases. The ripples percentages are provided in the tables for each parameter. Here, speed and torque ripples are the least for the proposed scheme. But the flux ripple is lesser using the proposed methodology, but not the least. Though it can be reduced using the proposed scheme compared to the first case. So, all total, the twelve sectors SMC-DTC method is far better than the other methods mentioned here to control PMSM.

6.11 Chapter Summary

This chapter consists of the simulation results obtained from the MATLAB software and a comparison of the results. Here, the ripple percentages are mentioned in the tables, the observations are stated below the simulation results and the values for different cases are discussed.

CHAPTER 7

CONCLUSION

7.1 Contributions to the work

Firstly, I did a literature survey related to the research area of different control techniques of PMSM.

PMSM is one of the most efficient machines used in Electric Drives. So, I decided to work with this machine as a plant for my project work. I studied PMSM in detail with all the important equations and relevant diagrams.

PMSM is not self-starting. So, I used Three-Phase Voltage Source Inverter to drive the PMSM. I studied the theory of the Three-Phase Voltage Source Inverter with the necessary circuit diagram and tables.

I found Direct Torque Control as the most advantageous technique to control PMSM. So, I decided to go for it. So, I studied the theory of Direct Torque Control in detail with important equations, necessary tables, and relevant diagrams for both six sectors and twelve sector operations.

The only disadvantage of Direct Torque Control is the torque and flux ripples which can be eliminated using Sliding Mode Control. So, I studied the methodology in detail and discussed it with all formulas and necessary diagrams. Then, I used it in the system to reduce the ripples.

I simulated the total system in MATLAB software successfully and compared the response and ripple percentages. I found twelve sectors modified SMC-DTC as the best among all four cases.

7.2 Scopes of the future work

This system can be implemented in hardware to compare the response with the simulation results.

Other efficient control methodologies can be applied to continue smooth control operation and more ripple-free response.

The response obtained from other methods can be compared with my current works and if it is better, it can be implemented in hardware also.

References

[1] R. Krishnan, *Permanent magnet synchronous and brushless DC motor drives*, CRC Press, 2009.

[2] A. Sant, V. Khadkikar, W. Xiao, and H. Zeineldin, “Four-axis vector controlled dual-rotor PMSM for plug-in electric vehicles”, *IEEE Trans. Ind. Electron*., vol. 62, no. 5, pp. 3202–3212, May 2015.

[3] F. Abrahamsen, F. Blaabjerg, and J. K. Pedersen, “Efficiency improvement of variable speed electrical drives for HVAC applications”, *Energy Efficiency Improvements in Electronic Motors and Drives. Springer*, 2000, pp. 130–135.

[4] P. Kshirsagar, R. P. Burgos, J. Jang, A. Lidozzi, F. Wang, D. Boroyevich, and S.K. Sul, “Implementation and sensorless vector-control design and tuning strategy for SMPM machines in fan-type applications”, *IEEE Trans. Ind. Appl*., vol. 48, no. 6, pp. 2402–2413, Nov. 2012.

[5] Y.C. Hung, F.J. Lin, J.C. Hwang, J.K. Chang, and K.C. Ruan, “Wavelet fuzzy neural network with asymmetric membership function controller for electric power steering system via improved differential evolution”, *IEEE Trans. Power Electron*., vol. 30, no. 4, pp. 2350 2362, Apr. 2015.

[6] I. Boldea, “Control issues in adjustable speed drives”, *IEEE Ind. Electron. Mag*., vol. 2, no. 3, pp. 32–50, Sept. 2008.

[7] J. Rivera Dominguez, A. Navarrete, M. Meza, A. Loukianov, and J. Canedo, “Digital sliding-mode sensor less control for surface-mounted PMSM”, *IEEE Trans. Ind. Informant*., vol. 10, no. 1, pp. 137–151, Feb. 2014.

[8] H. H. Choi, H. M. Yun, and Y. Kim, “Implementation of evolutionary fuzzy PID speed controller for PM synchronous motor”, *IEEE Trans. Ind. Informant*., vol. 11, no. 2, pp. 540–547, Apr. 2015.

[9] T. Pajchrowski, K. Zawirski, and K. Nowopolski, “Neural speed controller trained online by means of modified RPROP algorithm”, *IEEE Trans. Ind. Informant*., vol. 11, no. 2, pp. 560–568, Apr. 2015.

[10] T. Tarczewski and L. M. Grzesiak, "Constrained State Feedback Speed Control of PMSM Based on Model Predictive Approach", *IEEE Transactions on Industrial Electronics*, vol. 63, no. 6, pp. 3867-3875, June 2016, doi: 10.1109/TIE.2015.2497302.

[11] G. F. Franklin, J. D. Powell, and M. L. Workman, *Digital control of dynamic systems*. Reading, MA, USA: Addison-Wesley, 1998.

[12] B. Ufnalski, A. Kraszewski, and L. M. Grzesiak, “Particle swarm optimization of the multi-oscillatory LQR for a three-phase four-wire voltage-source inverter with an LC output filter”, *IEEE Trans. Ind. Electron*., vol. 62, no. 1, pp. 484–493, Jan. 2015.

[13] I. Roband, K. Nishimori, R. Nishimura, and N. Ishihara, “Optimal feedback control design using genetic algorithm in multimachine power system”, *Int. J. Elec. Power & Energy System*., vol. 23, no. 4, pp. 263–271, May 2001.

[14] P. Cortes, M. Kazmierkowski, R. Kennel, D. Quevedo, and J. Rodriguez, “Predictive control in power electronics and drives”, *IEEE Trans. Ind. Electron*., vol. 55, no. 12, pp. 4312–4324, Dec. 2008.

[15] F. Bianchini and S. Miani, *Set-theoretic methods in control*. Springer Science, 2007.

[16] A. Formentini, A. Trentin, M. Marchesoni, P. Zanchetta, and P. Wheeler, “Speed finite control set model predictive control of a PMSM fed by matrix converter”, *IEEE Trans. Ind. Electron*., vol. 62, no. 11, pp. 6786– 6796, Nov. 2015.

[17] S. Chai, L. Wang, and E. Rogers, “A cascade MPC control structure for a PMSM with speed ripple minimization”, *IEEE Trans. Ind. Electron*., vol. 60, no. 8, pp. 2978–2987, Aug. 2013.

[18] A. Damiano, G. Gatto, I. Marongiu, A. Perfetto, and A. Serpi, “Operating constraints management of a surface-mounted pm synchronous machine by means of an FPGA-based model predictive control algorithm”, *IEEE Trans. Ind. Informant*., vol. 10, no. 1, pp. 243–255, Feb. 2014.

[19] S. Ding and S. Li, "Second-order sliding mode controller design subject to mismatched term", *Automatic a*, vol. 77, pp. 388-392, Mar. 2017.

[20] L. Liu, W. X. Zheng, and S. Ding, "An adaptive SOSM controller design by using a Sliding-Mode-Based filter and its application to buck converter", *IEEE Trans. Circuits Syst. I Reg. Papers*, vol. 67, no. 7, pp. 2409-2418, Jul. 2020.

[21] S. Chai, L. Wang, and E. Rogers, "A cascade MPC control structure for a PMSM with speed ripple minimization", *IEEE Trans. Ind. Electron*., vol. 60, no. 8, pp. 2978-2987, Aug. 2013.

[22] X. Zhang, L. Zhang and Y. Zhang, "Model predictive current control for PMSM drives with parameter robustness improvement", *IEEE Trans. Power Electron*., vol. 34, no. 2, pp. 1645-1657, Feb. 2019.

[23] H. Fan and Y. C. Wang, "Research on the characteristics of PMSM vector control system based on speed sliding mode controller", *Appl. Mech. Mater*., vol. 130, pp. 1142-1147, Oct. 2011.

[24] J. Liu, M.-Z. Huang and Y. Wang, "Research on vector-control system of PMSM based on internal model control of current loop", *Proc. 2nd Int. Workshop Compute. Sci. Eng*., pp. 297-301, Oct. 2009.
[25] C. Xia, J. Zhao, Y. Yan, and T. Shi, "A novel direct torque and flux control method of matrix converter-fed PMSM drives", *IEEE Trans. Power Electron*., vol. 29, no. 10, pp. 5417-5430, Oct. 2014.
[26] M. H. Vafaie, B. Mirzaeian Dehkordi, P. Moallem, and A. Kiyoumarsi, "A new predictive direct torque control method for improving both steady-state and transient-state operations of the PMSM", *IEEE Trans. Power Electron*., vol. 31, no. 5, pp. 3738-3753, May 2016.
[27] M. H. Vafaie, B. M. Dehkordi, P. Moallem, and A. Kiyoumarsi, "Improving the steady-state and transient-state performances of PMSM through an advanced deadbeat direct torque and flux control system", *IEEE Trans. Power Electron*., vol. 32, no. 4, pp. 2964-2975, Apr. 2017.
[28] L. A. Adase, I. M. Alsofyani and K.-B. Lee, "Predictive torque control with simple duty-ratio regulator of PMSM for minimizing torque and flux ripples", *IEEE Access*, vol. 8, pp. 2373-2381, 2020.
[29] K. T. Chau, C. C. Chan, and C. H. Liu, “Overview of permanent-magnet brushless drives for electric and hybrid electric vehicles”, *IEEE Trans. Ind. Electron*., vol. 55, no.6, pp. 2246-2257, Jun. 2008.
[30] N. Bianchi, S. Bolognani, and M. Zigliotto, “High-performance PM synchronous motor drive for an electrical scooter”, *IEEE Trans. Ind. Appl*., vol. 37, no. 5, pp. 1348–1355, Sep./Oct. 2001.
[31] Hui Yang, Z. Q. Zhu, Heyun Lin, Pelin Xu, Hanlin Zhan, Shuhua Fang, and Yunkai Huang, “Design synthesis of switched flux hybrid-permanent magnet memory machines”, *IEEE Trans. Energy Convers*., vol. 32, no.1, pp. 65-79, Mar. 2017.
[32] Yuan Ren, and Z. Q. Zhu, “Reduction of both harmonic current and torque ripple for dual three-phase permanent-magnet synchronous machine using modified switching-table-based direct torque control”, *IEEE Trans. Ind. Electron*., vol. 62, no. 11, pp. 6671-6683, Nov. 2015.
[33] Atheer H. Abosh, Z. Q. Zhu, and Yuan Ren, “Cascaded direct torque control of unbalanced PMSM with low torque and flux ripples”, *IEEE Trans. Power Electron*., vol.33, no.2, pp.1740-1749, Feb.2018.
[34] Mohammad Hossein Vafaie, Behzad Mirzaeian Dehkordi, Payman Moallem, and Arash Kiyoumarsi, “Improving the steady-state and transient-state performances of PMSM through

an advanced deadbeat direct torque and flux control system", *IEEE Trans. Power Electron*., vol. 32, no. 4, pp. 2964-2975, Apr. 2017.
[35] Masao Yano, Isao Kamiyama, and Sadanari Yano, "Microprocessor-Based Vector Control System for Induction Motor Drives with Rotor Time Constant Identification Function", *IEEE Trans. Ind. Appl*., vol. 22, no. 3, pp. 453-459, 1986.
[36] Tsuneo Kume, and Takanobu Iwakane, "High-Performance Vector-Controlled AC Motor Drives: Applications and New Technologies", *IEEE Trans. Ind. Appl*., vol. 23, no. 5, pp. 872-880, 1987.
[37] L. Zhong, M. F. Rahman, W. Y. Hu, and K. W. Lim, "Analysis of direct torque control in permanent magnet synchronous motor drives", *IEEE Trans. Power Electron*., vol. 12, pp. 528–536, May 1997.
[38] Lixin Tang, Limin Zhong, M. F. Rahman, and Yuwen Hu, "A novel direct torque control for interior permanent-magnet synchronous machine drive with low ripple in torque and flux-a speed-sensor less approach", *IEEE Trans. Ind. Appl*., vol. 39, no.6, pp. 1748–1756, Nov.-Dec. 2003.
[39] I. Takahashi and T. Noguchi, "A new quick-response and high efficiency control strategy of an induction machine", *IEEE Trans. Ind. Appl*., vol.22, pp. 820-827, Sept./Oct. 1986.
[40] K. D. Hoang, Z. Q Zhu., and M. P. Foster, "Influence and compensation of inverter voltage drop in direct torque-controlled four-switch three phase PM brushless AC drives", *IEEE Trans. Power Electron*., vol. 8, no.26, pp.2343-2357, Aug. 2011.
[41] Y. Xu, N. Parspour, and U. Vollmer, "Torque ripple minimization using online estimation of the stator resistances with consideration of magnetic saturation", *IEEE Trans. Ind. Electron*., vol. 61, no. 9, pp. 5105-5114, Sep. 2014.
[42] J. H. Leong, Z. Q. Zhu, and J. M. Liu, "Space-vector PWM based direct torque control of PM brushless machine drives having non-ideal characteristics", *Ecological Vehicles and Renewable Energies (EVER)*, 8th International Conf. and Exhibition, 2013, pp.1-6.
[43] Z. Xu and M. F. Rahman, "Direct torque and flux regulation of an IPM synchronous motor drive using variable structure control approach", *IEEE Trans. Power Electron*., vol. 22, no. 6, pp.2487-2498, Nov. 2007.
[44] G. Foo and M. F. Rahman, "Sensor less direct torque and flux-controlled IPM synchronous motor drive at very low speed without signal injection", *IEEE Trans. Ind. Electron*., vol. 57, no. 1, pp. 395–403, Jan. 2010.

[45] M. Preindl and S. Bolognani, “Model predictive direct speed control with finite control set of PMSM drive systems”, *IEEE Trans. Power Electron*., vol. 28, no. 2, pp. 1007–1015, Feb. 2013.
[46] J-H Lee, C-G Kim, and M-J Youn, “A dead-beat type digital controller for the direct torque control of an induction motor”, *IEEE Trans. On Power Electron*., vol. 17, no. 5, pp.739-746, Sept. 2002.
[47] Y. Cho, K.-B. Lee, Song, J.-H. Lee, “Torque ripple minimization and fast dynamic scheme for torque predictive control of permanent magnet synchronous motors”, *IEEE Trans. Power Electron*., vol. 30, no.4, pp.2182-2190, Apr. 2015.
[48] Y. Wang, L. Geng, W. Hao, and W. Xiao, "Control Method for Optimal Dynamic Performance of DTC-Based PMSM Drives", *IEEE Transactions on Energy Conversion*, vol. 33, no. 3, pp. 1285-1296, Sept. 2018, doi:10.1109/TEC.2018.2794527.
[49] L. Meng and X. Yang, "Comparative analysis of direct torque control and DTC based on sliding mode control for PMSM drive", *29th Chinese Control and Decision Conference (CCDC)*, 2017, pp. 736-741, doi: 10.1109/CCDC.2017.7978529., 2017.
[50] Markus Lindegger. *Economic viability, applications and limits of efficient permanent magnet motors*, Switzerland, Swiss Federal Office of Energy, 2009.
[51] Jacek F. Gieras, Mitchell Wing, *Permanent Magnet Motor Technology Design and Applications*, 2nd Edition, Marcel Dekker Inc., New York, Basel, USA, 2002.
[52] https://www.elprocus.com/what-is-a-permanent-magnet-synchronous-motor-its-working/
[53] https://en.wikipedia.org/wiki/Synchronous_motor
[54] Yihua Liu, Jiayi Wen, Dacheng Xu, “The decoupled vector control of PMSM based on nonlinear multi-input multi-output decoupling ADRC”, *Sage Journal of Advances in Mechanical Engineering*, vol. 12, doi: 10.1177/1687814020984255, 2020.
[55] Maha Sabra, Bashar Khasawneh, Mahamed A. Zohdy M., “Nonlinear Control of Interior PMSM using Control Lyapunov Functions”, *Journal of Power and Energy Engineering*, vol. 2, pp. 17-26, doi: 10.4236/jee.2014.21003, 2014
[56] D. C. Hanselman, *Brushless Permanent Magnet Motor Design*, Magna Physics Pub, 2006.
[57] P. C. Krause, O. Wasynczuk, S. D. Sudhoff, *Analysis of electric machinery*, in IEEE Press, 1995.
[58] O'Rourke, Colm J. et al. "A Geometric Interpretation of Reference Frames and Transformations: dq0, Clarke, and Park", *IEEE Transactions on Energy Conversion* 34, December 2019.

[59] Y. Inoue, S. Morimoto, and M. Sanada, "Control Method Suitable for Direct-Torque-Control-Based Motor Drive System Satisfying Voltage and Current Limitations", *IEEE Transactions on Industry Applications*, vol. 48, no. 3, pp. 970-976, May-June 2012, doi:10.1109/TIA.2012.2191170.

[60] M. Preindl and S. Bolognani, "Model Predictive Direct Torque Control with Finite Control Set for PMSM Drive Systems, Part 2: Field Weakening Operation", *IEEE Transactions on Industrial Informatics*, vol. 9, no. 2, pp. 648-657, May 2013, doi:10.1109/TII.2012.2220353.

[61] Y. Cho, K. Lee, J. Song, and Y. I. Lee, "Torque-Ripple Minimization and Fast Dynamic Scheme for Torque Predictive Control of Permanent-Magnet Synchronous Motors", *IEEE Transactions on Power Electronics*, vol. 30, no. 4, pp. 2182-2190, April 2015, doi:10.1109/TPEL.2014.2326192.

[62] S. A. Saleh and A. Rubaai, "The Development and Performance Evaluation of a Frame-Angle-Based Direct Torque Controller for PMSM Drives", *IEEE Transactions on Industry Applications*, vol. 54, no. 3, pp. 2806-2820, May-June 2018, doi:10.1109/TIA.2018.2794958.

[63] F. Niu et al., "A Simple and Practical Duty Cycle Modulated Direct Torque Control for Permanent Magnet Synchronous Motors", *IEEE Transactions on Power Electronics*, vol. 34, no. 2, pp. 1572-1579, Feb. 2019, doi:10.1109/TPEL.2018.2833488.

[64] Y. Ren, Z. Q. Zhu, J. E. Green, Y. Li, S. Zhu, and Z. Li, "Improved Duty-Ratio-Based Direct Torque Control for Dual Three-Phase Permanent Magnet Synchronous Machine Drives", *IEEE Transactions on Industry Applications*, vol. 55, no. 6, pp. 5843-5853, Nov.-Dec. 2019, doi:10.1109/TIA.2019.2938468.

[65] X. Wang, Z. Wang, Z. Xu, M. Cheng, and Y. Hu, "Optimization of Torque Tracking Performance for Direct-Torque-Controlled PMSM Drives with Composite Torque Regulator", *IEEE Transactions on Industrial Electronics*, vol. 67, no. 12, pp. 10095-10108, Dec. 2020, doi:10.1109/TIE.2019.2962451.

[66] S. Sakunthala, R. Kiranmayi, and P. N. Mandadi, "A study on industrial motor drives: Comparison and applications of PMSM and BLDC motor drives", *International Conference on Energy, Communication, Data Analytics and Soft Computing (ICECDS)*, 2017, pp. 537-540, doi: 10.1109/ICECDS.2017.8390224.

[67] N. Celanovic and D. Boroyevich, "A fast space-vector modulation algorithm for multilevel three-phase converters", *IEEE Transactions on Industry Applications*, vol. 37, no. 2, pp. 637-641, March-April 2001, doi: 10.1109/28.913731.

[68] K.-B. Lee, J.-H. Song, I. Choy, and J.-Y Yoo, “Improvement of low-speed operation performances of DTC for 3-level inverter-fed induction motors”, *IEEE Trans. Ind. Electron*., vol. 48, no. 5, pp. 1006-1014, Oct. 2001.

[69] D. Casadei, F. Profumo, G. Serra, and A. Tani, “FOC and DTC: Two viable schemes for induction motors torque control”, *IEEE Trans. Power Electron*., vol. 17, no. 5, pp. 779–787, Sep. 2002.

[70] G. H. B. Foo and M. F. Rahman, “Direct torque control of an IPM synchronous motor drive at very low speed using a sliding-mode stator flux observer”, *IEEE Trans. Power Electron*., vol. 25, no. 4, pp. 933-942, Apr. 2010.

[71] I. R. Akhil and C. K. Vijayakumari, "Modified Direct Torque Control scheme for PMSM", *IEEE International Conference on Power Electronics, Drives and Energy Systems (PEDES)*, 2012, pp. 1-6, doi: 10.1109/PEDES.2012.6484328.

[72] Ouboubker Lahcen, Khafallah Mohamed, Essaadi Mouna, Lamterkati Jawad, Chaikhy Hamid, Elafia Aziz, “An Implementation of a Twelve Sectors Direct Torque Control Strategy of Induction Machine using DSPACE TMS 320F2812”, *Communications on Applied Electronics, Foundation of Computer Science*, New York, USA, vol. 3, no. 1, October 2015, ISSN: 2394-4714.

[73] V.I. Utkin, “Variable Structure systems with Sliding Modes”, *IEEE Transaction on Automatic Control*, 22, 2, 212-222, 1977.

[74] Raymond A. DeCarlo, Stanislaw H. Zak, and Gregory Mathews, "Variable Structure Control of Nonlinear Multivariable Systems: A Tutorial", *Proceedings of the IEEE*, vol. 76, No. 3, Mar. 1988.

[75] J. Y, Hung, W. Gao, and J.C Hung, "Variable Structure Control: A Survey", *IEEE Trans. on Industrial Electronics*, vol. 40, No. 1, Feb. 1993.

[76] K.D. Young, V.I. Utkin and Ü. Özgüner, “A control engineer’s guide to Sliding Mode Control”, *IEEE Transactions on Control Systems Technology* 7 (3), pp. 328–342., 1999.

[77] G. Bartolini, L. Fridman, A. Pisano, E. Usai (Eds.), *Modern Sliding Mode Control Theory - New Perspectives and Applications*, Springer Lecture Notes in Control and Information Sciences, Vol. 375.

[78] Arie Levant, “Sliding order and sliding accuracy in sliding mode control”, *International Journal of Control*, 58(6), 1993, 1247-1263).

[79] G. Bartolini, A. Ferrara, A. Levant, E. Usai, “On second order sliding mode controller in Variable structure systems, sliding mode and nonlinear control”, *Springer Lecture Notes in Control and Information Sciences*, Volume 247/1999.

[80] V.I. Utkin, “Sliding mode control design principles and applications to electric drives”, *IEEE Transactions on Industrial Electronics*, 40, 1, 23.36, 1993.

[81] Damiano A., Gatto G.L., Marongiu I., PISANO A.,” Second-order sliding-mode control of DC drives” *IEEE Trans. on Industrial Electronics*, vol. 51, n. 2, pp. 364-373, 2004.

[82] A.G. Loukianov, J.M. Cañedo, V.I. Utkin, J. Cabrera-Vázquez, “Discontinuous Controller for Power Systems: Sliding-Mode Block Control Approach”, *IEEE Transactions on Industrial Electronics*, 51, 2, 340-353, 2004.

[83] Y.B. Shtessel, ME Jackson, “Sliding mode thermal control system for space station furnace facility”, *IEEE transactions on control systems technology*, vol. 6, n 5, pp. 612-622, 1998.

[84] S. K. Spurgeon, C. Edwards “Sliding Mode Output Tracking with Application to A Multivariable High Temperature Furnace Problem”, *International Journal of Robust and Nonlinear Control*, 7, 4, 337-351, 1998.

[85] Bartolini G., Pisano A., Punta E., Usai E., "A survey of applications of second-order sliding mode control to mechanical systems", *International Journal of Control*, vol. 76, n. 9/10, pp. 875-892, 2003.

[86] Bartolini G., PISANO A., Usai E., "Output-feedback control of container cranes: a comparative analysis", *Asian Journal of Control*, vol. 5, n. 4, pp. 578-593, 2003.

[87] Bartolini G., PISANO A.., Usai E., "Second Order Sliding Mode Control for Container Cranes" *Automatica*, vol. 38, pp. 1783-1790, 2002.

[88] Bartolini G., Orani N. PISANO A., Punta E., Usai E., “A combined first/second order sliding-mode technique in the control of a jet-propelled vehicle”, *International Journal of Robust and Nonlinear Control*. Vol. 18, n. 4/5, pp. 570-585, 2007.

[89] PISANO A. Usai E., “Output-feedback control of an underwater vehicle prototype by higher-order sliding modes”, *Automatica*, vol. 40, n. 3, pp. 1525-1530, 2004.

[90] www.ansaldoenergia.com